BUILDING BLOCKS OF CONTINUOUS PHARMACEUTICAL MANUFACTURING

By

GOLSHID KEYVAN

A dissertation submitted to the

School of Graduate Studies

Rutgers, The State University of New Jersey

In partial fulfillment of the requirements

For the degree of

Doctor of Philosophy

Graduate Program in Chemical and Biochemical Engineering

Written under the direction of

Fernando J. Muzzio

And approved by:

_____

_____

_____

_____

New Brunswick, New Jersey

October, 2020

ABSTRACT OF THE DISSERTATION

Building blocks of continuous pharmaceutical manufacturing

By GOLSHID KEYVAN

Dissertation Director:

Fernando J. Muzzio

Continuous manufacturing (CM) is gaining popularity within the pharmaceutical industry as it is undergoing a shift from the conventional batch manufacturing of the last century to a new continuous paradigm that greatly enables use of advanced manufacturing methods. Continuous manufacturing offers many advantages such as flexibility, quality, robustness, higher yield, and lower manufacturing costs. Although CM is common in other industries (e.g., food and chemicals), it is an emerging technology in the pharmaceutical industry. Undoubtedly, continuous processing lends itself to in-process monitoring and closed-loop control. Process understanding, control strategies, and on-line, in-line, or at-line measurements of critical quality attributes provide for control strategies that include real-time quality evaluation of products. Under CM, real-time product quality assurance has been widely investigated under the Quality-by-Design (QbD) guidelines recommended by the FDA to advance the pathway to Real Time Release testing (RTRt).

Solid oral dosage products such as tablets and capsules constitute about 60% of global drug prescriptions, and their critical quality attributes (CQAs) such as hardness and dissolution, are well defined. Historically, they have been manufactured using batch methods and

quality is evaluated by extracting a small number of samples that are subsequently subjected to destructive testing to evaluate quality. More recently, as the result of continuous processing, there is a movement away from end-of-line sample testing towards the adoption of in-process measurement strategies that ensure product quality in real-time. The first step in implementing an in-process test methodology towards RTRt is to identify the critical steps in the manufacturing processes, understand their failure modes, and develop design methodologies to prevent them from defeating the process.

In this work, we examined building blocks of two continuous manufacturing processes; DCCM (Direct Compression Continuous Manufacturing) and CHME (Continuous Hot Melt Extrusion). In both operations, we identified the critical processing parameters so that it could lead to implementing in-process testing methodologies that would enable RTRt. We characterized the process and examined the interplay between the process parameters and the product quality. This was accomplished by executing designed experiments on both processes and characterizing the tablets in terms of their critical quality attributes (CQAs) such as dissolution and hardness. Furthermore, we found a correlation between the tensile strength and dissolution of the continuously manufactured tablets and the processing parameters in the manufacturing line that can predict process performance. The predictive approach will not only enable us to develop a control strategy to determine the process parameters values that keep the process within the control space but also facilitate development of new solid oral dose products in the event of an emergency or drug shortages.

ACKNOWLEDGMENTS

I would like to thank my supervising professor, Dr. Fernando Muzzio, for his support and guidance. His advice and principles will serve me for the rest of my life. I would also like to thank the members of my committee: Dr. Alberto Cuitino, Dr. Ravendra Singh, and Dr. San Kiang. Thanks also to my colleagues for their friendship and support: Krizia Karry, Dina Ameen, Tannaz Ramezanli, Mania Dorrani, Francisco Palma, late Tara Tsai, Xue Liu, Thamer Omar, Savitha Panikar, Jen Winkler, Yifan Wang, Pallavi Pawar, Sarang Oka, Zhanjie Liu, Tianyi Li, Yi Tao, Jingzhe Li, Qiushi Zhou, Shashwat Gupta, Andres Romam-Ospino, James Scicolone, Gerardo Callegari, Wei Meng, Sonia Razavi, Elaheh Ardalani, and Justin Hendrix. Without them and other friends, my goals would not have been achieved.

I gratefully acknowledge the funding I received during my years at the ERC. Throughout these years I had the pleasure to collaborate with great colleagues and professors from Rutgers, NJIT, University of Puerto Rico, and Purdue University. Thanks to Atul Dubey for the collaborative work we had together during my first year at Rutgers. I am grateful to Professor Bo Michniak from the Rutgers Pharmacy School, Xiangxin Meng from Professor Mitra's group, Ezinwa Elele from professor Khusid's group, and Lucus Sievens-Figueroa from Professor Dave's group from NJIT, and Eduardo Hernandez from Professor Romanach's group from University of Peurto Rico for the collaborative work.

Most of all, I would like to thank my incredible husband, Farhad, for his unwavering devotion and love of our family, my children, Arya and Kurosh, for their continued encouragement to finish my dissertation, unending love and support, and for always

reminding me that family is the most important thing in life. I am also thankful to my parents, Molood and Mohsen, for leading me into intellectual pursuits.

Table of Contents

List of Tables

List of Figures

Chapter 1: Introduction

1.1 Background and motivation

Continuous manufacturing has been used in the chemical and food industries for decades [1]. However, pharmaceutical companies have only recently recognized the advantages of this manufacturing approach. In recent years, the pharmaceutical industry has suffered from a shortage of new blockbuster drugs, expiration of patents on some of its most lucrative drugs, and reduction in productivity in research and development in generating new patent-protected products. These issues have put pressure on pharmaceutical companies to improve the efficiency of their manufacturing operations, especially in cases involving mergers and acquisitions of the largest companies. Furthermore, competition imposed by generic pharmaceutical companies has increased, and expectations of better quality by regulatory agencies have increased. These factors have fueled interest in the more efficient continuous operations, which the industry is currently adopting at a growing rate [2-4].

1.2 Drug shortages

While the most common method for oral solid dosage manufacturing is batch processing, such processes involve hurdles with scale up and storage of intermediate products, long manufacturing cycle times, issues with tablet quality, low yield (large waste), and inefficient manufacturing [5]. They are poor in flexibility and robustness leading to frequent product failures that may lead to drug shortages [6]. The majority of drug shortages derive from failures due to product quality. In particular, manufacturing issues cause the majority of drug shortages and drug recalls in the US. Overall drug product recalls

have been increasing [7], and the industry has limited ability to rapidly increase production in the event of emergencies. Continuous manufacturing, which can address many of these issues, is thus a promising opportunity that has been described by Dr. Janet Woodcock, the long-term director of the FDA Center for Drug Evaluation and Research, as "the future of Pharmaceutical Manufacturing" [8].

1.3 Real time release testing (RTRt)

Important advances in science and technology have taken place over the past fifteen years to support the implementation of continuous pharmaceutical manufacturing processes. The US Food and Drug administration has taken proactive steps to facilitate the pharmaceutical industry's implementation of continuous manufacturing, seeking to improve product quality and to address the underlying causes of drug shortages and recalls [9]. Process analytical technology (PAT) has progressed in developing online measurement tools for analyzing critical quality attributes (CQAs) of intermediates and products. The rapid response of continuous processes greatly facilitates implementation of QbD, so that quality is designed into the process, rather than checked afterwards. Thus, PAT and QbD are key elements of continuous manufacturing. However, importantly, Real Time Release testing (RTRt) of final products still remains a challenge that prevents continuous manufacturing from reaching its full potential.

1.4 Advantages of continuous manufacturing

Continuous manufacturing can transform the drug manufacturing process to become a faster, better understood, and a better controlled process [10]. The output material in a batch process is sampled and tested to determine whether it has the expected quality, and

if it does not the entire batch must be reprocessed or discarded. On the other hand, in continuous processes, the quality of output material is tested in real-time, and then an active control strategy adjusts the process parameters to maintain product quality. Thus, an understanding of the process dynamics, as impacted by the interaction of process parameters with material attributes, is required. In general, to operate at full efficiency, the continuous process requires some level of closed-loop control, including material controls, process monitoring, and detecting and handling perturbations in real-time to be able to support Real Time Release testing (RTRt) [11]. RTRt consists of a combination of process control and process analytical technology (PAT). Analytical data are obtained from instruments such as near infrared spectroscopy (NIR), Raman spectroscopy, terahertz pulsed imaging, acoustic techniques as well as from soft sensors that predict hard-to-measure material attributes based on more easily measurable attributes or measured process variables. These techniques are non-destructive, i.e., they have the benefit of measuring material attributes without destroying the samples. This makes it possible for further characterization of the same sample by multiple methods, which enables the correlation of multiple critical quality attributes (CQAs) and a better understanding of the process.

1.5 Oral solid dosages

Oral solid dosage products such as tablets and capsules constitute the majority of global drug prescriptions. Hardness, dissolution, content uniformity, and weight variability of tablets are the quality attributes that are usually critical in pharmaceutical manufacturing. Typically, product must comply with pre-set limits in these attributes to be dispensed to patients. Failure to adhere to the limits can lead to product failure.

1.6 Tensile strength

Tablet hardness, or more correctly, tensile strength, is an important physical-mechanical property that is known to affect the disintegration and dissolution of the drug in the body. Therefore, it has become common practice to evaluate tablet tensile strength as an at-line method. Currently, this critical quality attribute is evaluated by a diametrical compression test that is destructive. As the pharmaceutical industry continues to shift towards continuous processes, it would be very useful to be able to evaluate tensile strength and tablet hardness in-line and non-destructively, so that the measurement can be used to control the process. Therefore, there has been a growing interest in the development of non-destructive predictive tools for tablet tensile strength. Acoustic measurements, which are effective, non-destructive, and only take a few microseconds, have been shown to be a suitable option for RTRt [12].

1.7 Acoustic measurements at ultrasound frequencies

In the last half a century, the potential of acoustic measurements has been explored multiple times for characterization of the physical-mechanical attributes of pharmaceutical tablets [13-17]. Acoustic measurements involve determination of ultrasound velocity of tablets from their transmission measurements. Ultrasound, sound waves above 20 kHz frequency, is a mechanical wave that propagates through a medium such as air, water and solids. This technique is fast, non-invasive, and can provide useful physical and chemical information about the tablet in real-time. Different studies have utilized ultrasonic testing techniques to predict tablets capping [18], to investigate the effects of compaction force and level of shear strain on tablets [19], and to analyze the effect of particle size distribution, lubricant

concentration, and mixing time on tablet tensile strength [20]. Clearly, one of the major advantages of an ultrasonic technique is its speed and simplicity in the evaluation of tablet properties. Although the ultrasound system must be calibrated to insure the time of flight (TOF) of the samples are accurate, it has the advantage that it does not require a calibration model to predict the time of flight of the samples. To date, there have been no studies using ultrasonic techniques involving tablets manufactured in a Continuous Direct Compaction (CDC) line. None of the studies mentioned above have investigated the multivariate effects of the processing variables using Quality-by-Design methods to measure tablet tensile strength. Although dependence of ultrasound on tablet density has been studied in the past [13, 21], the acoustic properties of tablets have never been correlated with formulation. Given that there has been growing interest in the use of non-destructive methods of analyzing tablet tensile strength by ultrasound, this dissertation receives special attention in this dissertation.

1.8 Dissolution

As stated in the FDA guidance [22, 23], drug release rate, as measured by dissolution testing, is one of the quality attributes that assures continued product quality and performance characteristics of a dosage form. The FDA has placed substantial emphasis on dissolution profile comparisons for post approval changes [24]. The most important application of the dissolution profile is its role as a surrogate for *in vivo* bioequivalence for generic products, where *in-vitro/in-vivo* correlations (IVIVC) can be developed subsequently to reduce the need to perform costly bioavailability human volunteer studies and speed-up product development. Hence, it is important to evaluate tablet in-vitro dissolution before the drug product is released to the market. Currently, the only method

of dissolution testing is the offline laboratory-based method of dissolving samples in agitated liquid baths, which is destructive, so that the samples are no longer available for further characterization. Dissolution testing is a lengthy procedure that is time-consuming, expensive, requires media preparation, and generates substantial waste. As continuous manufacturing becomes a common processing method that requires real-time evaluation of drug release, tablet critical quality attributes such as dissolution profile needs to be controlled in-line and non-destructively. Therefore, development of non-destructive predictive methods for tablet dissolution testing towards RTRt is essential. Building models for predicting tablet dissolution profiles will enable rapid techniques in continuous assessment of tablets ensuring the desired quality attributes.

There are diverse methods for prediction of dissolution profiles, and multiple strategies have already been studied. Multivariate approaches have been used by other investigators [25, 26] [27] [28, 29], and dependence of dissolution profiles on formulation and physio-chemical characteristics of tablets have been analyzed. Wang *et al*. studied different methodologies for comparison of dissolution profiles and utilized MANOVA to assess similarity of profiles for controlled release tablets [30]. MANOVA is simply an ANOVA (Analyis of Variance) with several dependent variables that are correlated. MANOVA differentiates between profiles based on mean vectors rather one mean at each time point, thus, has the advantage of comparing dissolution profiles as a whole.

Different from the other studies mentioned above, NIR spectroscopy will not be used in the work reported in this dissertation for dissolution prediction. Methods relying on NIR testing can be defeated by sensor fouling and lack of maintenance and updated calibration. Fouling is one of the concerns associated with the operation and maintenance of sensing

technologies, such as NIR. Periodic cleaning of the NIR system to meet the target performance level is usually required. Updated calibration is required on a regular basis to prevent incorrect processing decisions and to compensate for changes in raw materials. Thus, the methodology introduced here for predicting dissolution performance by statistical analysis that does not rely on NIR testing can be extremely useful in the aforementioned cases.

1.9 Hot melt extrusion

Hot melt extrusion (HME), a manufacturing technique traditionally used in the plastic and food industries, has attracted significant interest from the pharmaceutical manufacturing sector [31]. Hot melt extrusion was originally used to process poorly soluble APIs and biocompatible polymers to create solid dispersions with enhanced dissolution characteristics [32]. More recently however, with the advent of the opioid crisis, more recently however, HME has emerged as a manufacturing technology to produce abuse deterrent formulations (ADF) [33].

1.10 Opioids and the FDA

Opioids are medication for pain that are prescribed on a daily basis to millions of patients. While opioids have led to many benefits to patients suffering from intense acute and chronic pain, they have also caused enormous addiction problems throughout the United States due to prescription misuse and overdose. More than 200,000 people died from overdoses related to prescription opioid in the United States between 1999 and 2016 [34].

In 2015, in reaction to the opioid crisis, the US Food and Drug Administration (FDA) published a guidance for industry regarding evaluation and labeling of abuse-deterrent

opioids [35]. Abuse-deterrent formulations (ADF) make manipulation of opioid more difficult or less rewarding. The guidance focused on how the studies on ADF formulations should be conducted to demonstrate abuse-deterrent properties. Various categories of abuse deterrent technologies consisted of physical/chemical barriers, agonist/antagonist combinations, aversion, delivery system, new molecular entities (NMEs) and prodrugs, and other novel approaches. While different abuse deterrent methodologies are reported in the literature, they have only reduced the risk of abuse and not yet proven successful at complete removal.

Polyethylene Oxide (PEO) has been a common excipient to formulate abuse deterrent oral solid opioids such as OxyContin™ (oxycodone HCL) [36] and Hysingla™ (hydrocodone bitartrate) ER tablet [37]. Application of PEO in hot melt extrusion was first studied by Zhang and McGinity [38]. The authors used different grades of PEO, 7M and 1M molecular weight, to investigate the properties of PEO as drug carrier. They demonstrated that hot melt extrusion was not only a novel method to prepare sustain-release tablets but also that PEO was a suitable polymeric carrier for HME process. PEO is commercially available in different grades and has several advantages: its gelling property makes PEO a good candidate for sustained release formulation; PEO particles fuse together at relatively low temperatures and result in tablets with high tensile strength; and the high viscosity grades make solutions very viscous and difficult to inject. Due to these unique properties, PEO has attracted considerable attention for its suitability as an abuse deterrent formulation enhancer. However, these formulations are prepared by batch processes which involve many unit operations and are costly. Therefore, there is a need to advance the

manufacturing method and apply continuous manufacturing where products with optimum abuse deterrence and less cost can be achieved.

As with many continuous processes, HME can be readily coupled with process analytical technology such as Near Infrared spectroscopy (NIR), which allows for real-time feedback and control of the chemical composition of the extruded materials, leading to enhanced control of the HME process itself. While extrusion is an intrinsically continuous processing step, an overall continuous process including upstream feeding and blending and downstream tableting has not been completely implemented in the industry. Thus, there exists a critical need to develop methodologies and approaches to manufacturing abuse deterrent products by continuous HME.

1.11 Dissertation objectives and organization

The four specific aims of this dissertation are achieved through the completion of the following aims:

Aim 1: To set up a direct compression continuous manufacturing line (DCCM) and design a study to integrate RTRt tools into the manufacturing process (Chapters 2, 3, and 4)

Aim 2: To conduct a study to examine the impacts of the process parameters on process and product performance and to build predictive models for tablet hardness and dissolution based on process parameters (Chapters 3 and 4)

Aim 3: To use ultrasound as a PAT method to enable an approach for real time release testing (RTRt) of tablet hardness (Chapter 3)

Aim 4: To examine the effects of formulation properties and performance of PEO (polyethylene oxide) tablets (Chapter 5)

The 1st aim of this dissertation was accomplished by conducting a case study for continuous manufacturing of tablets in the pilot plant at Rutgers University. The DCCM line was comprised of gravimetric feeders, a de-lumping mill, a continuous mixer, and a tablet press. The case study used designed experiments to evaluate the effect of variability in critical process parameters (CPP) on the critical quality attributes (CQA) of tablets. Tablets were characterized for their tensile strength and dissolution. The aim was to understand the effect of the continuous process on tablet properties.

The data compiled in Aim 1 was examined using ANOVA methods to identify the process operating conditions that contributed significantly to variability in product quality attributes such as tensile strength and dissolution. To address the auto-correlated nature of the dissolution profile results, for dissolution test results, MANOVA was used to identify the operating conditions affecting the dissolution profiles of the tablets. Multi-linear regression models were developed to predict tablet tensile strength and dissolution profiles of the tablets manufactured in Aim 1. A predictive model was built to correlate the tensile strength with speed of sound (SOS) and relative density of the tablets. The model was verified using an independently manufactured validation set, and the predicted values from the model were compared with the experimental results. Statistical models were also built to predict tablet dissolution profiles. The predicted dissolution profiles were compared to the experimental profiles. This work completed Aim 2.

In Aim 3, we investigated the use of Ultrasound for monitoring tablet tensile strength. The objective was to demonstrate a general methodology for Real Time Release testing (RTRt) of directly compressed tablets manufactured in the continuous line and to develop a statistical model to predict tensile strength. Multivariate effects were analyzed using Quality-by-Design methods. Ultrasound transmission speed was determined by measuring the sound wave time-of-flight (TOF) using transducers with a frequency of 2.25 MHz. The speed of sound (SOS) was calculated by dividing the measured tablet thickness by the TOF. The same tablets were characterized for diametrical crushing strength using a mechanical hardness tester. ANOVA was be used to reveal the main parameters affecting the tensile strength and the SOS of the tablets in this process.

The aim of the 2nd case study was to investigate the properties of polyethylene oxide (PEO) with different nominal molecular weight (MW) to manufacture tamper resistant formulations using high molecular weight PEO by hot melt extrusion (HME). We investigated the correlation between MW of PEO and extrudate attributes such as viscosity and dissolution. The benefits in this work will be better characterization of the relevant properties of various PEOs and to determine combination ratios of different PEOs in order to make tablets with intended abuse-deterrent properties to subsequently enable real time realease testing in opioid manufacturing processes. This work completed Aim 4.

Chapter 2: Experimental Methods

2.1 Introduction

The work in this study was based on two platforms; DCCM (Direct Compression Continuous Manufacturing) and CHME (Continuous Hot Melt Extrusion), and the methodologies of both have been discussed in detail in this chapter. Material characterization and analytical techniques utilized to characterize performance and quality of each platform are detailed in the following sections.

2.2 Direct compression continuous manufacturing line (DCCM)

The continuous direct compaction (CDC) line is a full-scale manufacturing line in the engineering building at Rutgers University by C-SOPS in collaboration with Janssen Pharmaceutical. The direct compaction equipment was arranged in a top down configuration so each unit operation can gravity feed powder to the next (Figure 1). The process was constructed on three levels and included four unit operations; feeders, comil, blender, and tablet press (Figure 1). Three types of Loss-in-Weight (LIW) Coperion-K-Tron feeders were used for the continuous line runs, including a KT-20 for acetaminophen, KT-35 for lactose, and a MT-12 for magnesium stearate. Once the acetaminophen and lactose were fed, they passed through a conical mill (Comil - Quadro S197) with a 800 nm screen, at a 50% motor speed setting, and round impeller (Model # 1601). The magnesium stearate feeder was placed after the comil to avoid potential over lubrication of the blend in the high shear environment of the comil. The total throughput of the line was 20 kg/hr. Acetaminophen and lactose mixture exited the mill, met the feed stream of the magnesium stearate, and entered into a Glatt GCG-70 blender with 24 blades on the mid-level. The

blades had the “1/3 forward+1/3 alternate +1/3 forward” configuration [39]. The material was conveyed down the length of the Glatt blender by the internal blades of the mixer. The exit of the blender was connected to a transitional chute, where the powder mixture traveled downward through an NIR interface (to determine blend homogeneity) and into the feed frame of the tablet press on the ground floor. A semi-stable bed height was maintained from the tablet press into the chute, allowing the NIR to scan the powder bed that was not interrupted by air. A 36-station Kikusui Libra 2 tablet press, fitted with a type B round tooling at 10 mm diameter, was used to compact the blend into tablets. A target tablet weight was set at 350 mg.

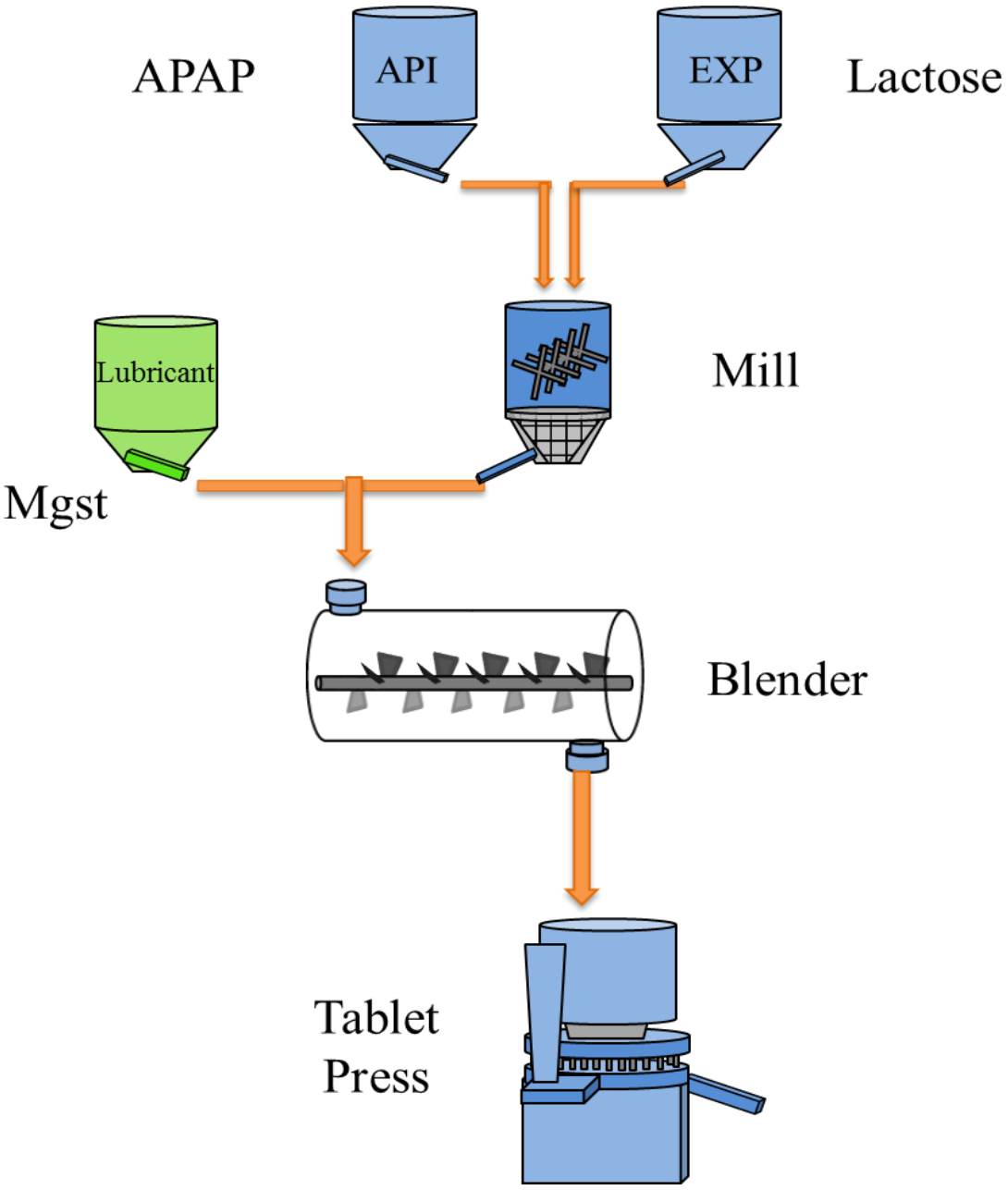

Figure 1: Continuous direct compression line at Rutgers University

2.2.1 Equipment

2.2.1.1 Feeders

The feeders in this work were characterized offline to identify appropriate screws were used. Fine auger screws were used for acetaminophen, and fine concave screws were used for lactose and magnesium stearate (Table 1).

Table 1: Tooling configuration and feed rates for each feeder

Material	**Feeder type**	**Screw Type**	**Feed rate @20 kg/hr**
Acetaminophen	KT-20	Fine auger	1-2.6
Lactose	KT-35	Fine concave	17.2-18.8
Magnesium Stearate	KT-12	Fine concave	0.2

2.2.1.2 Mill

The comil was used to de-lump the process stream after the initial feeding. Based on previous studies it was found that the combination of an 800μm hole diameter screen and a 50% motor speed setting led to the optimal de-lumping [40].

2.2.1.3 Blender

The blender configuration of the Glatt GCG-70 blender was previously explored with three different configurations; “all forward”, “1/2 forward + 1/2 alternate”, and “1/3 forward +

1/3 alternate + 1/3 forward". In the "all forward" case, all blades were set to a forward 45° angle. In the "1/2 forward + 1/2 alternate" case, the first 12 blades were set to a forward 45° angle, and the second 12 blades were alternated between forward 45° and backward 45°. Likewise, in the "1/3 forward + 1/3 alternate + 1/3 forward" case only the middle 1/3 were alternated between forward 45° and backward 45°. The authors concluded that based on "1/3 forward + 1/3 alternate + 1/3 forward" configuration the highest number of blade passes and the best performance was obtained, and that indicated the best condition of the blade configuration [39].

The Glatt blender impeller speed was operated using a speed range that avoided choking and fluidization. If the speed was set too high the blades would fluidize the powder, which could lead to a significantly reduced residence time which would consequently lead to reduced axial mixing risking product quality, and if the speed was set too low, the blender would choke.

2.2.1.4 Tablet Press setup

The tablet press was a 36-station Kikusui Libra 2 fitted with a type B round tooling at 10 mm diameter. The feed frame was set up to run at a very low range to accommodate the low throughput at 20 kg/hr.

2.2.2 Materials

Semi-fine acetaminophen (Mallinckrodt, Raleigh, NC) was used as the model active pharmaceutical ingredient (API), lactose 310 monohydrate NF (Foremost Farms, Rothschild, Wisconsin) was used as the filler/binder, and magnesium stearate NF (Mallinckrodt, St. Louis, Missouri) as the lubricant. The particle size distribution of the

ingredients was measured using a laser diffraction technique (Beckman Coulter LS 13 320). The values are reported in Table 2, and each value is an average of three measurements.

Table 2: Tablet ingredients and particle size

Material	**d10(µm)**	**d50(µm)**	**d90(µm)**
Semifine acetaminophen	6	43	103
Lactose 310 monohydrate NF	10	71	146
Magnesium Stearate	2	9	15

2.2.3 Experimental Design & Sampling

The overall experimental design was a $3^{(4-1)}$ fractional factorial experiment with three center points for a total of 30 experimental runs (Table 3). Treatments included %API, compaction force, blender speed, and feed frame speed with three levels of each. Based on prior studies on feeding, blending, and tableting four factors were selected: blender speed, feed frame speed, compaction force, and %API. It should be noted that %API is the nominal value of API used in the tablets. The % drug content that is used throughout the dissertation refers to the amount of drug predicted by NIR.

The experiment was performed in three days. Tablets containing 5% acetaminophen were manufactured on the first day, 9% on the second day, and 13% on the third day. Each time the API concentration, blender speed, feed frame, and compaction levels changed, the system required a certain interval until the system was again at steady state so that tablet

samples could be collected. The waiting interval used was set at 60 minutes for API concentration changes, 30 minutes for blender speed changes, and feed frame speed, and 5 minutes for compaction force changes. At each steady state experimental run, tablets were collected for ten minutes in ten bags. Tablets in the first minute were collected in the first bag, and tablets in the tenth minute were collected in the tenth bag. Only tablets in the tenth bag were analyzed.

Table 3: Fractional factorial experimental design with 4 factors and three center points

Run	**API(%)**	**Blender speed(rpm)**	**Feed frame speed(rpm)**	**Compression force(KN)**
1	5	150	20	8
2	5	150	25	16
3	5	150	30	24
4	5	200	20	16
5	5	200	25	24
6	5	200	30	8
7	5	250	20	24
8	5	250	25	8
9	5	250	30	16
10	9	150	20	16
11	9	150	25	24
12	9	150	30	8
13	9	200	20	24
14	9	200	25	8

15	9	200	30	16
16	9	250	20	8
17	9	250	25	16
18	9	250	30	24
19	13	150	20	24
20	13	150	25	8
21	13	150	30	16
22	13	200	20	8
23	13	200	25	16
24	13	200	30	24
25	13	250	20	16
26	13	250	25	24
27	13	250	30	8
28	9	200	25	16
29	9	200	25	16
30	9	200	25	16

2.2.4 Characterization methods

2.2.4.1 Particle Size Distribution

The particle size of ingredients was measured using a laser diffraction particle size analyzer (Beckman Coulter, LS 13 320) shown in Figure 2. This device works on the principle of diffraction patterns of a laser beam. It correlates the pattern of scattering light, as measured by the intensity at different angles, to the particle size distribution of the sample. The

measurement results in a volume percent as a function of the particle size, a data series from which the particle distribution parameters such as d10, d50 and d90 can be computed. The associated software of the equipment computes the particle size distribution parameters. Each measurement was performed in triplicate, and the average value of the three measurements has been reported.

Figure 2: Beckman Coulter LS 13 320 Laser diffraction particle size analyzer [41]

2.2.4.2 Relative density

Each tablet was accurately weighed, and their diameter and thickness were measured with a digital caliper (Marathon CO030150). Relative density of the tablets was calculated using the equation

$$\rho_{R} = \frac{\rho_b}{\rho_t}$$

where ρ_b is the bulk density and ρ_t is the true density. The bulk density of tablets was calculated by dividing the tablet weight by its volume. The true density of the individual components was estimated as per the supplier MSDS (lactose 1.54g/cc, semi-fine acetaminophen 1.29 g/cc, magnesium stearate 1.03g/cc), and the true density of the blend was calculated using the weight percent of each component.

2.2.4.3 Tensile strength

The hardness of the same tablets was measured using a destructive diametrical compression test apparatus (Dr. Schleuniger, Pharmatron 6D). The tablets were diametrically broken into two pieces, and the crushing hardness, defined as customary as the force required to break the tablet, was recorded for each tablet. With the acquired data, the tensile strength (σ) was calculated according to the equation below described by Fell and Newton (1970) [42].

$$\sigma_L = \frac{2F}{\pi dt}$$

where σ_L is the tensile strength, F is the applied force, t the tablet thickness, and d is the tablet diameter.

2.2.4.4 Content uniformity by high performance liquid chromatography (HPLC)

The tablets were analyzed for their API content using an in-house validated HPLC method. The acetaminophen method was adapted from USP 37 [43]. HPLC analysis was conducted using an Agilent 1100 HPLC system (Wilmington, DE, USA) equipped with a solvent

degasser, pump, auto-sampler, and PDA detector. A Waters Xterra RP 18 colum (Waters, Milford, MA) with 150 mm length, 4.6 mm inside diameter, and 5 μm particle size was used. The mobile phase consisted of water and methanol (3:1). The flow rate and the injection volume were set to 1.5 ml/min and 10 μl respectively. The column temperature was kept at 35 °C. The experiment was run for 6 minutes, and acetaminophen was detected at 243 nm.

Standards were prepared by dissolving accurately weighed quantities of acetaminophen in the mobile phase to obtain solutions at concentrations in the range of 0.0 mg/ ml to 0.01 mg/ ml. The standards were analyzed by the HPLC according to the method explained above, and the peak area of acetaminophen was recorded for each solution. A calibration curve was built by plotting peak areas against concentrations, and a best fit straight line was drawn to determine the calibration curve. Next, tablets were dissolved in the mobile phase to obtain solutions at concentrations within 0.0 - 0.01 mg/ml range. They were subsequently analyzed by the HPLC, and the quantity of acetaminophen was calculated based on the calibration curve.

2.2.4.5 Content uniformity by NIR

The tablets were measured for drug content by Near IR spectroscopy (Bruker Optics Multipurpose Analyzer, Billerica, Massachusetts). Tablets spectra were collected in transmission mode over the range of 12500 to 5800 cm^{-1} with a resolution of 64 cm^{-1}. Each spectrum was the average of 256 scans. The background spectrum was obtained prior to taking transmission scans of tablets to assure the accuracy of the spectra. NIR spectra data were processed using the chemometric software Unscrambler v. 10.2 (Camo, Oslo,

Norway). The standard normal variate (SNV) method was used as a spectral pretreatment. The 2nd derivative spectra were obtained subsequently by using the Savitzky-Golay algorithm with an 11-point moving window and a 2nd order polynomial. As with the HPLC, a calibration model was required to predict the API content of the collected tablets from the continuous manufacturing line run. Calibration tablets were made spanning the content range (±) 20% around the nominal API value and subjected to NIR transmission with the same pretreatment. The same tablets used to build the NIR model were measured for their actual drug content using HPLC to assure the NIR tablets matched the predetermined weight percentage of API. A multivariate PLS calibration model was constructed using the NIR spectra and their reference drug content measured by the HPLC. The calibration model was used to predict the %API of the tablets manufactured in the continuous line. Table 4 lists the model parameters.

Table 4: PLS model parameters

Spectral range (cm^{-1})	Number of latent variables	RMSEP (%w/w)	Bias (%w/w)
9087-8740	2	0.6	-0.05

2.2.4.6 In-vitro dissolution testing

Drug release studies were performed using the USP paddle method at a rotational speed of 50 rpm in an Agilent 708-DS dissolution apparatus (Agilent Technologists, Santa Clara, CA). The dissolution media was composed of 900 ml phosphate buffer pH 5.8, and the temperature was maintained at 37 +- 0.5 °C. Six tablets were each placed in vessels in the dissolution apparatus and ejected into the dissolution vessels simultaneously. Aliquots of

the dissolution medium were pumped at 3 min time intervals using an Agilent 810 peristaltic pump. The medium was filtered using 35μm full flow filters prior to detection using a Cary 60 UV-Vis spectrophotometer (Agilent Technologies). A wavelength of 243 nm, the standard for acetaminophen, was used to analyze the samples. Absorbance values for each tablet were converted to the percent of drug released at each analysis time.

2.2.4.7 Ultrasonic measurements

Ultrasound is a mechanical wave within a range of wavelengths, below the human auditory range, that can propagate through a medium. Ultrasound transmission measurements through tablets were performed using ultrasound pulser/receiver unit (Panametrics, 5077PR), a pair of 13 mm diameter ultrasound transducers (Panametrics, V606-RB) with a frequency of 2.25 MHz, and digitizing oscilloscope (Tektronix TDS3052) (Figure 3). The sound wave TOF was determined from the transmitted ultrasound signal. The time between the transmitted pulse and the received pulse is considered the time of flight (TOF). The speed of sound (SOS) was calculated by dividing the measured tablet thickness by the TOF. Prior to tablet measurements, a set of steel and aluminum samples with known time of flight (TOF) were used for calibration of acoustic property measurement. They both showed a time delay of 1.1μs which indicated that the steel and aluminum standards had 1.1μs higher TOF than the expected values. This time was subsequently subtracted from the tablets TOF to calibrate the ultrasound system. For the tablet measurements, the tablet was placed between a pair of transducers, one generating the ultrasound pulse and the other receiving the transmitted ultrasound pulse. The contact between the transducers and the tablet was ensured by applying a constant force on the transducers. In this study, TOF was measured for 6 to 12 tablets in each experimental run, therefore, the number of

measurements varied in each experimental run. The variation was due to having initially multiple measurements in order to find a representative number of measurements. After calculating the standard deviation, it was concluded that six measurements were adequate. The same tablets were also measured for relative density and the destructive diametrical compression test.

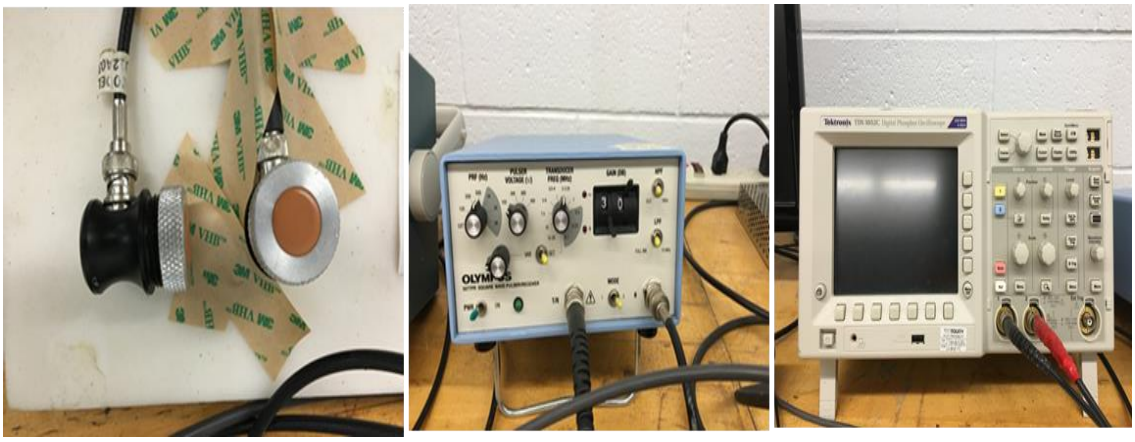

Figure 3: Schematic of the nondestructive ultrasonic experimental setup consisting of two transducers, pulser/receiver, and digitizing oscilloscope

2.3 Continuous hot melt extrusion (CHME)

The hot melt extrusion line consisted of two unit operations: a LIW feeder and a twin-screw extruder (Figure 4). The process was configured so that the mixture of the API and the polymer was gravity fed into the extruder (Thermo Scientific^{TM} Pharma 11). The outlet of the feeder was connected to a rubber flexible connection where the powders traveled downward towards the extruder inlet funnel at the furthest upstream port on the extruder. The HME process was carried out using two co-rotating screws that transported material inside a heated cylindrical barrel. After the extruded product exited the die in the form of continuous strand, it was manually pulled at a constant speed to achieve a uniform

thickness throughout the length of the extrudate. The extrudate was then cut into lengths of 20-30 cm, and were left to cool down at room temperature overnight.

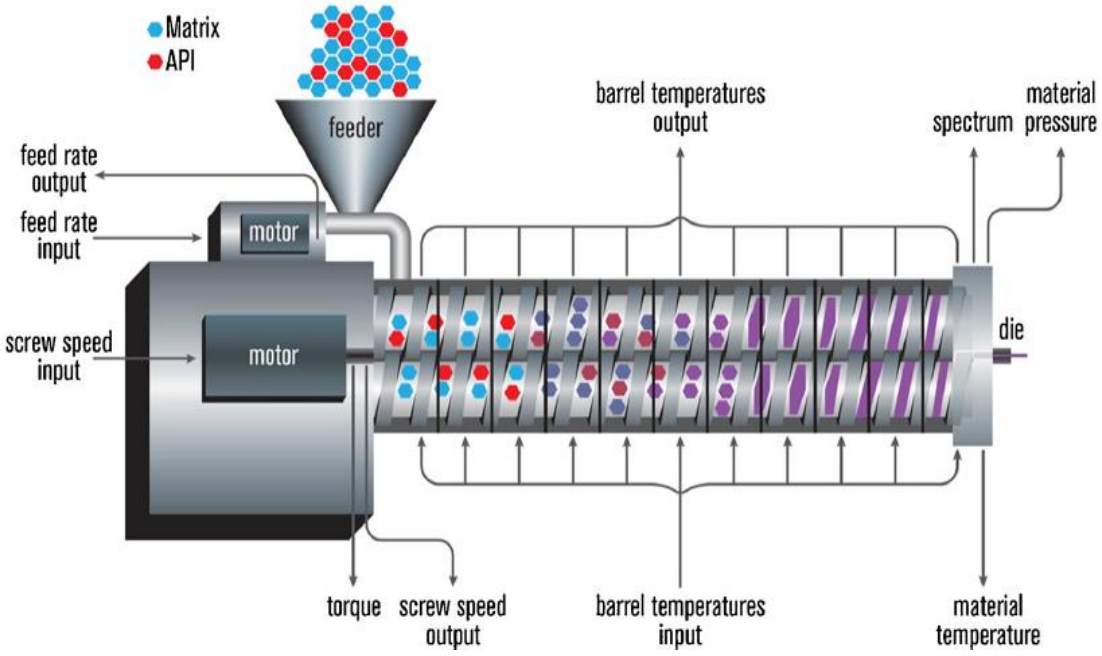

Figure 4: Schematic of Continuous Hot Melt Extrusion line. Adapted from [44]

2.3.1 Equipment

2.3.1.1 V-blender

Chlorpheniramine Maleate and PEO were weighed and pre-mixed in a 2-qt V-blender (The Patterson Kelley Co., East Stroudsburg, USA) prior to extrusion. The V-blender operated at 20 rpm for 30 minutes. Each formulation blend weighed 500 g.

2.3.1.2 Feeder

A Coperion K-Tron MT-12 loss-in-weight feeder was used to feed the pre-mixed materials into the hot melt extruder. The feeder was characterized offline and appropriate screws were identified, coarse concave, based on desired throughput of 0.4 Kg/hr.

2.3.1.3 Extruder

Hot melt extrusion was performed using a co-rotating twin-screw extruder (Pharma 11, Thermo Scientific™, Karlsruhe, Germany). Pharma 11 is a flexible machine which offers several options for customizing; the process of HME (Hot Melt Extrusion) or TSG (Twin Screw Granulation). In our experiments, the Pharma 11 was configured to work in the HME mode. The extruder specifications are listed in Table 5. The extruder consisted of two co-rotating 11 mm screws inside a cylindrical barrel. The barrel was composed of 8 segmentations (barrel zones) with 8 independently controlled heating zones; 7 internal zones and 1 external zone for the die. The barrel zones were heated individually with electric heaters, and the zones were set to the following temperatures; zone 1 (feeding zone) to 85 °C, zones 2 -7 to 125 °C, and zone 8 (die temperature) to 125 °C**.** Barrel length to diameter ratio (L/D) was 40:1, and the screw speed was 100 rpm. The throughput and the die diameter were 0.4 Kg/hr and 6 mm respectively. The extruder operation settings are listed in Table 6. Extrudate exiting the die can be seen in Figure 5.

Table 5: Specifications of Thermo Fischer Pharma 11 Extruder

Operating temperatures	10 - 280 °C
Pressure (max)	100 bar
Screw diameter	11 mm
Screw type	Co-rotating parallel twin-screw
Screw speed	Variable speed 10 – 1000 rpm
Throughput	20 g/h – 2.5 Kg/h
Torque (max)	6 Nm/shaft, 12 Nm both screws
Processing length	40:1 L/D ratio

Table 6: Hot Melt Extrusion processing parameters

Temp Zone 2-7 (°C)	125
Temp Zone 1 (°C)	80
Temp Die (°C)	125
Screw speed (RPM)	100
Gravimetric Feed Rate (kg/hr)	0.4
Screw Configuration	HME Standard Configuration
Die Diameter	6 mm

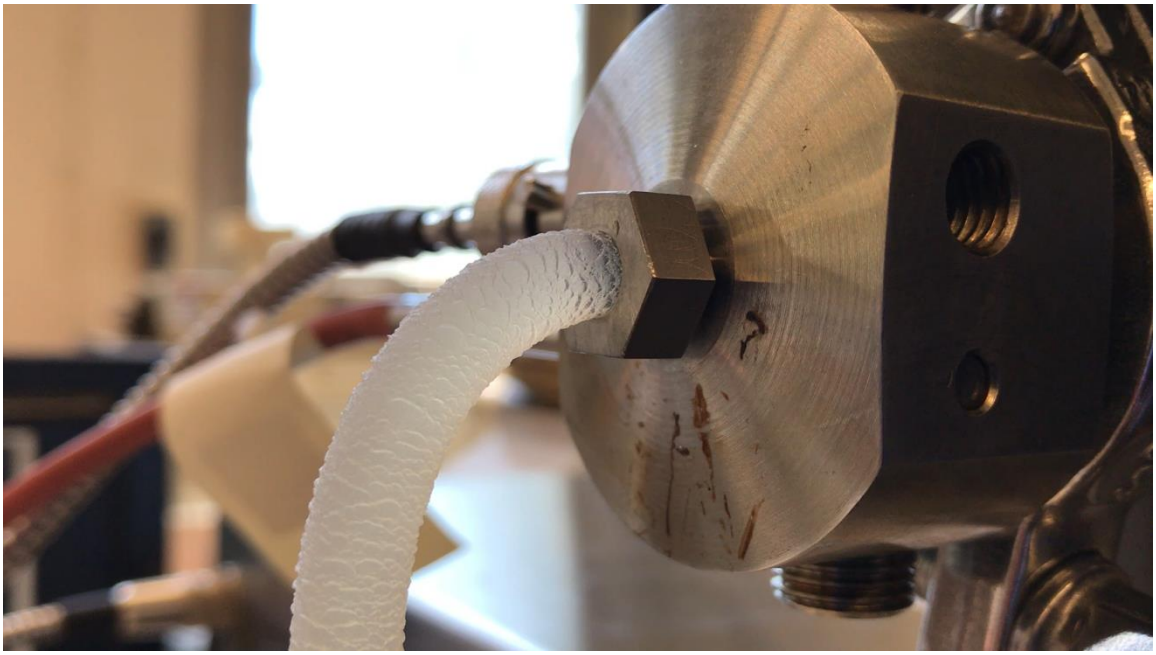

Figure 5: Extrudate exiting the 6 mm die

The standard twin-screw configuration for HME suggested by the manufacturer, Thermo Scientific, was used in the hot melt extrusion process. The screws consisted of conveying elements and mixing elements, and the screw configuration was designed to have two mixing zones separated by a section of conveying elements. Conveying elements were rounded channels angled to convey material downstream towards the die and had 1.0 L/D

ratio (See Figure 6). The mixing sections were created by combination of several single mixing elements of 0° and 90° (See Figures 7 and 8). The offset angle between neighbored elements determined the conveying and mixing properties. The elements were alternated with 0° and 90° to achieve 90°, 60°, and 30° offsets. In extreme 90° offset there was pure mixing and no conveying capabilities. And the 60° and 30° offsets provided both mixing and conveying. Screw configuration is shown in Figure 9.

Figure 6: Conveying element (Feed Screw) with 1.0 L/D

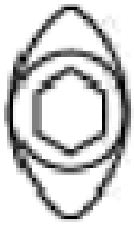

Figure 7: Mixing element 0° with 1/4 L/D

Figure 8: Mixing element 90° with 1/4 L/D

The rotation of the screws in the barrel created distributive and dispersive mixing regions. Distributive mixing provided rearranging the solid phase in the polymer melt in order to

improve the homogeneity of the melt [45]. This mixing mechanism can be characterized by the total strain the screw elements induce on the melt. Local variations in solid concentration can occur if the distributive mixing is not sufficient which would result in a non-homogeneous product. On the other hand, dispersive mixing provided by mixing elements subjected the melt to mechanical stress and broke down the solids particles into a finer state [46].

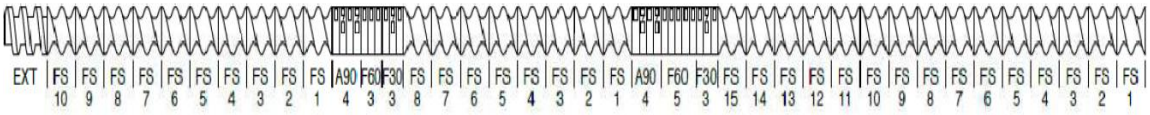

Figure 9: Screw design in the study (22 Kneading elements in each screw)

The feeder was filled with material and calibrated, and the barrel heaters were thermally stabilized. The extruder speed was decided based on prior studies on Pharma 11 extruder and was set to 100 rpm [47]. Next, the feeder was set to 0.1 Kg/hr to initiate the process. The feed rate was gradually increased and adjusted to increase and maintain the pressure and the torque close to and below the maximum at 100 bar and 12 Nm respectively. Steady conditions were reached when the feeder rate was at 0.4 Kg/hr. After enough samples were collected, the feeder was stopped, and the extruder continued to run until the screws pushed out all of the material left in the barrels. Once all the material was ejected, the screws were stopped from rotating, and the feeder hopper was vacuumed, cleaned, and calibrated for the next formulation. The process was repeated for all the formulations studied. The cooled extrudates were cut into portions of 200 mg and characterized for dissolution and viscosity. Extrudates from formulations 1 -10 are depicted in Figure 10 and 200 mg extrudate in Figure 11. The detailed formulations can be found in section 2.3.3

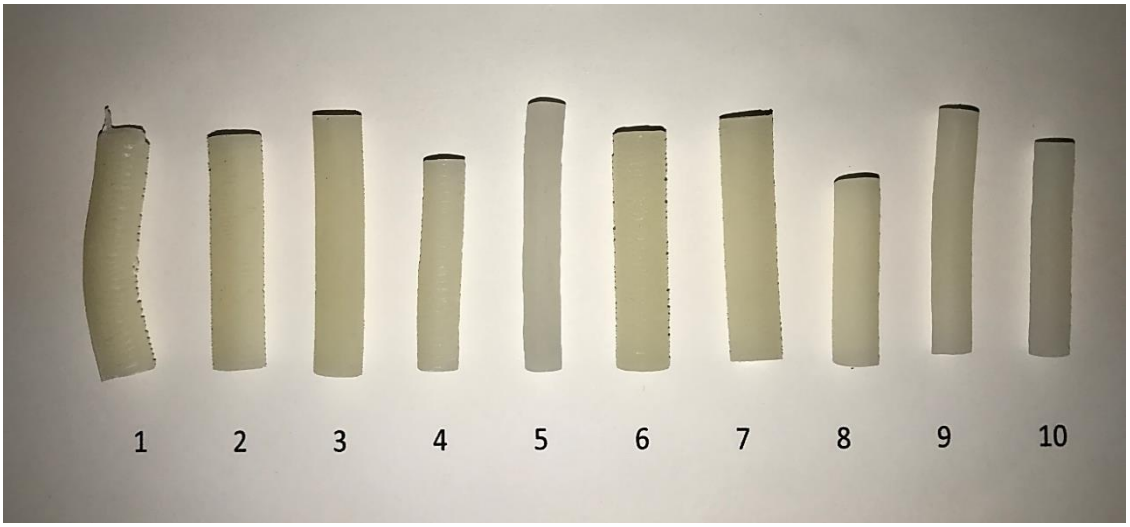

Figure 10: Extrudates – Formulations 1 – 10

Figure 11: Extrudate strand, extrudate cut into a 200 mg tablet

2.3.2 Materials

Chlorpheniramine Maleate was used as the model active pharmaceutical ingredient (API) and supplied by Spectrum. Polyethylene Oxide, manufactured by Dow Chemical Company under the trade name of POLYOX^{TM} Water Soluble Resins (WSR) and supplied by Colorcon, was used as a polymer carrier in the formulation. Polyethylene Oxides (PEOs) are high molecular weight hydrophilic (water-soluble) polymers which come in different grades. Formulations in our study were composed of three different grades of Polyethylene Oxide (PEO); WSR N-750 NF, WSR 301 NF, and WSR 303 NF with 0.3 million Da, 4 million Da, and 7 million Da molecular weight respectively. The physical properties of polymers depend heavily on their molecular weights, which vary according to the number of repeating monomer units in their molecular structure [48].

2.3.3 Experimental design & sampling

The experiments were designed so that each formulation had a specific weight-average molecular weight (Table 7). All formulations consisted of 6% API, and 94% polymer. Each of the formation had a different ratio of the polymers. Formulation 1 solely contained PEO 750, formulation 5 solely contained PEO 301, and formulation 10 solely contained PEO 303. Formulations 2-4 had various ratios of PEO 301 and PEO 750. Formulations 6-9 had various ratios of PEO 303 and PEO 750.

The experiments were performed over a three day period. The blends were prepared on the first day. Extrudates containing PEO 301 (Formulations 1 – 5) were manufactured on the second day and extrudates containing PEO 303 (Formulations 6 -10) on the third day. Each time the formulation was changed, the system required an interval until the system reached

a new steady state so that extrudate samples could be collected. The waiting interval was set at 3 minutes, and the extrudates collected during the waiting period were placed in waste. At each steady state experimental run, extrudates were collected for 15 - 20 minutes and left to cool down overnight.

Table 7: Formulations for extrusion by HME

Formulations	CPM (%)	PEO (303) 7M (%)	PEO (301) 4M (%)	PEO (750) 300K (%)	Average MW (Mw)
1	6	0	0	94	300K
2	6	0	7.5	86.5	600K
3	6	0	17.9	76.1	1M
4	6	0	43.2	50.8	2M
5	6	0	94	0	4M
6	6	4.2	0	89.77	600K
7	6	9.9	0	84.13	1M
8	6	23.9	0	70.1	2M
9	6	52	0	42	4M
10	6	94	0	0	7M

2.3.4 Characterization methods

2.3.4.1 Viscosity measurements by rheometer

Viscosity is the rheological property of a material which is defined as the study of the flow and deformation. It describes the interrelation between force, deformation and time [49]. We tested the rheological characteristics of the extrudates as a function of shear rate using

a Malvern Kinexus ultra+ rheometer with a torque range of 0.5nNm – 250mNm and a cup & bob geometric attachment (Figure 12). The properties were collected with a cylindrical bob diameter of 25 mm and a cup diameter of 27.5 mm. Dilute solutions of 2% were prepared by dissolving 2 grams of sample (200 mg) in 100 ml of water in a 250 ml flask. The solutions were stirred with a rectangular magnetic bar on a stirring hot plate at 25 °C for 3 days. The solutions were prepared for both pre-mixed blends and extrudates of each formulation. The goal was to compare the viscosity of the formulation before and after the hot melt extrusion process. A viscosity vs. shear rate test was run from 1 to 100 s^{-1} with a collection rate of 10 points over the range.

.

Figure 12: Malvern Kinexus ultra+ rotational rheometer, cup & Bob attachment

2.3.4.2 In-vitro dissolution testing

Drug release studies were performed using the USP basket method at a rotational speed of 100 rpm in an Agilent 708-DS dissolution apparatus (Agilent Technologists, Santa Clara, CA). The dissolution media was composed of 900 ml DI water, and the temperature was maintained at 37 ± 0.5 °C. Six tablets were each placed in individual baskets in the dissolution apparatus, and the baskets were immersed into the dissolution vessels simultaneously. Aliquots of the dissolution medium were pumped at 15 min time intervals using an Agilent 810 peristaltic pump. The medium was filtered using 35 μm full flow filters prior to detection using a UV spectrophotometer. A wavelength of 263 nm was used to analyze the samples using a Cary 60 UV-vis spectrophotometer (Agilent Technologies,). Absorbance values for each tablet were converted to the percent of drug released at each analysis time.

Chapter 3: Real-time prediction of tablet tensile strength by ultrasound in continuous manufacturing

3.1 Introduction

Conversion to continuous manufacturing can transform the drug manufacturing industry into a faster, better understood, and a better controlled process [10]. In batch manufacturing, the output material (tablets, capsules, etc.) are selectively tested to determine whether an entire batch has the expected quality, and the analysis of the selected batch will determine if the entire batch will have to be reprocessed or discarded. On the other hand, in continuous processes, the quality of output material can be tested by an active control strategy that adjusts the process parameters [50-52].

Therefore, an understanding of the process dynamics as impacted by the interaction of process parameters with material attributes is required. In order to operate at full efficiency, the continuous process requires some level of control, either open-loop or closed-loop [53]. Closed-loop control requires material controls, process monitoring, and detecting and handling deviation in real-time to be able to support the Real Time Release testing (RTRt) [11]. RTRt consists of a combination of process controls which may utilize process analytical technology (PAT). Analytical data is produced from instruments such as near infrared spectroscopy (NIR), Raman spectroscopy, terahertz pulsed imaging, and acoustic techniques as well as from soft sensors that predict hard-to-measure material attributes based on other attributes or measured process variables [54-57]. These techniques are non-destructive, i.e., they have the benefit of measuring material attributes without destroying the samples. This makes it possible for further characterization of the same sample by

multiple methods enabling the correlation of multiple critical quality attributes (CQAs) for a better understanding of the process.

Tablet hardness, or more correctly, tensile strength, is an important physical-mechanical property that is known to affect the disintegration and dissolution of the drug in the body. Therefore, it has become common practice to evaluate tablet tensile strength at-line. This critical quality attribute is currently evaluated by a diametrical compression test which is a destructive method. As the pharmaceutical industry continues to shift towards continuous processing it would be extremely beneficial to be able to evaluate tensile strength and tablet hardness in-line and non-destructively so that the measurement can be used to control the process. Therefore, there is a growing interest in the development of non-destructive predictive tools for tablet tensile strength towards RTRt. Acoustic measurements which are effective, non-destructive, and only take a few microseconds, have been identified as a good option for RTRt [12].

Ultrasound has been studied extensively and continues to be explored for new applications. Hakulinen *et al*. studied tablets with different solid fraction and particle size using ultrasound [13]. They showed that the velocity of ultrasound was negatively correlated with tablet porosity. Ultrasound was used by Akseli *et al.* in the characterization of the physical-mechanical attributes such as the Young's moduli of coated tablets [14]. Liu and Cetinkaya demonstrated the use of an ultrasonic technique to measure the thickness and mechanical properties of controlled release tablets [15]. The authors suggested that further advancement in the technique could allow ultrasonic testing to be used in real-time online monitoring of tablet quality through integration with the die-punch set. Stephens *et al.* investigated ultrasonic testing for real-time monitoring of physical-mechanical behavior of

tablets during compression [16]. The goal of the Stephens study was to demonstrate the feasibility of ultrasonic non-destructive characterization of the geometric/mechanical properties and integrity of tablets during compaction. In a subsequent study, the use of a wireless transceiver for analyzing the tablets' geometric and microstructural properties in real-time by ultrasound was reported [17]. Akseli *et al.* utilized an ultrasonic testing technique for the prediction of tablets capping and the quantitative correlation of capping with the viscoelastic characteristics of tablets measured axially and radially [18]. The use of ultrasound coupled with air (known as the air-coupled acoustic technique) has also been used for tablet characterization [14, 18, 58-60]. This technique is similar to acoustic emission except that it involves the use of an air-coupled transducer. Akseli *et al.* used this technique to analyze the physical-mechanical properties of pharmaceutical tablets.

Razavi *et al.* studied the characterization of pharmaceutical tablets and investigated the effect of compaction force and level of shear strain on tablets strength using ultrasound [19]. They concluded that both relative density and Young's modulus were required to predict tablet tensile strength. In later studies, the effect of particle size distribution, lubricant concentration, and mixing time on the tensile strength and acoustic properties of tablets using two grades of lactose, monohydrate and spray-dried, were investigated [20]. Xu *et al.* studied the relationship between the acoustically extracted mechanical properties of pharmaceutical compacts made from different ratios of spray-dried lactose and microcrystalline cellulose to porosity and tensile strength [61].

Advantages of ultrasonic techniques are simplicity and speed in the evaluation of tablet properties. In addition, they do not need a calibration model to predict the TOF of the tablets. In the present study, we investigated the acoustic properties of tablets manufactured

in a continuous process based on an experimental design. The compaction force has been studied as a process variable by previous researchers. However, for the first time, we have demonstrated that the acoustic properties of tablets could be correlated with both the formulation and process variables.

3.2 Materials and methods

3.2.1 Materials

The materials are described in chapter 2, section 2.2.2.

3.2.2 Methods

3.2.2.1 Production of tablets by continuous direct compression

The production method is described in chapter 2, section 2.2.

3.2.2.2 Experimental design

The experimental design is described in chapter 2, section 2.2.3. It should be noted that API weight percent (%API) is the nominal value of API used in the tablets. The drug content (%w/w) that is used throughout this dissertation refers to the amount of drug predicted by NIR.

3.2.3 Tablet characterization

3.2.3.1 Ultrasonic measurements

The ultrasonic measurement technique is described in chapter 2, section 2.2.4.7.

3.2.3.2 Relative density

Each tablet was accurately weighed, and their diameter and thickness was measured with a digital caliper (Marathon CO030150). Relative density of the tablets was calculated using the equation

$$\rho_{R=}\frac{\rho_b}{\rho_t}$$

where ρ_b is the bulk density and ρ_t is the true density. The bulk density of tablets was calculated by dividing the tablet weight by its volume. The true density of the individual components are estimated as per the supplier MSDS (lactose 1.54g/cc, semi-fine acetaminophen 1.29 g/cc, magnesium stearate 1.03g/cc).

3.2.3.3 Tensile strength

The hardness of the same tablets was measured with destructive diametrical crushing test apparatus (Dr. Schleuniger, Pharmatron 6D). The tablets were diametrically broken into two pieces, and the hardness was recorded for each tablet. With the acquired data, the tensile strength (σ) was calculated according to the equation described by Fell and Newton [42]

$$\sigma = \frac{2F}{\pi dt}$$

where σ is the tensile strength, F is the applied force, t the tablet thickness, and d is the tablet diameter.

3.2.3.4 Tablet content uniformity

Tablet content uniformity measurement technique is described in chapter 2, section 2.2.4.5.

3.3 Results & discussion

3.3.1 Effects of process parameters on the speed of sound

In this work, only %API was changed as part of the formulation, and the other constituents remained consistent. Therefore, API concentration was considered the only material attribute. The effects of processing variables on the tablet speed of sound (SOS) were examined. Since the weight and volume of the tablet affect the properties of the tablet, relative density was considered as the processing parameter in place of compaction force. Figure 14 shows the SOS of the tablets as a function of relative density. The plot was marked based on different levels of compaction force. As expected, based on previous studies [13, 21], SOS increased with compaction force (Figure 14). Hakulinen *et al.* found that the sound waves will propagate much faster through the tablets as tablets get harder and denser. The speed of sound waves in a medium depends on how quickly the energy of the vibration could be transferred across the medium. Therefore, the speed will vary depending on the state of the tablet. Dependence of ultrasound velocity on material density has also been observed for tablets consisting of starch acetate powders at different particle sizes [13]. An increase in tablet density led to an increase in its elastic modulus [21], and therefore, an increase in the sound velocity.

Figure 15 shows that SOS was sensitive to the amount of acetaminophen in the tablet. The plot was marked based on different levels of drug content. Tablets with the lowest amount

of drug showed lower SOS. That means that the sound waves were travelling more slowly in the tablets with low drug content. According to the Newton-Laplace equation

$$c = \sqrt{\frac{E}{\rho}}$$

where c is the speed of sound, E is the elastic modulus, and ρ is the density of the medium. The fastest sound wave will be in a material that is rigid (hard) and that has a large elastic modulus and/or low density. This explains why tablets with very low drug content may have a less rigid structure. Leskinen *et al.* studied the compaction dynamics of tablets made with acetaminophen using a tableting press that was implemented with ultrasound transducers inside the punches [12]. They monitored the speed of sound as a function of time during the tablet compression process for binary blended tablets with 0%, 5%, and 10% acetaminophen mixed with microcrystalline cellulose (MCC). They observed that the speed of sound decreased as the percentage of acetaminophen increased. Even though their results contradict the results observed in this study, it is worthwhile to mention that the tablets in this study had lactose as the main excipient and also magnesium stearate as a lubricant, in addition to acetaminophen. Evidently, the addition of these two excipients has changed the elastic properties of the tablets and subsequently their speed of sound. Undoubtedly, the sensitivity of speed of sound to acetaminophen particles cannot be ignored in either study and should be further investigated. More extensive research would be required to clearly demonstrate the effect of drug concentration on the acoustic properties of tablets.

Response surface regression was used to determine the effect of the processing variables, %API, blender speed, feed frame speed, and relative density, on the acoustic properties of

the tablets. Statistical analysis was performed using Minitab 18 confirmed that relative density highly affected the ultrasound velocity of the tablets. The ANOVA results in Table 9 indicate that the linear and quadratic terms of the relative density were both significant ($p<0.05$). A p-value of 0.05 or less typically represents a significant term. All the non-significant terms with p-values of 0.6 and larger were removed from the model, of which, those terms included %API, feed frame speed, blender speed, the interaction terms, and the quadratic terms of feed frame and blender speed.

It is well known that feed frames and blenders impart shear to the powder blend and affect the mechanical properties of the tablet [62]. The feed frame is a device inside the tablet press that drives the powders into the compression dies, and it can affect the flow properties of the blend and subsequently the mechanical properties of the tablets. It is well known that the speed of the paddles in the feed frame can change the properties of the blend such as particle size, density, and cohesion [63]. Additionally, the shear can change the history of the applied stress [64]. Hypothetically, similar shearing effects can occur within the continuous blenders that could cause shearing in the powder blend which causes over-lubrication of the powder blend by smearing the particles with MgSt. The faster the paddles in the feed frame run, the more energy can be imparted into the system increasing the shear rate and subsequently increasing the strain. Similarly, the total amount of strain generated by a continuous blender depends on the number of blender blade passes [65]. The blend strain consequently affects the degree of MgSt smearing on API particles [66]. In our study, the feed frame and the blender speed could operate at a maximum speed of 100 rpm and 900 rpm respectively. However, since these two parameters were not statistically significant, it can be concluded that within the range studied, the shear effects were not

significant enough to change the internal particle structure of the powder bed before it was compressed into a tablet. While it was not a significant effect in this study, it warrants the mention that the continuous line was operated at a low range of blender speed and feed-frame speed, and if higher shearing rates or different formulations more sensitive to shear were to be studied, the shear effects could alter the bulk properties of the blend and representative tablets.

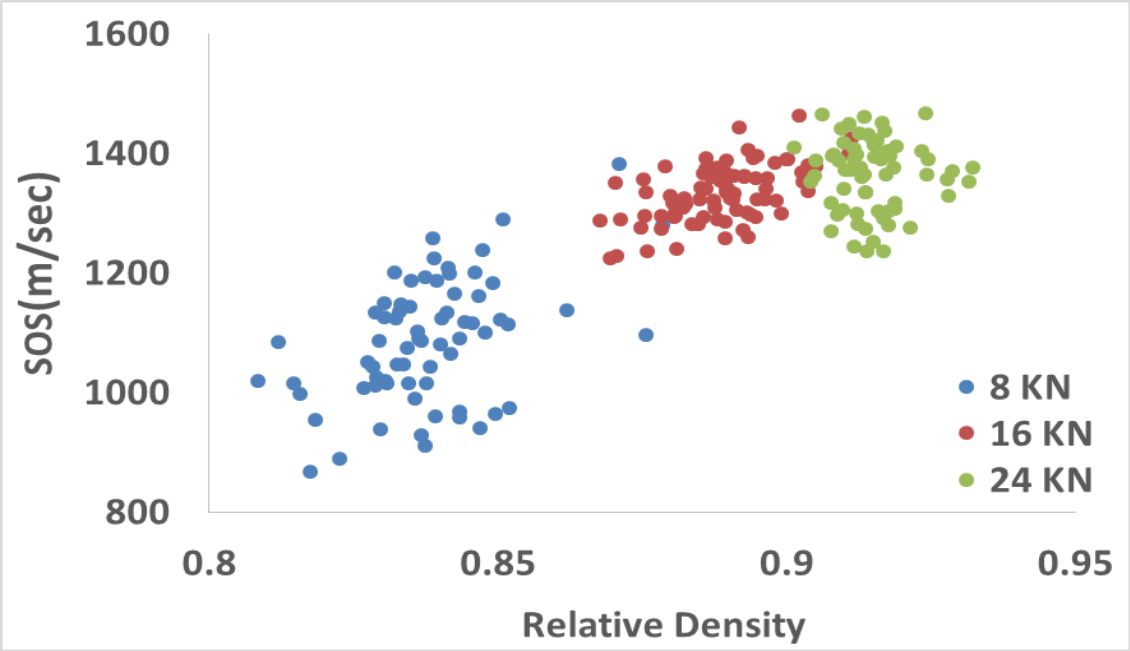

Figure 14: Speed of sound (SOS) as a function of relative density marked based on the level of compaction

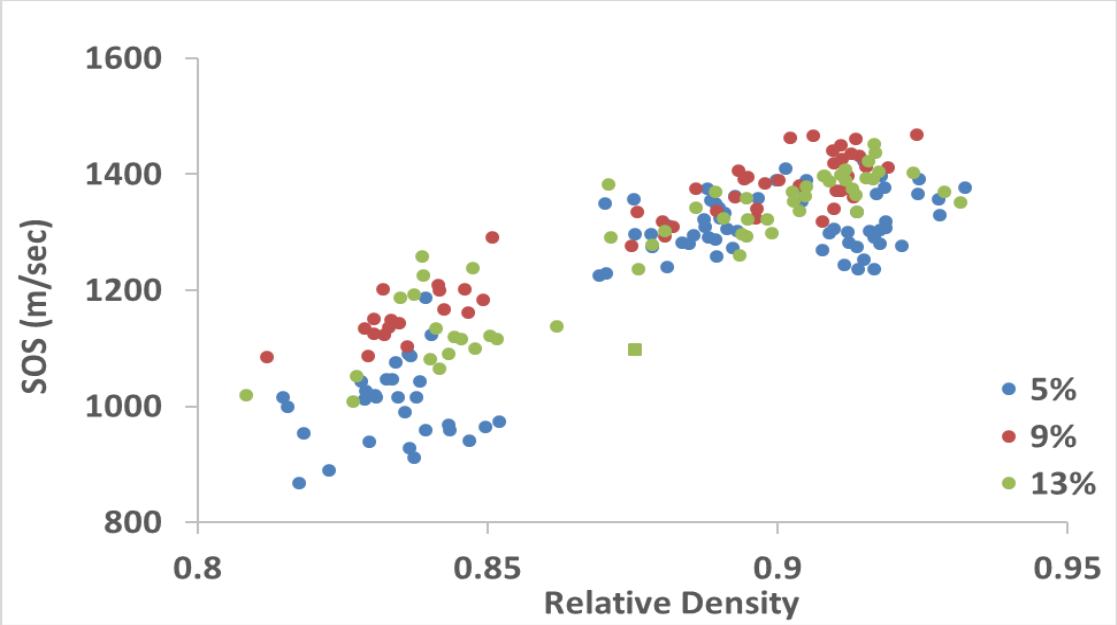

Figure 15: Speed of sound (SOS) as a function of relative density marked based on the level of drug

Table 9: Response surface regression for speed of sound (SOS)

Estimated regression coefficients for speed of sound (SOS)

Term	Coef	SE Coef	T-Value	P-Value
constant	1305.6	16.8	77.52	0
%drug	25.7	16.1	1.6	0.122
relative density	157.8	13.1	12.05	0
%drug*%drug	-65.9	32	-2.06	0.05
relative density*relative density	-69.4	25.8	-2.69	0.012

The analysis was done using coded units.

Model Summary	S	R_{sq}	R_{sq}(adj)	R_{sq}(pred)
	46.7579	88.21%	86.32%	82.07%

3.3.2 Effects of processing parameters on the tensile strength

In Figure 16, the measured tensile strength of tablets is presented as a function of relative density, while the tablets are identified based on their compaction force. Tensile strength increases exponentially as the relative density of the tablets increases. The exponential increase of tensile strength versus relative density has been studied in the past [67, 68]. Figure 17 shows the same data as Figure 16, however, the tablets were identified based on their drug content. Even though the effect of %API was significant based on statistical analysis in Table 5, but Figure 17 indicates that the trend with respect to the amount of API is not as apparent. ANOVA results also indicated that %drug and relative density both had a significant effect on tensile strength, but the interaction term between %drug and relative density was not significant and was removed from the model.

The ANOVA results in Table 10 indicate that the tensile strength of the tablets is negatively correlated with the %API. This suggests that tablets with a higher amount of acetaminophen had lower tensile strength, and therefore, were softer. This can be explained by the extremely brittle nature and highly elastic recovery of acetaminophen particles [69, 70]. It is suggested that the tableting materials that have poor compression properties and deform with high elastic recovery produce tablets with weaker bonding that can result in lower tensile strength.

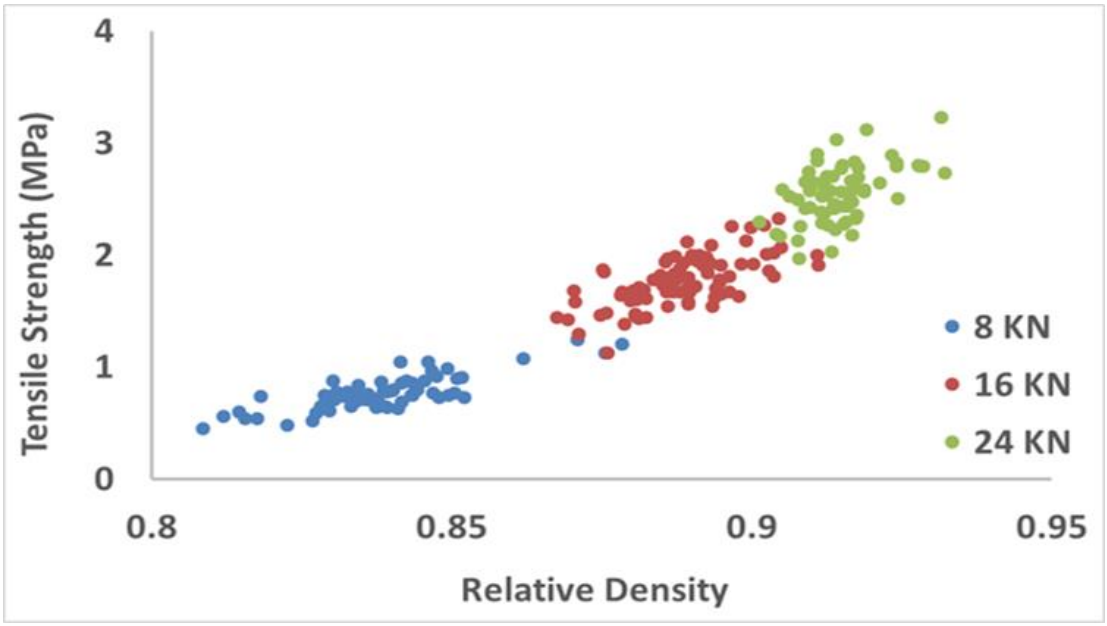

Figure 16: Tensile strength as a function of relative density marked based on the level of compaction force

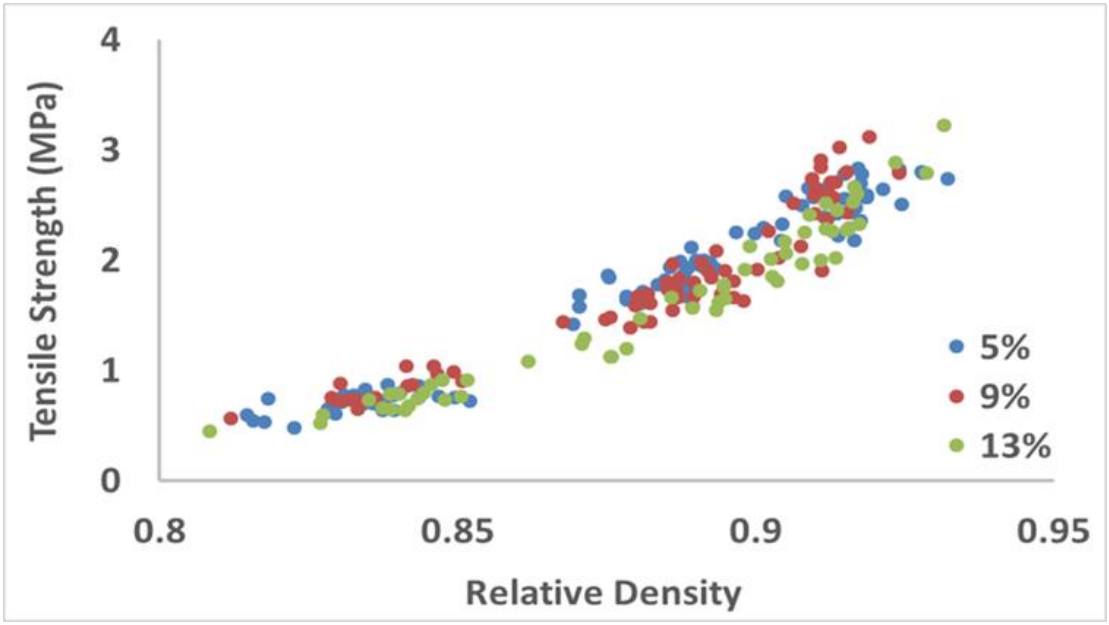

Figure 17: Tensile strength as a function of relative density marked based on the level of drug content

Table 10: Response surface regression for tensile strength (TS)

Estimated regression coefficients for tensile strength (TS)

Term	Coef	SE Coef	T-Value	P-Value
constant	1.465	0.0475	30.87	0
%drug	-0.1188	0.0453	-2.62	0.015
relative density	0.9948	0.0369	26.95	0
%drug*%drug	-0.1528	0.0903	-1.69	0.103
relative density*relative density	0.2622	0.0727	3.61	0.001

The analysis was done using coded units.

Model Summary	S	R_{sq}	R_{sq}(adj)	R_{sq}(pred)
	0.131774	96.98%	96.49%	95.94%

3.3.3 Tensile strength correlation/prediction

According to previous studies, tablets tensile strength depends not only on the density of the tablets but also on the shear strain. Pawar *et al.* studied the tensile strength of tablets manufactured under different levels of compaction force and shear strain [71]. The authors concluded that relative density alone was not sufficient to predict tablet tensile strength and shear-strain should be an additional predictor. Razavi *et al.* studied tablets that were compacted and sheared at different levels [19]. The authors measured the level of shear by ultrasound and concluded that Young's modulus (an indicator of shear-strain) was

necessary for predicting tablets tensile strength in addition to relative density. In this study, the aim was to correlate the tensile strength of tablets to their relative density based on the speed of sound (a metric for shear strain).

Figure 18 shows a three-dimensional response surface plot for the tensile strength of tablets in terms of relative density and speed of sound. The key parameters that had the greatest influence on the tensile strength were studied by statistical analysis. ANOVA results in Table 11 indicate that the relative density and speed of sound both have a significant effect on tensile strength ($p \leq 0.05$). The fitted model equation has an $R^2_{adjusted}$ of 97.35%. The residuals were normally distributed, as shown in Figure 19. The predicting power of the model was tested by a set of tablets that were analyzed as part of the design of experiment (DOE), but their values were not incorporated into the model. The predicted versus experimental values of the tensile strength of the tablets are depicted in Figure 20. The predicted values were in good agreement with the experimental values with an R^2 value of 0.96. As shown in Table 11, it is evident that the magnitude of the effect of the speed of sound was very small. This can be explained by the minimum strain experienced by the tablets manufactured in the continuous line.

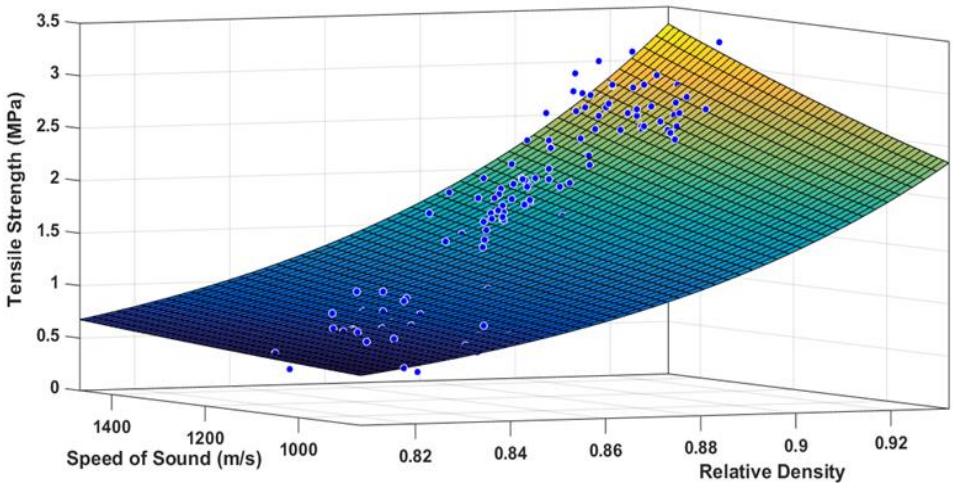

Figure 18: Tensile strength as a function of relative density and speed of sound (SOS)

Table 11: Response surface regression for transformed tensile strength ln (TS)

Estimated regression coefficients for tansformed tensile strength (lnTS)

Term	Coef	SE Coef	T-Value	P-Value
Constant	0.2745	0.0217	12.65	0
relative density	0.579	0.0466	12.43	0
SOS	0.1724	0.0639	2.7	0.012

The analysis was done using coded units.

Model Summary	S	R_{sq}	R_{sq}(adj)	R_{sq}(pred)
	0.0779253	97.54%	97.35%	97.11%

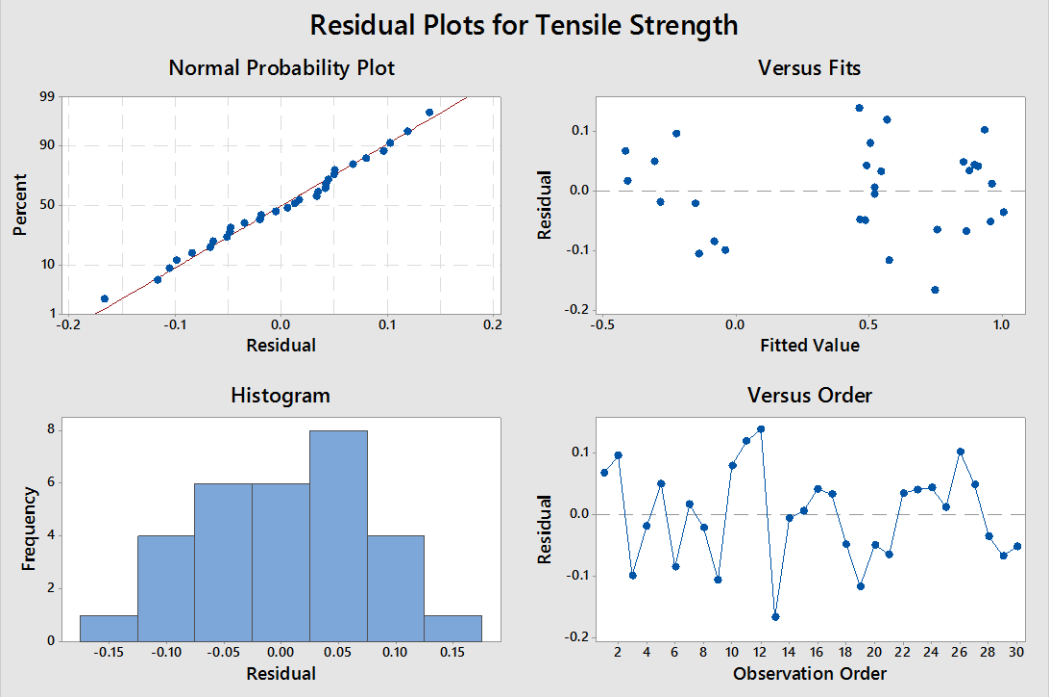

Figure 19: Residual plots for tensile strength

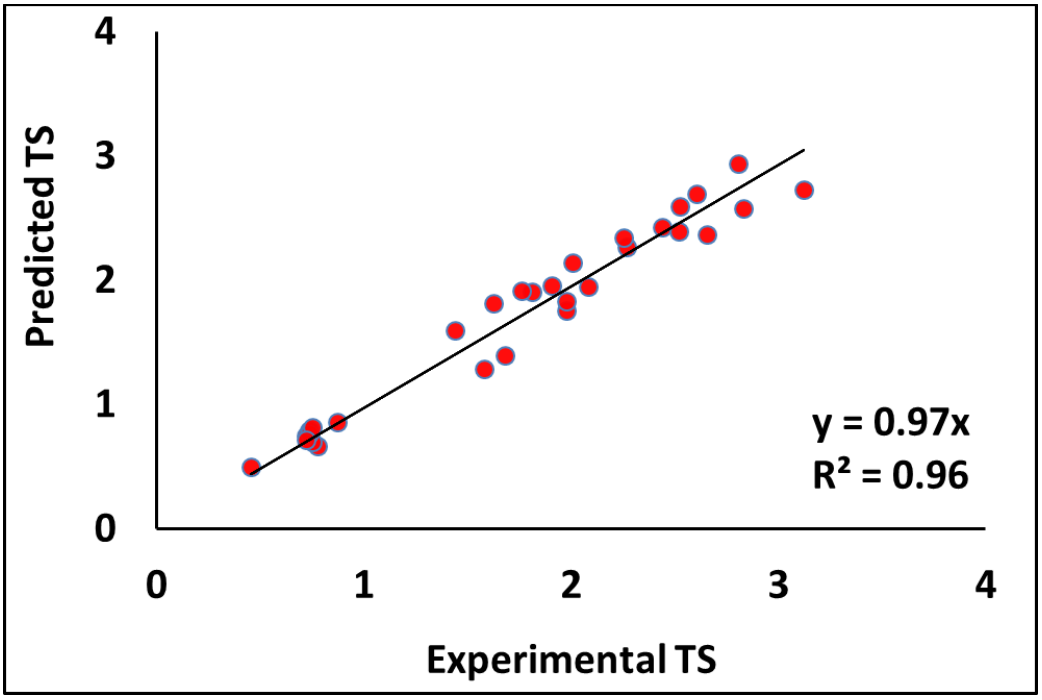

Figure 20: Linear regression of experimental vs. predicted value of tensile strength

The correlation between tensile strength and the processing variables, without the use of ultrasound, was also explored. The analysis is shown in Table 12. It was determined that the effect of relative density and %drug content was significant with an $R^2_{adjusted}$ of 96.49%. The validity of the correlation was further tested using the same tablets (as explained above). The predicted values were in good agreement with the experimental values with an R^2 value of 0.88 (Figure 21). It should again be noted that the results were in good agreement only because the tablets were minimally strained

Table 12: Response surface regression for tensile strength (TS)

Estimated regression coefficients for tensile strength (TS)

Term	Coef	SE Coef	T-Value	P-Value
Constant	1.465	0.0475	30.87	0
%drug	-0.1188	0.0453	-2.62	0.015
relative density	0.9948	0.0369	26.95	0
%drug*%drug	-0.1528	0.0903	-1.69	0.103
relative density*relative density	0.2622	0.0727	3.61	0.001

The analysis was done using coded units.

Model Summary	S	R-sq	R-sq(adj)	R-sq(pred)
	0.131774	96.98%	96.49%	95.94%

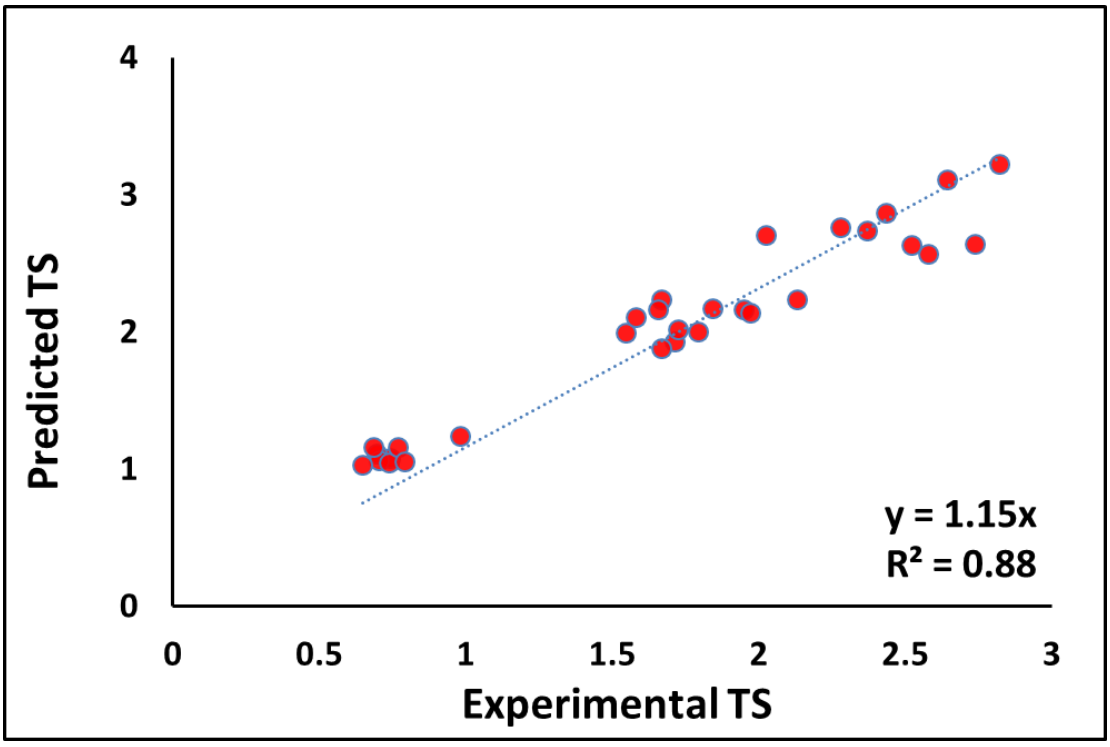

Figure 21: Linear regression of experimental vs. predicted value of tensile strength

3.4 Conclusion

The present study provides a novel approach to the implementation of real-time release testing to predict the tensile strength of tablets in a continuous manufacturing line. This was accomplished by characterizing tablets at line using ultrasound and diametrical compression test while correlating the tensile strength of the tablets to the relative density as well as to the speed of sound. A quality-by-design approach was used to understand the impact of various process changes on the tensile strength of the tablets, and a multilinear regression was used predict the tensile strength of the tablets in a nondestructive way. The validity of the correlation was tested by a set of tablets not incorporated in the model. There was a strong agreement between the predicted and experimental values.

This methodology for predicting the critical quality attributes (CQA) of the tablets will enable RTRt in continuous manufacturing. RTRt enables the generation of an enormous amount of data while the manufacturing process is taking place and can subsequently improve process control, unlike the traditional method of release testing conducted on only a few samples. The real-time analysis of data on the continuously manufactured tablets enables closed-loop control strategies to ensure that the tablets have the intended quality before being released to the market. This will not only enable rapid techniques in continuous assessment of tablets, but will also be economically beneficial in continuous manufacturing.

As the pharmaceutical industry is experiencing significant changes and continuous manufacturing processes are being implemented, there are a lot of benefits to be gained from RTRt applications. Despite the potential gains, the pharmaceutical industry is still trying to work out the practicalities of implementing the approach. The ultimate aim of a tablet manufacturing process that is implemented with RTRt is to compress powder into a tablet and ensure that the tablet has the desired hardness. The results of our study and using techniques such as ultrasound can help in the development of reliable non-destructive methods for hardness. They can provide a pathway for RTRt and the potential reduction in manufacturing costs associated with large waiting-for-release inventories and failed batches. Therefore, using ultrasound as a non-destructive tool has both scientific and economic impact. And it is a critical step toward improving quality and control of pharmaceutical products.

Chapter 4: An approach to predictive dissolution modelling in continuous manufacturing of solid dosage forms

4.1 Introduction

As stated in the FDA guidance, drug in-vitro release profile is a quality attribute that helps to assess batch-to-batch consistency and to predict in-vivo drug release profiles [72-74]. It is a graphical representation of complete release of drug from a dosage form in an appropriately selected dissolution medium with respect to time. Hence, it is imperative to evaluate tablet in-vitro dissolution during the lifecycle of a drug product. Currently, the only method of dissolution testing is the offline laboratory-based method of dissolving samples in agitated liquid baths which is destructive and no longer available for further characterization. Currently, the only method widely used in dissolution testing is the lengthy procedure of dissolving samples in agitated liquid baths which is time-consuming, expensive, and generates substantial waste. As the pharmaceutical industry embraces continuous manufacturing, tablet critical quality attributes such as dissolution profile needs to be controlled in-line and non-destructively. Therefore, development of non-destructive predictive methods for tablet dissolution testing towards RTRt is growing, and predictive dissolution models will enable rapid techniques in continuous assessment of tablets ensuring the desired quality attributes.

There have been many studies on understanding the parameters that affect and predict dissolution profiles by multivariate approaches. Mercuri *et al.* studied the effects of dissolution variables such as dissolution apparatus [USP1 apparatus (basket) and USP2 apparatus (paddle)], rotational speed of the basket/or paddle, the operator conditions (dissolution apparatus brand and operator), the volume, the pH, and the ethanol content of

the dissolution medium. They used multilinear regression to correlate percent dissolution at each time point to the test parameters. They were able to optimize the dissolution setup to predict an *in-vitro/in-vivo* correlations [25]. Huang *et al.* conducted multivariate analysis to understand the relationship between the variables from an experimental design to dissolution. They used PLS models to correlate the variables to the percent dissolution at different time points [26]. Kaul *et al*. used multivariate data analysis to investigate the role of poloxamer in the dissolution of immediate-release tablets [27]. Andersson *et al*. utilized multivariate methods in a screening design to obtain a predictive model to optimize tablets CQAs with the desired strength and a fast drug release profile [28]. Ring *et al*. [29] used statistical methods to understand the relationship between high shear wet granulation processing parameters and the granule properties with the dissolution of modified release dosage forms.

Sustained-release dosage forms are dosage forms designed to release a drug at a predetermined rate in order to maintain a constant drug concentration for a specific period of time with minimum side effects. In this study, the dissolution profiles of acetaminophen sustained released tablets based on an experimental design will be analyzed using a multivariate analysis method. MANOVA (multivariate analysis of variance) will be used to compare the dissolution profiles of tablets manufactured based on an experimental design in a direct compression continuous manufacturing process and understand the impact of the processing parameters on the tablet dissolution profiles. Next, multilinear regression will be utilized to correlate the processing parameters to the tablet dissolution model parameters and predict the dissolution profiles for the validation set of tablets. This method can be used in addition to the NIR in-line as a redundant measurement technique

when there is no NIR used due to fouling and lack of maintenance and updated calibration. Hence, the methodology of dissolution prediction by statistical analysis will be extremely useful

4.2 Materials and methods

4.2.1 Materials

The materials are described in chapter 2, section 2.2.2.

4.2.2 Methods

4.2.3 Continuous manufacturing of tablets by direct compression

The production method is described in chapter 2, section 2.2.

4.2.4 General strategy for predicting dissolution profiles

In continuous processes, we have the opportunity to design the appropriate controls into the system, rather than relying mostly on testing materials at the end. However, there are some aspects to consider when establishing a control strategy. One is having a state of control that will provide assurance that the final product is consistently meeting the desired quality. There may be situations such as a sudden or uncontrolled change in a process variable where it is still crucial that the product is homogeneous and of acceptable quality. To establish the control strategy, we need to select the appropriate process attributes or ranges or use a multivariate process control approach. Therefore, we will present the strategy used to predict target tablets dissolution profiles as illustrated in Figure 22. The tablets were manufactured based on an experimental design, dissolved based on a

dissolution method, and dissolution profiles were acquired. Multivariate analysis of variance (MANOVA) was used to identify the critical process parameters (CPP) and their effects on dissolution profiles. The dissolution curves were fitted to Weibull model, and model coefficients, α and β, were obtained. Then the coefficients, α and β, were correlated with the process variables to create two multilinear equations; one correlating α and another one correlating β with the process parameters. These two equations were used for the prediction of the model parameters for the target tablets which were subsequently plugged into the Weibull model. The Weibull model was solved for the % drug released of the target tablets at all the sampling times. The dissolution profiles of the target tablets were acquired.

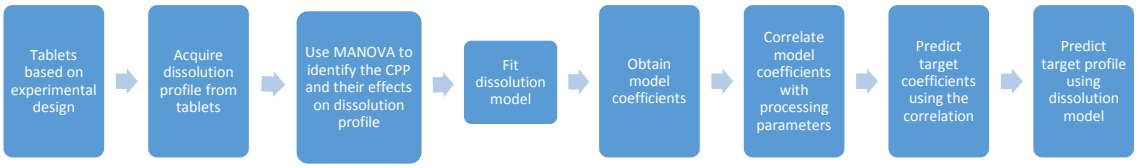

Figure 22: Methodology for predicting dissolution profiles

4.2.5 Experimental Design

The experimental design is described in chapter 2, section 2.2.3. It should be noted that API weight percent (%API) is the nominal value of API used in the tablets. The drug content (%w/w) that is used throughout this dissertation refers to the amount of drug predicted by NIR at-line.

4.2.6 In-vitro dissolution testing

Dissolution testing method is described in chapter 2, section 2.2.4.6.

4.2.7 Tablet content uniformity

Tablet content uniformity measurement technique is described in chapter 2, section 2.2.4.5.

4.3 Results & discussion

4.3.1 Effects of processing parameters on dissolution profiles

The dissolution profiles of all the tablets are shown in Figure 23. Each data point represents a mean of six measurements for each texperimental run. It is apparent that some of the profiles are different based on the process. The effect of compaction force, %API, and feed frame speed can be seen in Figures 24, 25, and 26 respectively. However, a thorough understanding of the different factors affecting the dissolution release rates requires analyzing the data by multivariate analysis of variance (MANOVA). MANOVA has been used in many studies to compare dissolution profiles [75] [30]. Repeated measures of MANOVA were used in this study, mainly because there were several correlated dependent variables (percent released at different time points).

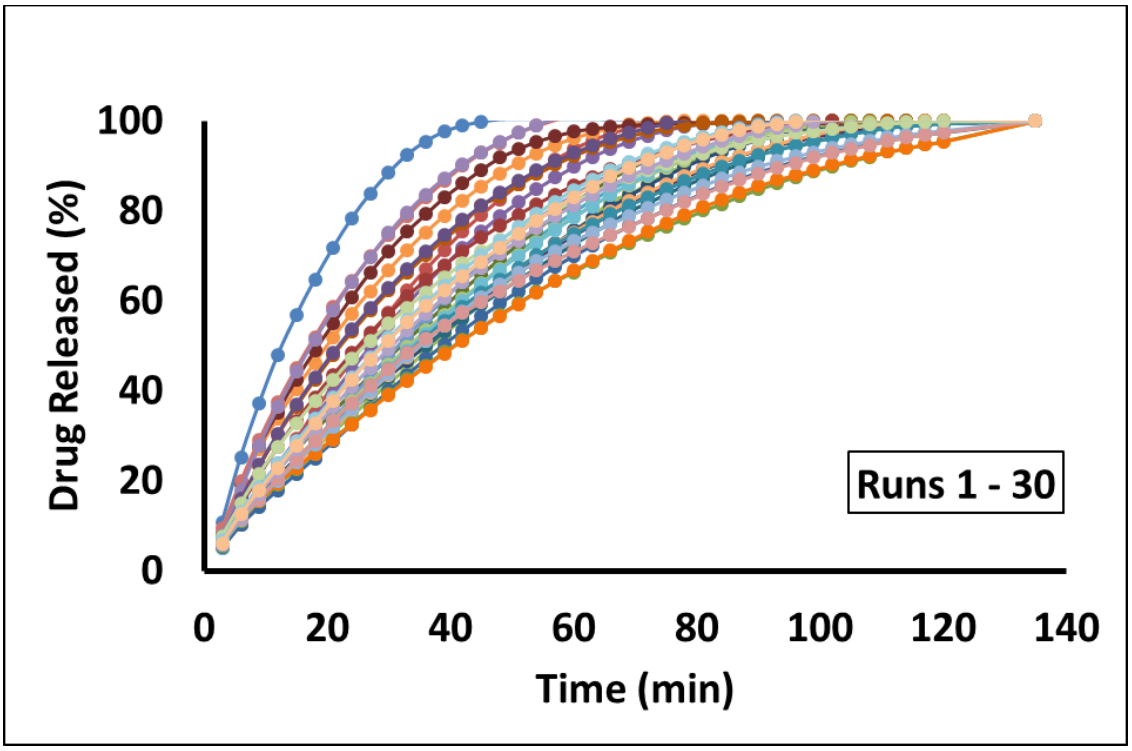

Figure 23: Mean (n=6) dissolution profiles of the tabets from 30 experimental runs

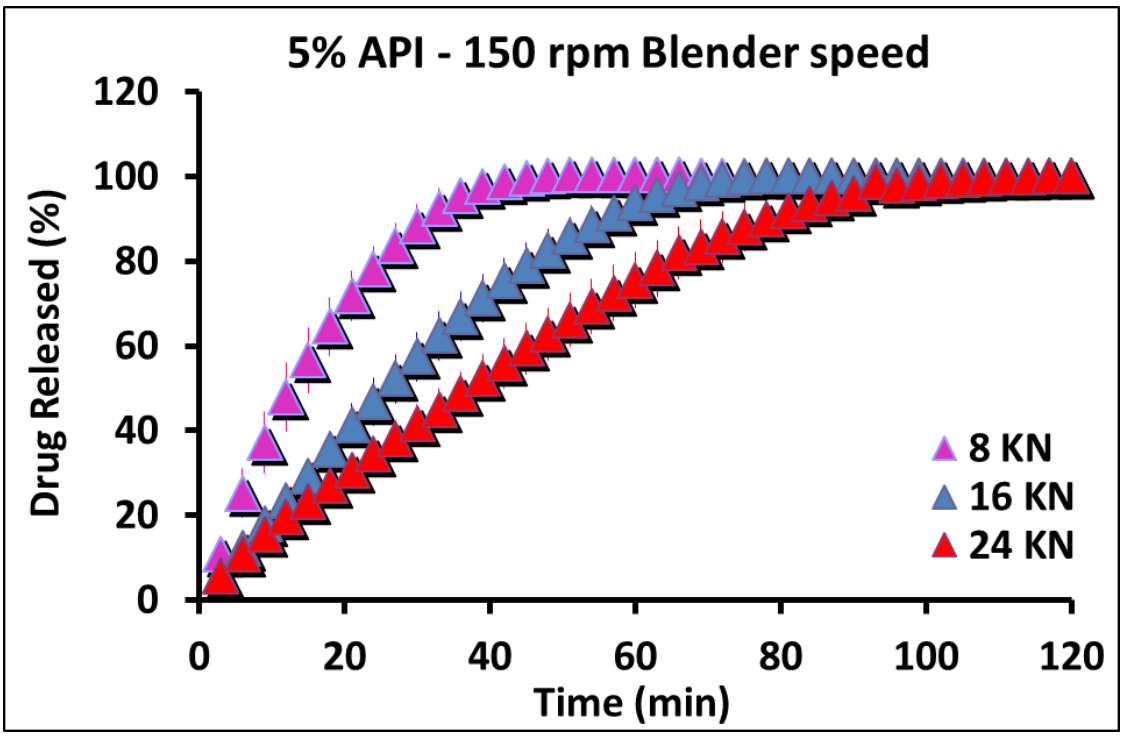

Figure 24: Mean (n=6) dissolution profiles of the tabets compacted at 8 KN (run 1), 16 KN (run 2), and 24 KN (run 3)

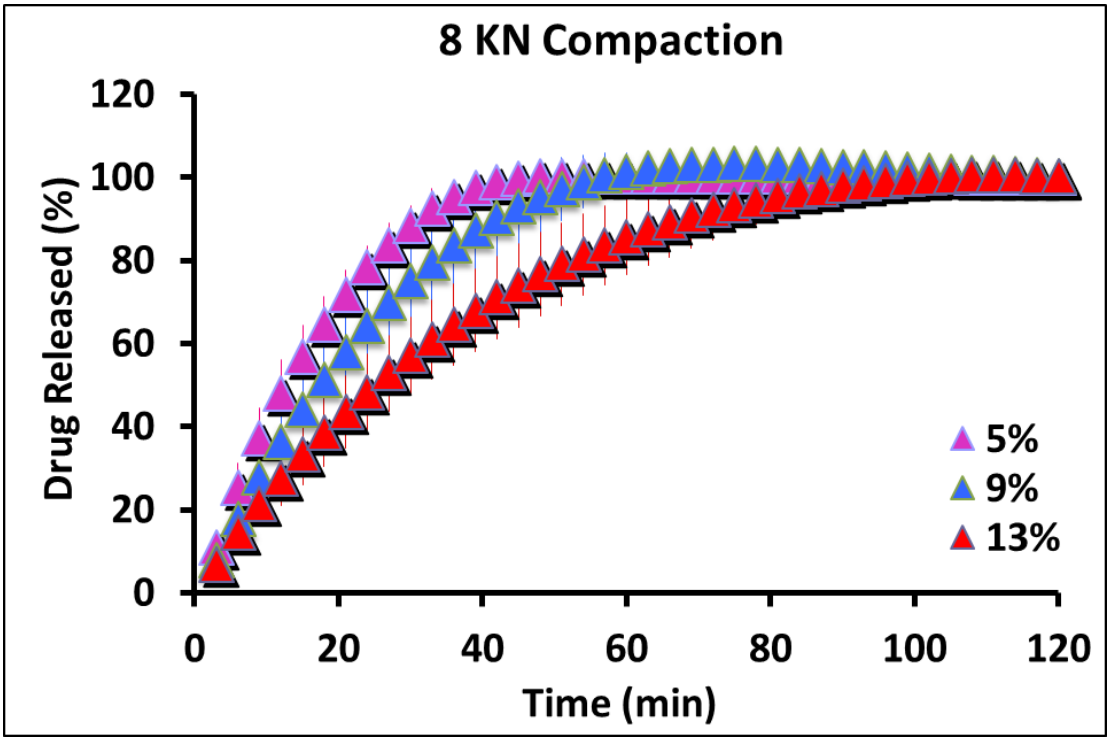

Figure 25: Mean (n=6) dissolution profiles of the tablets with %API at 5% (run 1), 9% (run 16), and 13% (run 20)

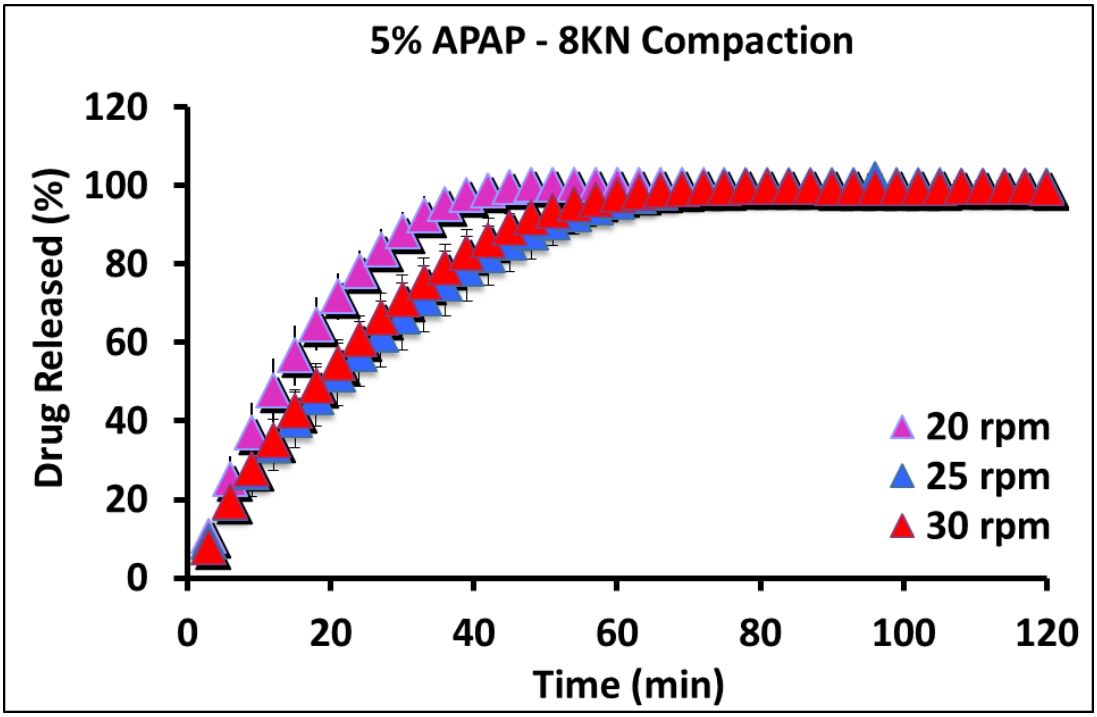

Figure 26: Mean (n=6) dissolution profiles of the tablets with feed frame speed of 20 rpm (run 1), 25 rpm (run 6), and 30 rpm (run 8)

The advantage of using MANOVA is that one overall test of equality of mean vectors will be given for several groups rather than one mean at each time point. MANOVA results consist of within-subject and between-subject analysis. There have been few studies that used MANOVA for comparing dissolution profiles. Wang *et al*. used MANOVA to understand whether the dissolution profiles of sustain released tablets were similar [30]. Yuksel *et al*. applied MANOVA to differentiate between dissolution profiles of immediate release tablets[76]. In this experiment, the percent dissovled at different time points were dependent variables, and time was the repeated factor. Sources of variation were the time, the processing parameters (%API concentration, blender speed, feed frame speed, and compactin force), and the interaction between time and processing parameters. MANOVA was applied to see whether there were significant differences among the percent dissolved

at each time level, meaning the profiles were time dependent. Then the MANOVA analysis was used to see whether there were differences between the profiles due to the processing parameters and their interaction with time. In this study, the software JMP 10 (SAS Institute Inc., , Cary, NC) was used to test the treatment effects for the MANOVA repeated measures analysis. Table 13 illustrates the reults. The between subject results clearly indicate that API concentration, feed frame speed, and compaction force have significant effects (p <0.05) on dissolution profiles, and therefore they are considered not parallel. Additionally, the within subject results indicate that the effect of time and their interactions with the processing parameters are statistically significant.

Table 13: MANOVA Results

	Term	**F value**	**Prob>F**
	API Concentration	78.8541	<.0001
	Blender Speed	0.0716	0.7894
	Feed Frame	17.7698	<.0001
	Compaction Force	258.2361	<.0001
Between Subjects	API Concentration*Blender Speed	3.8049	0.0528
	API Concentration*Feed Frame	0.1028	0.7489
	API Concentration*Compaction Force	1.2203	0.2709
	Blender Speed*Feed Frame	0.1791	0.6727

	Blender Speed*Compaction Force	0.5701	0.4513
	Feed Frame*Compaction Force	2.2578	0.1348

	Term	**F value**	**Prob>F**
	Time	882.8439	<.0001
	Time*API concentration	3.8652	<.0001
Within Subjects	Time*Blender speed	0.9568	0.5502
	Time*Feed frame	1.9412	0.0028
	Time*Compaction force	9.936	<.0001
	Time*API concentration*Blender speed	2.1138	0.0009
	Time*API concentration*Feed Frame	1.7388	0.0107
	Time*API concentration*Compaction Force	4.4588	<.0001
	Time*Blender Speed*Feed Frame	1.4664	0.0564
	Time*Blender Speed*Compaction Force	1.2861	0.1476
	Time*Feed Frame*Compaction Force	2.2006	0.0005

4.3.2 Fitting dissolution models

The dissolution profiles were analyzed using the model-dependent approach [77]. We fitted various models to the dissolution profiles [78]. The best fit was obtained by Weibull model based on the Akaike Information Criterion (AIC) [79]. The advantage of this model is its capability in dealing both with S-shaped curves (drug dissolution from disintegrating tablets) and curves with a fast initial release followed by a slower release (sustained release tablets). And it is useful for comparing release profiles of tablets with matrix type drug delivery. The model is

$$\%\, Dissolved = 100[1 - e^{\frac{(T0-t)^{\beta}}{\alpha}}]$$

where T_0 = lag time; α = a time parameter; β = a shape parameter. Since our tablets were sustained released the parameter T_0 would be equal to zero (Equation below). Model parameters α and β were calculated for each profile using DDSolver. DDSolver is an add-inn program for Microsoft Excel and holds a dissolution model library for fitting dissolution profiles using a nonlinear optimization method.

$$\%\, Dissolved = 100[1 - e^{\frac{-t^{\beta}}{\alpha}}]$$

The parameters, α and β, indicate the scale and shape parameter respectively [80]. The parameter β is characterized as exponential (β=1), sigmoidal (β>1), or parabolic (β<1).

Table 14 and 15 show the regression coefficients for α. As can be seen, compaction force had the highest effects on both α and β. Increasing compaction force decreases tablet

permeability and increases the time that water reaches the core of the tablet to dissolve all the API particles.

4.3.3 Multiple linear regression between process parameters & dissolution model coefficients

Multilinear regression (Response surface model) was used to study how critical process parameters impacted the dissolution model parameters, α and β, using Minitab 18. We examined the relationship between the process variables in the manufacturing line and the model parameters, α and β, extracted from the Weibull model. A good fit was observed for the multilinear regression models for α and β, and the regression models had an R^2 of 0.9 and 0.89 for α and β respectively. The model summaries for α and β can be seen in tables 14 and 15.

Table 14: Response surface regression for parameter α

Estimated regression Coded Coefficients for α				
Term	**Coef**	**SE Coef**	**T-Value**	**P-Value**
Constant	165.200	10.200	16.240	0.000
%API	-31.190	8.140	-3.830	0.001
Blender Speed	2.160	6.070	0.360	0.727
Feed Frame	-1.170	5.950	-0.200	0.847
Compaction Force	60.990	5.960	10.240	0.000

%API*%API	-33.300	18.700	-1.780	0.094
Blender Speed*Blender Speed	3.500	10.100	0.350	0.730
Feed Frame*Feed Frame	3.030	9.500	0.320	0.754
Compaction Force*Compaction Force	-25.020	9.620	-2.600	0.019
%API*Blender Speed	9.800	10.300	0.940	0.359
%API*Feed Frame	-11.800	10.500	-1.120	0.279
%API*Compaction Force	-35.600	10.300	-3.450	0.003
Blender Speed*Compaction Force	-7.460	7.500	-0.990	0.335
Feed Frame*Compaction Force	-3.120	7.630	-0.410	0.687

The analysis was done using coded units

Model Summary

S	R-sq	R-sq(adj)	R-sq(pred)
24.7195	0.901	0.820	0.599

Table 15: Response surface regression for parameter β

Estimated regression Coded Coefficients for β				
Term	**Coef**	**SE Coef**	**T-Value**	**P-Value**
Constant	1.405	0.016	89.430	0.000
%API	-0.107	0.013	-8.450	0.000
Blender Speed	0.009	0.009	0.980	0.341
Feed Frame	-0.032	0.009	-3.580	0.002
Compaction Force	0.032	0.009	3.500	0.003
%API*%API	-0.150	0.029	-5.230	0.000
Blender Speed*Blender Speed	0.007	0.016	0.470	0.646
Feed Frame*Feed Frame	-0.007	0.015	-0.440	0.662
Compaction Force*Compaction Force	-0.026	0.015	-1.720	0.104
%API*Blender Speed	0.049	0.016	3.080	0.007
%API*Compaction Force	-0.029	0.016	-1.800	0.090
Blender Speed*Compaction Force	-0.018	0.011	-1.640	0.119

Feed Frame*Compaction Force	0.005	0.012	0.450	0.662

The analysis was done using coded units

Model Summary

S	R-sq	Rsq(adj)	R sq(pred)
0.038	0.896	0.822	0.590

4.3.4 Dissolution prediction @ target point

To test the validity and the robustness of the prediction model, we maufacutred tablets at the target point of 5%API, 250 rpm blender speed, 25 rpm feed frame speed, and 24 KN compaction force. These tablets were considered as the external validation set. The processing parameters at the target point were used as inputs for the prediction model, however, drug content predicted by NIR in section 2.2.5 was used as %API input. Then α and β were predicted, and the predicted dissolution profile was constructed by Weibull model. Later the tablets were dissolved and the experimental profiles were calculated. The reference and the predicted dissolution profiles for individual tablets are depicted in Figures 7-10.

The mathmatical methods for the comparison of dissolution profiles has been described by Moore and Flanner [81]. Comparison of dissolution profiles were performed between the predicted and the reference profiles by the f_2 similarity factor and the f_1 difference factor (equations below). This method has been recommended for use in a number of FDA

guidance documents [22, 82] [23]. The equations can be seen below where Log=logarithm to base 10, n=number of sampling time points, R_t and T_t are the reference and test dissolution values at time t. The value of f1 and f2 are zero and hundred respectively when the test and reference mean profiles are identical.

$$f_1 = \{[\sum_{t=1}^{n} lR_t - T_t]/[\sum_{t=1}^{n} R_t] \times 100$$

$$f_2 = 50 \times \log \{[1 + (1/n) \sum_{t=1}^{n} (R_t - T_t)^2]^{-0.5} \times 100$$

The values of difference factor (f_1) and similarity factor (f_2) were computed for at least 25 time points up to the point when 85% of the drug was releasaed. The f1 and f2 are listed in Table 16 as well as on Figures 27-30, and it can be seen that they are within the expected limits. Figure 1 illustrates the dissolution profiles with the calculated f_1 and f_2.

Table 16: Difference and similarity factors (f_1 and f_2)

Tablet	f_1	f_2
1	9	77
2	9	74
3	5	83
4	9	76

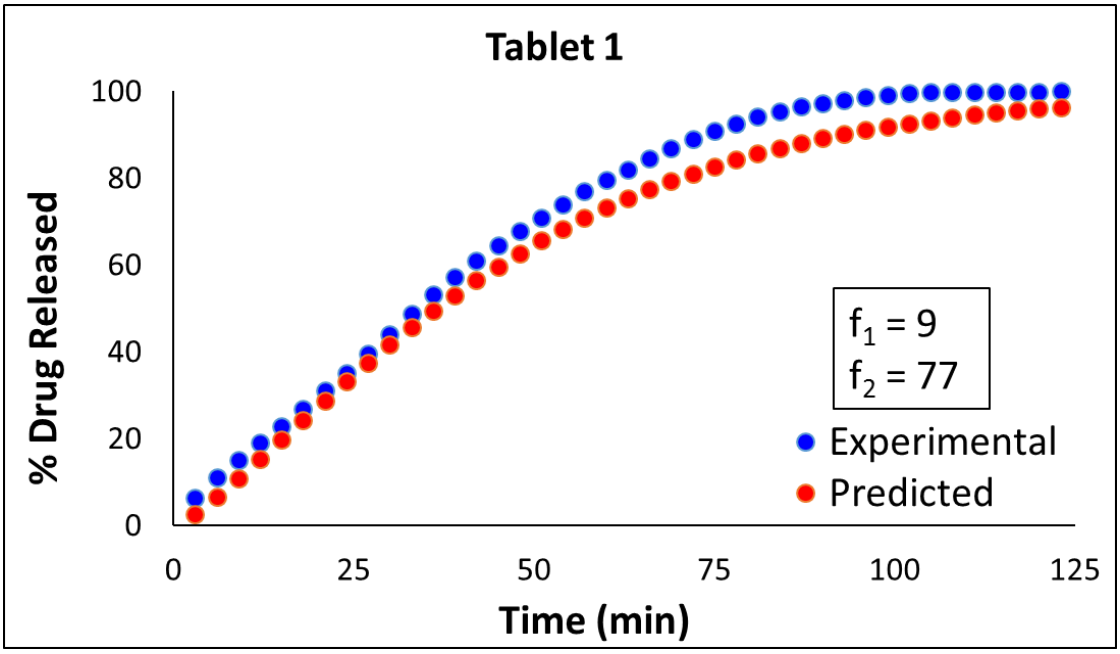

Figure 27: Dissolution profile comparison for tablet 1

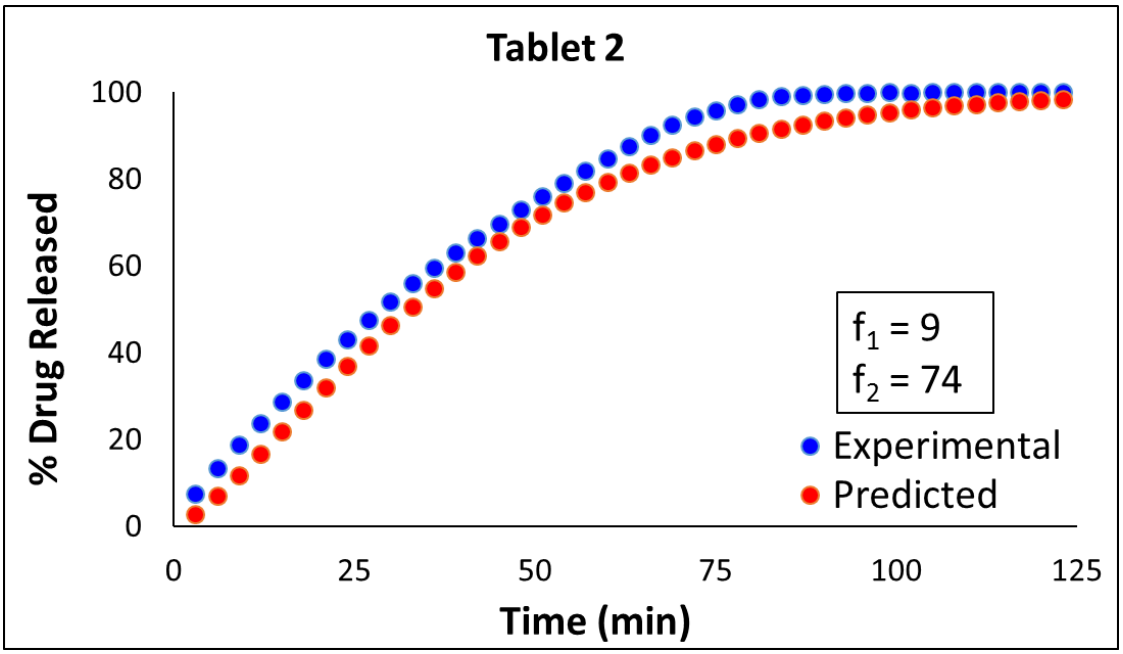

Figure 28: Dissolution profile comparison for tablet 2

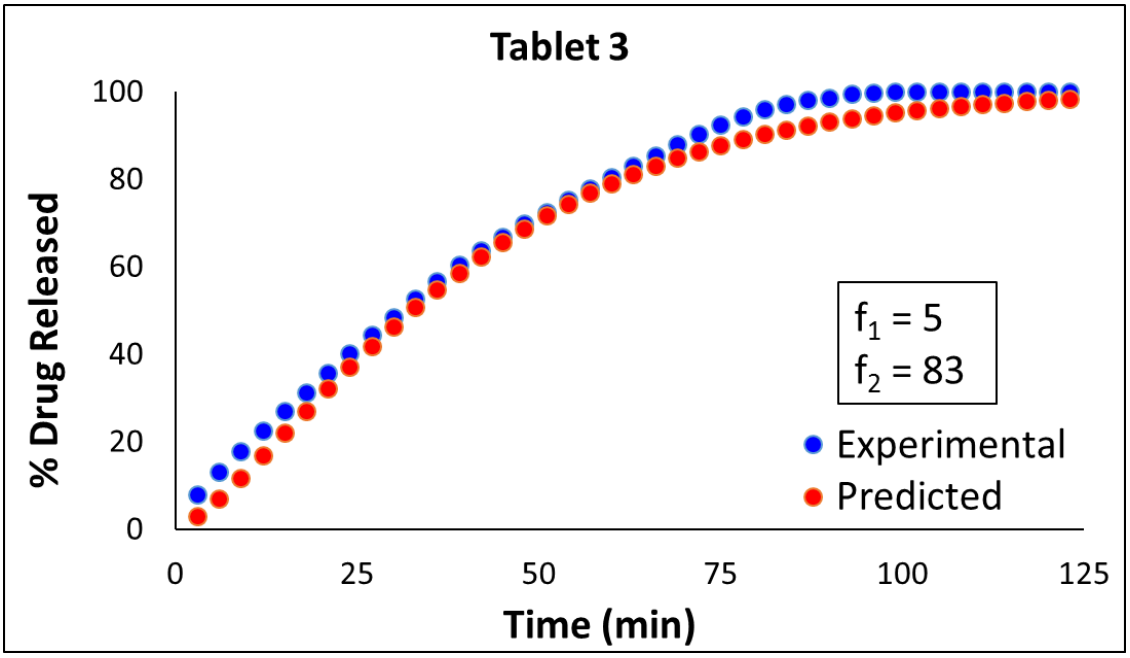

Figure 29: Dissolution profile comparison for tablet 3

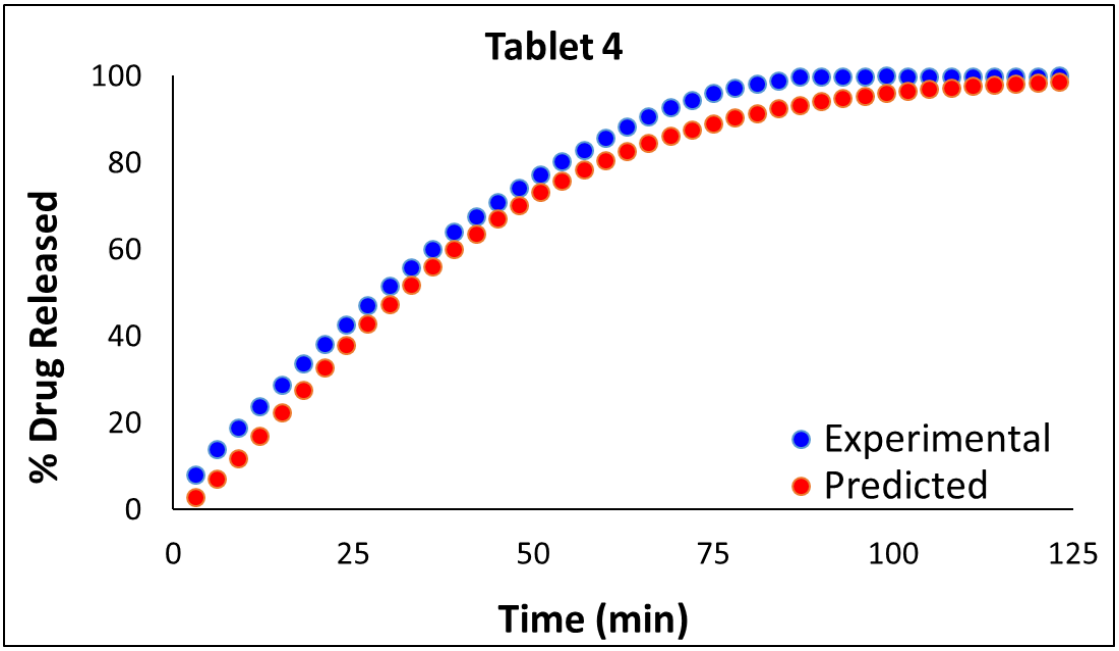

Figure 30: Dissolution profile comparison for tablet 4

4.4 Regulatory considerations

Pharmaceutical drug products will not have the intended quality without regulatory oversight. Regulators such as the FDA and the ICH review, inspect, and research across the product lifecycle. But within the regulatory framework and in the context of continuous manufacturing there has been some uncertainties in the evaluation and assurance of quality of products. There are differences between batch and continuous manufacturing in terms of regulatory expectations, and risk and control strategies have been in the center of attention. The ICH has developed over 45 harmonized guidelines that include categories such as quality, safety, efficacy, and multidisciplinary topics. Among those, ICH Q8 [83], Q9[84], and Q11 [85] were specifically developed to provide guidance on aspects involved with quality. In 2017, the ICH Q12 [86] was recommended for adoption to the regulatory bodies of the European Union, Japan, and USA to enhance the management of post-approval changes, and transparency between industry and regulatory authorities, leading to innovation and continual improvement [87].

There are some elements of ICH Q12 that are defined as “Established conditions” (ECs) and are necessary to assure product quality and changes to these information will have to be reported to the regulatory authority. Established Conditions (ECs) for manufacturing processes include relevant parameters and attributes that impact product quality or for which an impact on product quality cannot be ruled out. There are, however, different approaches in reporting them which include parameter based, enhanced, and performance-based approach. The first approach will only provide a limited understanding of the inputs and quality attributes relationships. An understanding of interaction between inputs and product quality attributes based on a control strategy can be used as part of the enhanced

approach. And finally, the performance based approach which will include manufacturing processes using in-line monitoring such as PAT technologies [86]. The concept of Established Conditions provides a risk-based categorization of post-approval CMC changes.

The proposed method for predictive dissolution modeling may find its applications in currently emerging regulatory environment. Our study can be considered as an example of what may be considered as established conditions when some of the critical process parameters are used for dissolution prediction for dosage units. This study demonstrated an approach to identify some of the critical or key process parameters such as blender speed and compression force, and their relationship with product attributes such as dissolution profile. We have briefly described the equipment and the sequence of the operation, the process these products were manufactured, and the ranges of the process parameters were used. Other considerations in the context of ECs can include maintenance, monitoring, and update of the dissolution prediction model, and implementation of the model as part of overall control strategy.

4.5 Conclusion

With the new paradigm in continuous manufacturing comes the need to have all the critical process attributes sufficiently controlled. This case study exemplified the methodology to be used for a model based prediction of dissolution performance based on processing variables in a continuous manufacturing line, advancing the process to real-time release testing (RTRt). This work showed the feasibility of predicting dissolution profiles and demonstrated that real-time prediction of dissolution profiles could be a possible control

method which can subsequently be integrated into the control strategy in continuous manufacturing to enable continued process performance and product quality. Application of such a strategy will add to the process knowledge and along with other PAT tools would not only lower laboratory and personnel costs but also increase product quality. A statistical model for predicting tablet dissolution profiles will enable rapid techniques in continuous assessment of tablets ensuring the desired quality attributes. In addition, the information in this study can provide some elements of a control strategy which is required as part of ECs and will allow the FDA to assess the manufacturing process as part of the review process.

While the pharmaceutical industry seeks to improve efficiency and reduce costs, clearly a need exists for an in-line real time alternative to the long offline end-product dissolution testing. The tests don't always correlate to in-vivo dissolution, depend heavily on hydrodynamics, and performances vary between apparatus. The FDA has been pushing for dissolution modelling for a long time, and the pharmaceutical industry has made progress in developing real-time alternatives to be used with continuous manufacturing but has also faced a lot of challenges. To implement RTRt for dissolution, the most important processing parameters have to be linked to process or product characteristics that can be measured inline. Some parameters are hard to measure inline which make the study complex. There is lack of information about product performance due to physical and chemical interactions during in-vitro dissolution process. Some processes cannot be easily modelled from first principals based on the product data available inline. Thus, the significance of this work lies in the development of prediction models for dissolution performance based on measurable process parameters and critical quality attributes which can overcome some of the aforementioned challenges with in-vitro dissolution testing.

Chapter 5: Effect of high MW PEO on properties of tablets in a hot melt extrusion process

5.1 Introduction

5.1.1 Hot melt extrusion (HME)

Hot melt extrusion (HME) has been commonly used in the plastic industry. It was introduced for pharmaceutical applications in the 1930's [31]. HME is an intrinsically continuous process enabling the formation of new dosage forms. The extrusion process operates by forcing a mixture through a die under controlled conditions [88]. The material is subjected to heating and intense mixing during the process resulting in a homogeneous dispersion of drug particles in molten carrier. The carrier is generally a polymeric or lipidic material [46].

The HME process is composed of several sub-systems; a feeder that brings the mix inside a heating barrel at a controlled rate, the screws with defined screw speed that convey the material while mixing them, and the die at the end that gives the final shape to the extrudate. There are two types of extruders; single screw extruder that are cheaper and easier to use, and twin screw extruders where the screws can turn in counter-rotating or co-rotating ways resulting in better mixing. The screws are composed of different elements with various functions. Conveying elements carry the mixture forward, and the kneading elements mix and densify the mixture. The elements and their design are very important in the manufacturing process and have a strong influence on the final product. The die, at the end of the screws, can have various shapes and diameters. The barrel is usually composed of

multiple heating zones which can be heated to different temperatures. A schematic of the HME process can be depicted in Figure 31.

The parameters that highly influence the products in an HME process are the screw design, the screw speed, the feed rate, and the extrusion temperatures at different barrels. It is important to keep these parameters in control as they would have an impact on the critical quality attributes of the final product such as drug homogeneity and drug release.

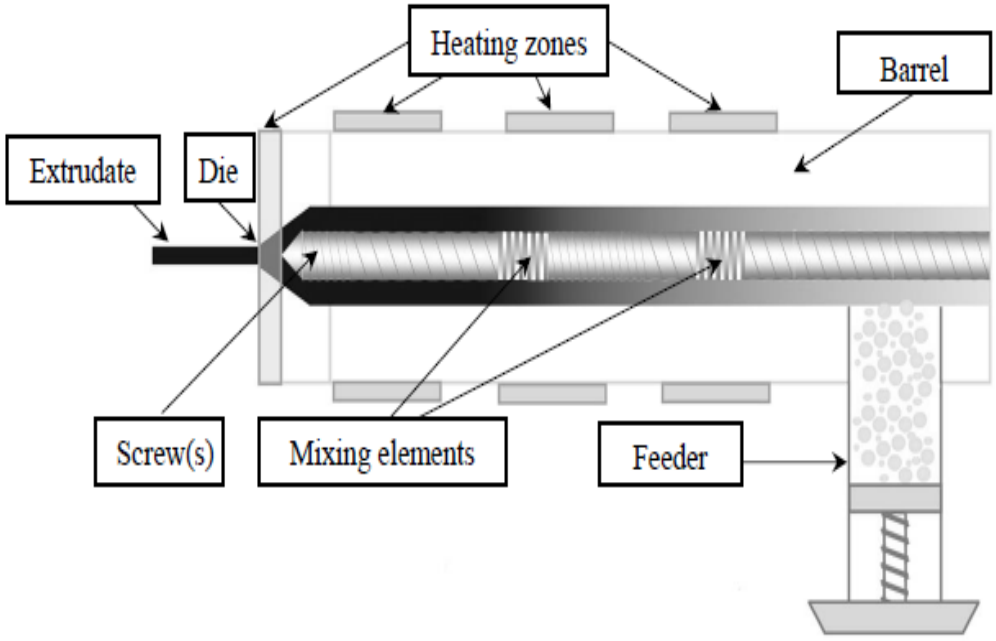

Figure 31: Schematic representation of the hot melt extrusion process. Adapted from [31]

5.1.2 HME applications

Some of the hot melt extrusion pharmaceutical applications are immediate release, modified release, and taste masking of drugs. Recent innovations include abuse-

deterrent/tamper-resistant formulations [89], co-extrusion [90], co-crystallization [91], and 3D printing [92]. In this dissertation, we focus mainly on abuse-deterrent formulations.

The goal of abuse-deterrent formulations (ADF) is to make manipulation more difficult or less rewarding. In 2015, the US Food and Drug Administration (FDA) published a guidance for industry regarding evaluation and labeling of abuse-deterrent opioids [35]. The guidance focused on how studies on abuse deterrent formulations should be conducted, and described seven categories of abuse-deterrent technologies. The categories consisted of physical/chemical barriers, agonist/antagonist combinations, aversion, delivery system, new molecular entities (NMEs) and prodrugs, and other novel approaches. An extensive list of technologies is listed in Table 17 [35].

With the recent growing interest in abuse-deterrent formulations, drug manufacturers have attempted to develop opioids with formulations designed to create barriers to tampering. Table 18 summarizes the opioid products that have been already approved and labeled ADF by the FDA.

Table 17: Technologies for deterring drug abuse. Modified from [35]

Technology	**Examples**
Physical/chemical barriers	• Physical barriers can prevent chewing, crushing, cutting, grating, or grinding of the dosage form. • Chemical barriers, such as gelling agents, can resist extraction of the opioid using common solvents like water, simulated biological media, alcohol, or other organic solvents. • Physical and chemical barriers can limit drug release following mechanical manipulation, or change the physical form of a drug, rendering it less amenable to abuse.
Agonist/Antagonist combinations	• An opioid antagonist can be added to interfere with, reduce, or defeat the euphoria associated with abuse. • The antagonist can be sequestered and released only upon manipulation of the product. • For example, a drug product can be formulated such that the substance that acts as an antagonist is not clinically active when the product is swallowed, but becomes active if the product is crushed and injected or snorted.
Aversion	• Substances can be added to the product to produce an unpleasant effect if the dosage form is manipulated or is used at a higher dosage than directed. • For example, the formulation can include a substance irritating to the nasal mucosa if ground and snorted.
Delivery System (including use of depot injectable formulations and implants)	• Certain drug release designs or the method of drug delivery can offer resistance to abuse. • For example, sustained-release depot injectable formulation or a subcutaneous implant may be difficult to manipulate.
New molecular entities and prodrugs	• The properties of a new molecular entity (NME) or prodrug could include the need for enzymatic activation, different receptor binding profiles, slower penetration into the central nervous system, or other novel effects. • Prodrugs with abuse-deterrent properties could provide a chemical barrier to the in vitro conversion to the parent opioid, which may deter the abuse of the parent opioid. • New molecular entities and prodrugs are subject to evaluation of abuse potential for purposes of the Controlled Substances Act (CSA).
Combinations	• Two or more of the above methods could be combined to deter abuse.
Novel approaches	• This category encompasses novel approaches or technologies that are not captured in the previous categories.

Table 18: FDA-approved Opioids with Abuse Deterrent Formulations (ADF) Labeling [93]

Generic Compound	Year of Approval	Availability on the Market	ADF Mechanism	Dosages Available
Oxycodone				
OxyContin (oxycodone extended-release)	2010	Available	Hinders crushing of the tablet into a fine powder. If powder of the tablet is formed and dissolved in solvent, the drug product becomes a viscous gel that is difficult to inject IV.	10 mg, 15 mg, 20 mg, 30 mg, 40 mg, 60 mg, 80 mg
Xtampza ER (oxycodone extended-release)	2016	Available	Capsules contain microspheres of oxycodone and inactive ingredients that hinder dosage dumping *via* intranasal and oral abuse. Microspheres cannot be readily dissolved and will solidify within a needle to resist injection.	9 mg, 13.5 mg, 18 mg, 27 mg, 36 mg
Troxyca ER (oxycodone + naltrexone extended-release)	2016	Unavailable (as of July 27, 2017)	Capsules consist of pellets containing oxycodone hydrochloride surrounding sequestered naltrexone hydrochloride. When crushed, sequestered naltrexone is released and able to impede the effects of extended-release oxycodone and block opiate-induced euphoria.	10 mg/1.2 mg, 20 mg/2.4 mg, 30 mg/3.6 mg, 40 mg/4.8 mg, 60 mg/7.2 mg, 80 mg/9.6 mg
Targiniq ER (oxycodone and naloxone extended-release)	2014	Unavailable (as of July 27, 2017)	Pill containing extended-release oxycodone and opioid antagonist naloxone in a 2:1 ratio. If the tablet is crushed for administration *via* nasal or IV routes, the naloxone will counteract the effects of oxycodone and impede opiate-induced euphoria. Tablet also has a polyethylene oxide matrix to resist mechanical stress, such as crushing.	10 mg/5 mg, 20 mg/10 mg, 40 mg/20 mg
RoxyBond (oxycodone IR)	2017	Unavailable (as of July 27, 2017)	Contains layered inactive ingredients that make the tablet resistant to physical manipulation (*e.g.*, crushing). Chemical extraction and dosage dumping are hindered by superabsorbent excipients and insoluble coatings within the layers. When taken as directed, extended-release of oxycodone is facilitated by the layers *via* diffusion.	5 mg, 15 mg, 30 mg
Hydrocodone				
Hysingla ER (hydrocodone extended-release)	2014	Available	Difficult to crush because of a polyethylene oxide matrix and, when dissolved, the tablet forms a viscous hydrogel that hinders an abuser's ability to inject the extracted product through a syringe in intravenous abuse.	20 mg, 30 mg, 40 mg, 60 mg, 80 mg, 100 mg, 120 mg
Vantrela ER (hydrocodone extended-release)	2017	Unavailable (as of July 27, 2017)	Designed with lipids and other excipients that resist crushing and maintain thermoplasticity. Fat and wax polymers present in the tablet's granules establish low solubility of the crushed drug product, hindering IV injection.	15 mg, 30 mg, 45 mg, 60 mg, 90 mg
Morphine				
Embeda (morphine + naltrexone extended-release)	2014	Available	Capsules contain pellets of morphine around a core of sequestered naltrexone. When taken as directed, morphine is released and absorbed and the naltrexone core passes through the gastrointestinal tract. If the pellets undergo physical manipulation, naltrexone is released from the core to block euphoria caused by rapid morphine release.	20 mg/0.8 mg, 30 mg/1.2 mg, 50 mg/2 mg, 60 mg/2.4 mg, 80 mg/3.2 mg, 100 mg/4 mg
MorphaBond ER (morphine extended-release)	2015	Unavailable (as of July 27, 2017)	The tablet contains multiple layers that are resistant to physical manipulation (*e.g.*, crushing). The layers also prevent chemical extraction and dosage dumping by utilizing superabsorbent excipients and insoluble coatings. When taken as directed, extended-release of morphine is facilitated by the layers *via* diffusion.	15 mg, 30 mg, 60 mg, 100 mg
Arymo ER (morphine extended-release)	2017	Available	Polyethylene oxide matrix and morphine polymers surrounded by a hard shell make the tablet dense, less porous, and resistant to physical manipulation (*e.g.*, crushing). When the manipulated product encounters a solvent, a viscous hydrogel is formed, preventing the abuser from drawing the product into a syringe for injection.	15 mg, 30 mg, 60 mg

ADF = abuse-deterrent opioid formulation; FDA = Food and Drug Administration; IR = immediate release.

5.1.3 Polyethylene Oxide (PEO)

Polyethylene oxide (PEO) has been widely used in abuse deterrent pharmaceutical products. Polyethylene oxide (PEO) is a semi-synthetic material derived from ethylene oxide and a linear polymer comprised of ethylene oxide rings. It is a nonionic polymer of ethylene oxide and chemically similar to polyethylene glycol, but it has molecular weight in the range of 100,000 to 7 million Daltons. PEOs are material with hydrophilic, highly swelling, and thermoplastic properties. Polyethylene oxide (PEO) is a thermoplastic semicrystalline polymer with a melting point of 60 °C – 75 °C and a glass transition temperature of -67 °C [94] [95]. The general physicochemical properties are given in Table 19 [96].

Table 19: Typical physicochemical properties of polyethylene oxide (PEO). Adapted from [96]

Physico-chemical properties	PEO	Comments
Bulk density (g/cm^3)	~ 0.47	Similar to commonly used excipient. Good blending characteristics. No segregation issues reported.
Packed density (g/cm^3)	~ 0.51	
Typical particle size (μ)	~ 150	Comparable to commonly used direct compression excipients. This additionally prevents any segregation issues after blending or flow of powder from hopper.
Crystallinity (%)	~ 95	Surface moisture adsorption is prevented due to high crystallinity. This gives low moisture content in polyethylene oxide
Moisture content (%)	< 1	
Melting point (°C)	~ 62 to 67	During drying or coating applications it is recommended to keep product bed temperature of polyethylene oxide containing formulations below 50 °C. Accelerated stability study (45°C/75%RH or 50°C) does not cause melting or affect physical stability of formulations. Low melting property has been used for hot melt extrusion applications.
Swellability in water	~7 times its initial dry size	Polyethylene oxide swells enormously, independent of pH. Higher viscosity grades swell more compared to lower viscosity grades. This ability has been utilized in gastro-retentive formulations.
Solubility in various solvents		
Water	Soluble with very high viscosity	Water has been used for aqueous granulation and coating under optimized conditions and use of spray system. Water can cause a sticky and highly slippery surface, so precautions should be taken when using water for PEO processing.
Isopropyl alcohol, IPA (91%)	Dissolves at room temperature	Hydro-alcoholic solution can be used for granulation and coating with or without a binder such as HPMC.

Pharmaceutical grades of PEO are commercially available under the trade name of POLYOX^{TM} water soluble resins (WSR). There are various grades of PEO available and can be seen in Table 20 [97].

Table 20: Approximate molecular weight (MW) and viscosity range for POLYOX water soluble resins for pharmaceutical applications

POLYOX Water-Soluble Resins, NF Grade	Approximate Molecular Weight	Viscosity Range at 25°C, cP			Brookfield Viscometer, Model RVF, Spindle No./Speed, rpm
		5% Solution	2% Solution	1% Solution	
WSR N-10 NF	100,000	30 – 50			1/50[1]
WSR N-80 NF	200,000	55 – 90			1/50[1]
WSR N-750 NF	300,000	600 – 1,200			1/10
WSR-205 NF	600,000	4,500 – 8,800			2/2
WSR-1105 NF	900,000	8,800 – 17,600			2/2
WSR N-12K NF	1,000,000		400 – 800		1/10
WSR N-60K NF	2,000,000		2,000 – 4,000		3/10
WSR-301 NF	4,000,000			1,650 – 5,500	2/2
WSR Coagulant NF	5,000,000			5,500 – 7,500	2/2
WSR-303 NF	7,000,000			7,500 – 10,000	2/2

Table 1 shows all the PEO products available from Dow Chemical with different nominal molecular weights. The difference in nominal molecular weight of various PEO products is reflected in the viscosity of an aqueous solution of a standard concentration. An increase in nominal molecular weight results in an increase in viscosity. Viscosity of polymer solutions is the result of hydration of polymer chains causing them to extend and form relatively open random coils. A given hydrated random coil is further H-bonded to additional water molecules, entrapping water molecules within, and may be entangled with other random coils. All these factors contribute to larger effective size and increased frictional resistance to flow. In discussions on controlled release, the term “viscosity” or “viscosity grade” and the associated value for the 2% w/w aqueous solution is frequently used as a way to refer to the molecular weight of the polymer. In fact, because molecular weights of these polymers are very difficult (if not impossible) to measure, the actual quality specification for their commercialization and use is the viscosity in solution.

PEO polymers are prone to auto-oxidation that leads to chain cleavage and loss of viscosity. The higher and medium viscosity grades are more prone to viscosity loss compared to lower viscosity grades. Therefore, PEO polymers are stabilized by addition of antioxidants such as butylated hydroxyl toluene (BHT) [96]. Polyethylene oxide (PEO) is prone to degradation due to thermal and mechanical stress, and the polymer degradation can be monitored using Gel Permeation Chromatography (GPC) and viscosity. Mechanical stresses such as shear and elongation stress cleaves the polymer chains and causes mechanical degradation [98]. This phenomenon occurs in hot melt extrusion processes where polymers are subjected to the shear effects induced by the rotating extruder screw in the presence of heat.

5.1.4 Sustained release formulations

Millions of Americans suffer from acute or chronic pain on a daily basis [99]. To alleviate the persistent and severe pain, opioids are prescribed by doctors. While opioids can effectively relieve pain, they carry some risks and can be highly addictive. The side effects are often associated with high blood concentration of the opioid. However, the side effects could be greatly reduced by using a sustained or controlled release dosage form. These formulations maintain therapeutically optimal blood levels of the opioid for an extended period of time without concurrent side effects. They are designed to provide continuous release of drug for a predetermined time at a predetermined rate.

Sustained release tablets can be formulated by using a variety of polymers [100]. Polyethylene oxide molecules (PEOs) have been extensively used in controlled release formulations because of their low toxicity, pH-independent swelling, and drug release

properties [101] [102] [103] [38] [96] [104] [105] [106] [107]. The use of PEO and their influence on release rate have been studied in tablets prepared by direct compression, and the results showed that high molecular PEO successfully delayed the release of drugs from tablets [108, 109]. Apicella *et al*. produced PEO buccal films using solvent casting methods [101]. In another study, sustained release gelatin capsules were produced using PEO as the rate-controlling carrier by Efentakis and Vlachou [110]. The drug release properties of sustained release tablets made by hot-melt extrusion using PEO has been investigated by Zhang and McGinity [38]. High molecular weight PEO was also studied by Maggi and *et al.* as an alternative to hydroxypropylmethylcellulose (HPMC) in controlled release matrix tablets [111]. The studies above gave rise to formulations that were releasing drug over a period of time to alleviate pain in a lot of patients.

5.1.5 Polyethylene oxide molecular weight

Similar to all polymers, PEO molecules exist as a distribution and may be characterized by parameters such as the number averaged molecular weight (Mn), the weight average molecular weight (Mw), and the polydispersity index (PI) which is the ratio of Mw to Mn [112]. These molecular weight attributes may be determined by a number of techniques such as osmometry, light scattering, or size exclusion chromatography [113].

The number average molecular weight, Mn, is the simplest of the molecular weights, because it corresponds to the usual notion of an arithmetic average. The weights of all the molecules are added together and then the sum is divided by the total number of molecules present. The equation of Mn is given below where Ni is the number of moles, and Mi is

the contributing molecular weight in the sample and, Ni is the corresponding number of moles [114].

$$M_n = \frac{\sum N_i M_i}{N_t}$$

The contributing molecular weight in the sample is multiplied by the corresponding number of moles. The sum is then divided by the total number of moles in the sample. Another commonly used quantity is the mass-averaged molecular weight, Mw, which is given mathematically by the equation below:

$$M_w = \frac{\sum W_i M_i}{W_t}$$

where Wi is the mass of polymer with molecular weight Mi. Mi is multiplied by the weight present in the sample, and the sum of all these contributions is divided by the by the total weight of the sample. The ratio of Mw to Mn is called the polydispersity, and is an indication of the width of the distribution of molecular weights in the sample. The distribution width increases with the polydispersity ratio [115].

In addition, molecular weight information can be obtained from intrinsic viscosity data using the Mark-Houwink-Sakurada equation and appropriate constants [116]. Mark-Houwink equation describes the relationship between the intrinsic viscosity and the molecular weight as seen in the equation below:

$$[\eta] = k\, M_v^{\alpha}$$

where [η] is the intrinsic viscosity in dL/g, M_v is the viscosity-average molecular weight, and k and α are coefficients for given solute-solvent system and temperature.

5.1.6 Plasticizers & antioxidants

Plasticizers are used to improve the flexibility and processability of polymers by lowering their glass transition temperature (T_g) [117]. The extent that T_g is reduced in the presence of a plasticizer can be used as a predictor to assess the plasticization efficiency. Plasticizers improve workability and flexibility of the polymer by increasing the intermolecular separation of the polymer molecules. In addition, plasticizers improve polymer toughness and flexibility and lower thermal processing temperatures of a process [118]. Plasticizers tend to lower the torque during the hot melt extrusion process and thus, thus minimizing the localized heating of the drug and polymer and improve the stability and processability of the solid dispersion. Selecting the ideal plasticizer is very important. Each application requires a particular plasticizer with specific attributes [119].

Hot melt extrusion subjects the polymers to thermal and shearing stresses. Depolymerization of polymer chains may occur due to high temperature, and chain scission as a result of shearing effects of the screw [38]. Some conventional plasticizers that reduce such effects include polyethylene glycol 400 (PEG 400), triethyl citrate (TEC), and acetyltributyl citrate (ATBC) that can prevent the aforementioned phenomena [38]. The use of Vitamin E TPGS (TPGS, D-α-tocopherylpolyethylene glycol 1000 succinate) as a plasticizer in hydrophilic films was tested by Repka and McGinity. They found Vitamine E was a good processing aid, decreasing barrel pressure and torque, and additionally, decreasing the polymer degradation [120]. Plasticizers must be efficient, and their

efficiency depends on their chemical structure and the interaction between its functional groups with those of the polymers in the formulations [121]. In another study, Crowly *et al.*, demonstrated that PEO 100K improved processing of PEO 1M and did not significantly influence the rate of release from matrix tablets [122]. Other plasticizers such as stearic acid, glyceryl behenate, and PEG 8000 have been evaluated based on their solubility parameters to evaluate their physical and mechanical properties as processing aids for HME process [123].

5.1.7 Mechanism of drug release from PEO formulations

When tablets including PEO are exposed to water they start to hydrate and swell, forming a gel layer outside the core. PEO polymeric chains begin to dissolve into medium after the swelling process is completed. The swelling and dissolution processes of PEO control the drug release [124]. The formation and erosion of the outer gel layer on the tablet has been studied in the past [125-132].

Three different boundaries exist when swelling and dissolution take place in polymeric PEO tablet matrices [124]. The swelling front, or the innermost boundary, separates the tablet core and the gel layer; the diffusion front, or the middle boundary, distinguishes the solid drug and drug solution; and the erosion front, or the outmost front, is a boundary between swollen matrix and the surrounding release media (Figure 32). Water penetrates the tablet matrix and causes the swelling front to move inward while the erosion front move outward until the whole tablet matrix is hydrated. Dissolution of the drug particles and release of drug molecules depend on the gel layer thickness. As the swelling process continues, the gel layer gradually thickens and results in slower drug-release rates. In our

study, the diffusion of dissolved chlorpheniramine maleate particles, a highly water soluble drug, across the gel layer, is the primary release manner. The matrix will provide a zero-order release kinetics if the swelling and erosion rates are approximately equal. Whether this occurs depends on the amount and viscosity grade of polymer in the formulation.

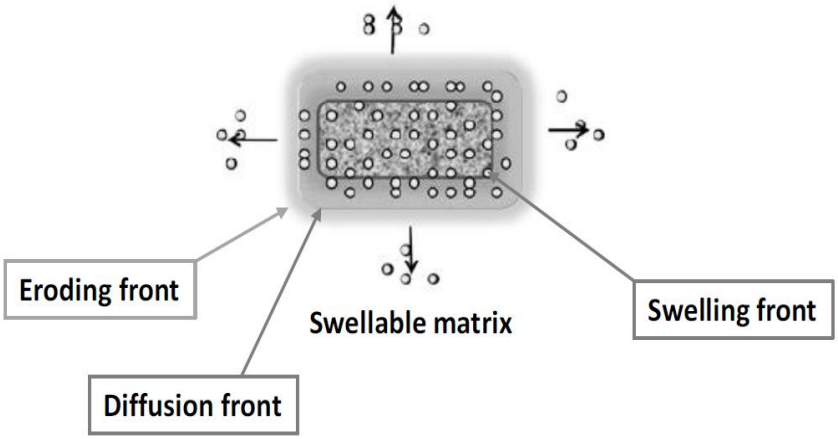

Figure 32: Schematic representation of the polymer matrix tablet during immersion. Liquid penetration forms eroding (outer) and swelling (inner) fronts, where the gel layer is formed in between [133].

5.1.8 Newtonian and non-Newtonian fluids

Fluids are characterized as Newtonian or non-Newtonian depending on their viscosity behavior as a function of shear rate, stress, and deformation history. Newtonian fluids are described as fluids with a linear relation between shear stress (mPa) and shear rate (1/sec). This is known as Newton's Law of Viscosity (Equation below), where the proportionality constant η is the viscosity (mPa-s) of the fluid [134] which in a Newtonian fluid is independent of the shear rate.

$$\underbrace{\tau}_{\text{Shear Stress}} = \underbrace{\eta}_{\text{Viscosity}} \times \underbrace{\dot{\gamma}}_{\text{Shear Rate}}$$

Most polymer solutions and polymer melts are, however, non-Newtonian, which means that their viscosities vary at different shear rates. Non-Newtonian fluids are broadly classified as shear thinning and shear thickening. In contrast to Newtonian fluids, non-Newtonian fluids display a non-linear relationship between shear stress and shear rate. A shear thickening fluid is described as a fluid whose viscosity increases as the shear rate increases. In contrast, fluids are shear thinning if the viscosity decreases as the shear rate increases. Plots of shear rate vs. shear stress for Newtonian, shear thickening, and shear thinning fluids are given in Figure 33.

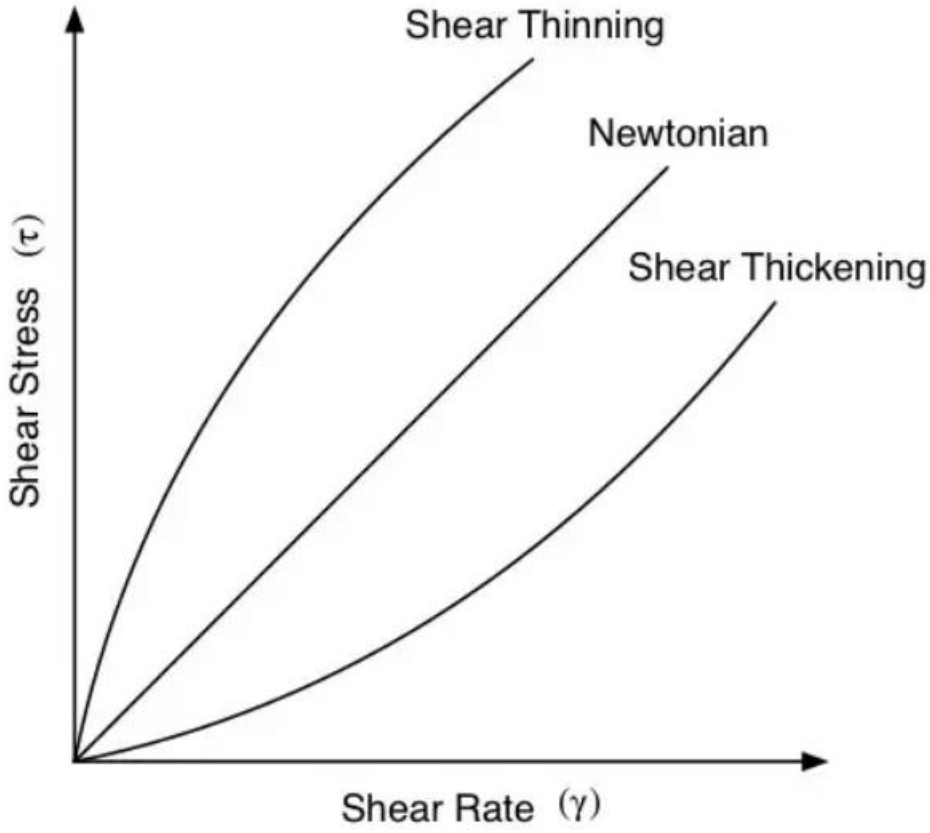

Figure 33: Plot of shear rate as a function of shear stress for shear thickening, Newtonian and shear thinning fluids [135]

5.2 Materials and methods

5.2.1 Materials

The materials are described in chapter 2, section 2.3.2. It is important to note that F1 – F10 refers to the extrudates prepared by HME. Additionally, tablets and extrudates are used interchangeably in this chapter of the dissertation.

5.2.2 Viscosity measurements

Viscosity measurements are described in chapter 2, section 2.3.4.1.

5.2.3 In-vitro dissolution testing

In-vitro dissolution testing is described in chapter 2, section 2.3.4.2.

5.3 Results and discussion

5.3.1 Drug release from extrudates

The dissolution behavior of the extruded tablets for F1 - F5 tablets and F6 - F10 tablets are shown in Figure 34 and Figure 35 respectively. Each data point represents a mean of six measurements for each tablet. As it is apparent from both Figures, the drug release rate decreases with increasing amount of PEO 301 in Figure 34 and PEO 303 in Figure 35. In Figure 34, F1 containing 94% PEO 750 (plasticizer) exhibits a significantly faster drug release rate, whereas F5 containing 94% PEO 301 is evidently the slowest in drug release. Similar trend is observed in Figure 35 where F6 tablets, containing the lowest amount of PEO 303 and the highest amount of plasticizer, have the fastest drug release rate, and F10 tablets, with the highest amount of PEO 303, have the slowest release rate. This can be explained by the extreme swelling property of the high molecular weight PEO polymer rather than polymer dissolution. The high MW polymers swelled and tended to form a strong gel upon hydration, which was slower to erode as compared to the lower molecular weight PEO. This gave rise to a continuous decrease of the drug's diffusion through the growing swollen layer, and consequently, to an unsteady release induced by diffusive control. Contrarily, drug release from the low molecular weight PEO was closely related to the polymer erosion and dissolution mechanism [101]. Similar results have previously been observed [136-138].

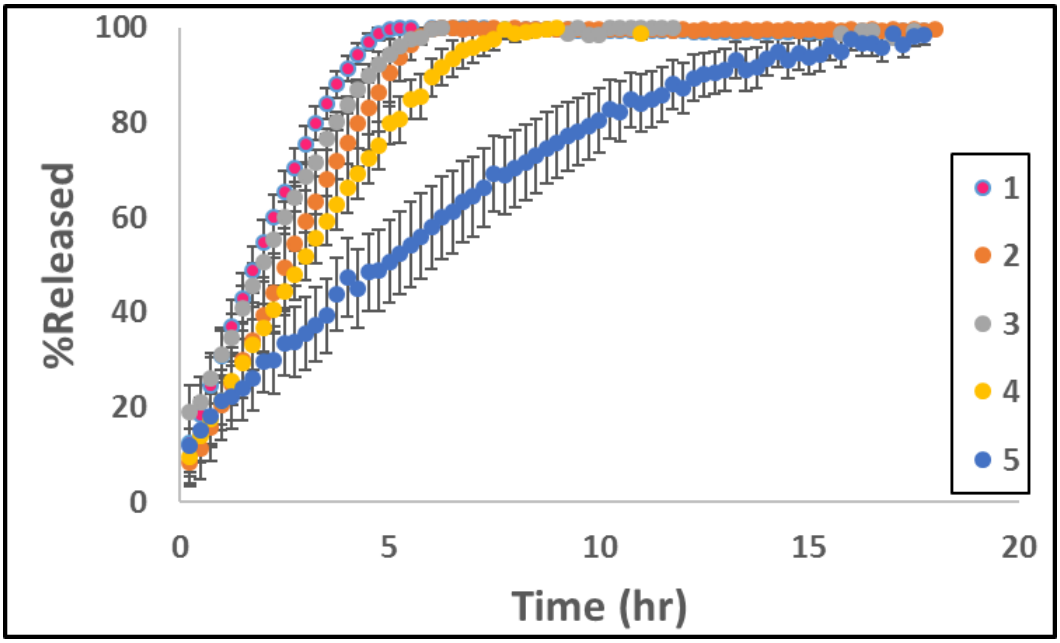

Figure 34: Dissolution profiles for HME F1 – F5 tablets

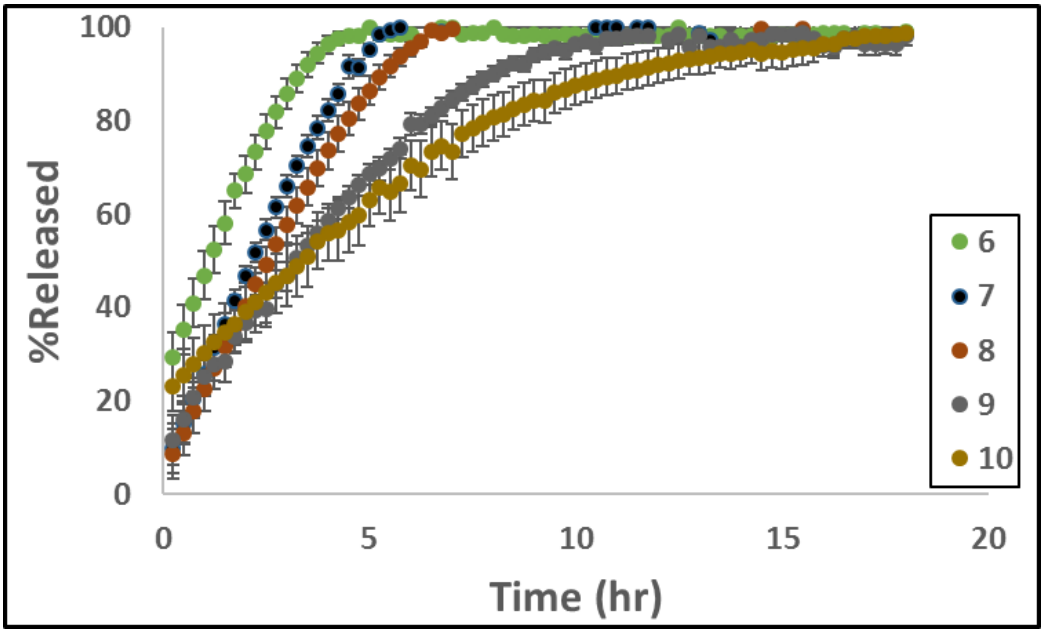

Figure 35: Dissolution profiles for HME F6- F10 tablets

To capture the release of the drug in terms of parameters that could have some physical meaning, the release profiles were regressed by a first-order kinetic model of the form:

$$f(t) = 100[1 - e^{-kt}]$$

where f(t) is the quantity released at time *t* and *k* is the fitted parameter. The *k* constant is a rate constant and quantifies the rate of release and physically indicates the rate at which one species from the boundary moves into the bulk of the phase. A large value of *k* implies fast mass transfer, and a small one means slow mass transfer. The kinetic model is based on Fick's first law that assumes the flux through a unit area of material is proportional to the concentration gradient measured normal to the material, where the constant of proportionality is known as the diffusion coefficient [134]. The rate of dissolution of a tablet may also be characterized by the time t_{50}, where 50% of the drug has been released from the tablet into the media. The values of rate constant (*k*) and t_{50} are listed in Table 21 and Table 22. In addition, Figure 36 and Figure 37 show the graphical representation of *k* and t_{50}.

Shown in Figure 36 is the effect of formulation on the rate constant. By comparing F1- F5 and F6 -F10 tablets it can be observed than an increase of high molecular weight of PEO results in a subsequent decrease in the k value. However, the release rate constant and t_{50} are surprisingly similar for F5 and F10 tablets even though they contain different grades of PEO. The similarity can be attributed to similar viscosities of the hydrated high molecular weight tablet matrices. Even though PEO 303 in F10 tablet has higher nominal molecular weight than PEO 301 in F5 tablet, it is likely that the thermal degradation of PEO 303 has

contributed to the decreasing viscosity and consequently a similar drug release rate [136-138].

Table 21: Rate constant values with their corresponding standard deviations (STDEV) for F1- F10 tablets

Experimental run	k (1/min)	STDEV
1	0.008	±0.001
2	0.006	±0.001
3	0.007	±0.001
4	0.005	±0.001
5	0.004	±0.0
6	0.011	±0.001
7	0.007	±0.0
8	0.006	±0.0
9	0.004	±0.0
10	0.003	±0.0

Table 22: t_{50} values with their corresponding standard deviations (STDEV) for F1-F10 tablets

Experimental run	t50 (min)	STDEV
1	89.7	±9
2	117	±17
3	97	±7
4	136	±14
5	190	±23
6	63	±7
7	102	±4
8	119	±9
9	167	±11
10	213.2	±24

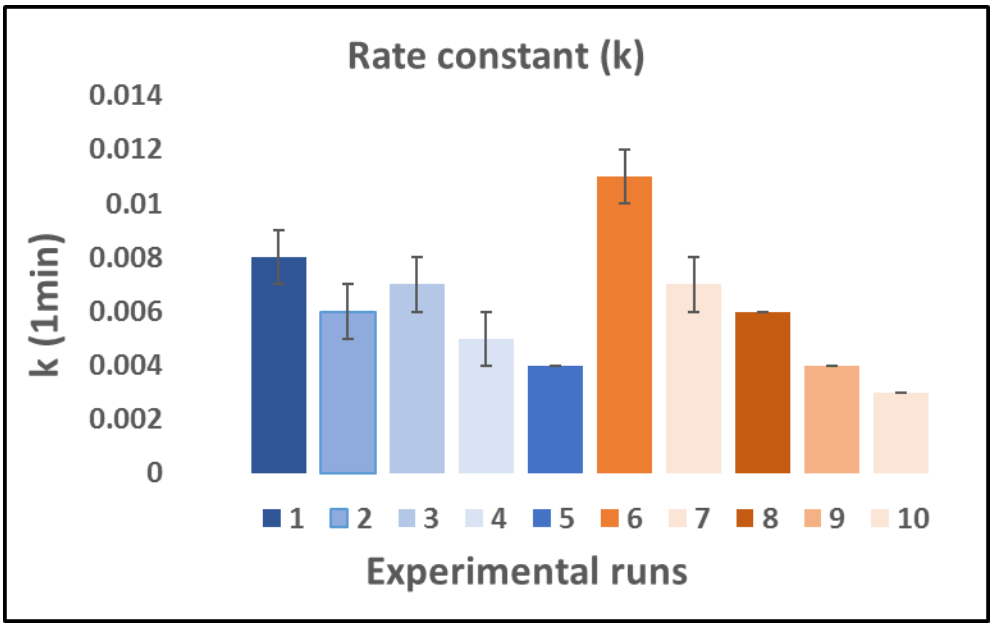

Figure 36: Rate constant of the release profiles for F1- F10

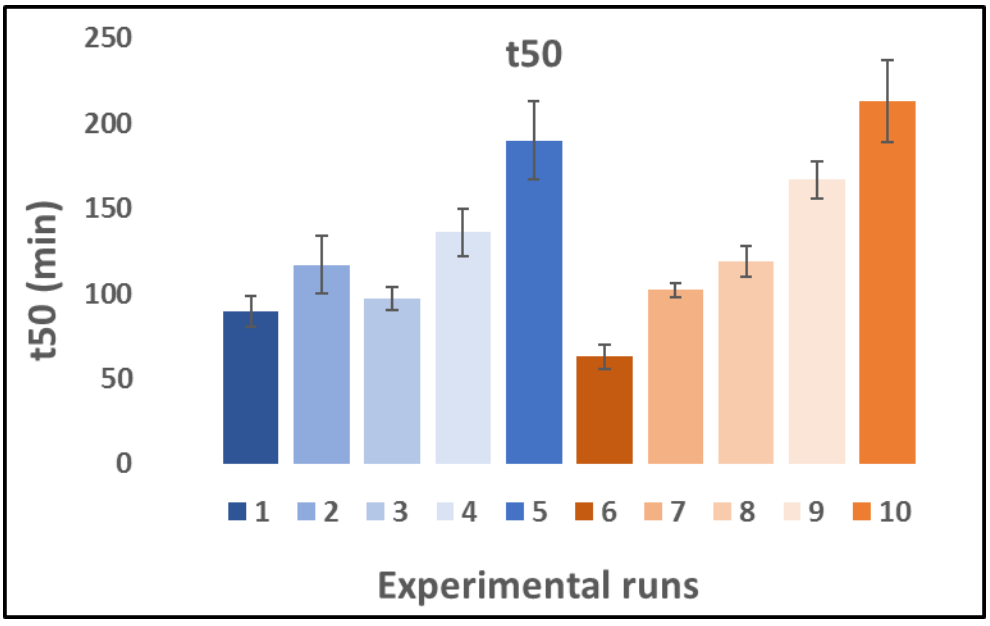

Figure 37: Corresponding t_{50} values of the dissolution profiles for F1 – F10 tablets

5.3.2 Influence of MW and PEO grade on viscosity before and after HME

Solutions prepared using tablets (post-HME) and also their corresponding powder blends (pre-HME) were subjected to a steady shear from 0.1 1/sec to 1000 1/sec in logarithmic steps with 10 points per decade. Each shear step was maintained for 20 sec to achieve a steady measurement. Figure 38 and Figure 39 show the measured viscosity vs. shear rate for powder and tablet solutions of F5 and F10 plotted over a log-log scale that covers nearly four decades of shear rate. For all the solutions, it can be clearly seen that the viscosity decreases with increasing shear rate indicating a shear thinning behavior. The shear thinning behavior can be explained by rupturing and dissociation of polymer entanglements [139]. For high molecular weight polymers such as PEO 301 and PEO 303, penetration of the polymer coils occurs and this results in the formation of entanglements of polymer segments of different polymer coils. As the shear rate increases the polymer coils disentangle and orient themselves in the direction of the flow resulting in the observed shear thinning behavior [140]. Analysis of the same data on Figure 38 and Figure 39 also indicates that tablet solutions (post-HME) have lower viscosity than their corresponding powders (pre-HME). This can be attributed to mechanical and thermal degradation in addition to oxidative degradation of the PEO molecules during the extrusion process. Mechanical degradation is induced by shear forces due to the rotating screws and thermal degradation due to the high extrusion temperatures. Oxidative degradation occurs due to the reaction of PEO with oxygen molecules [122, 141]. In the degradation process, the C-O bonds in the PEO molecule separate and result in smaller molecules with lower molecular weight.

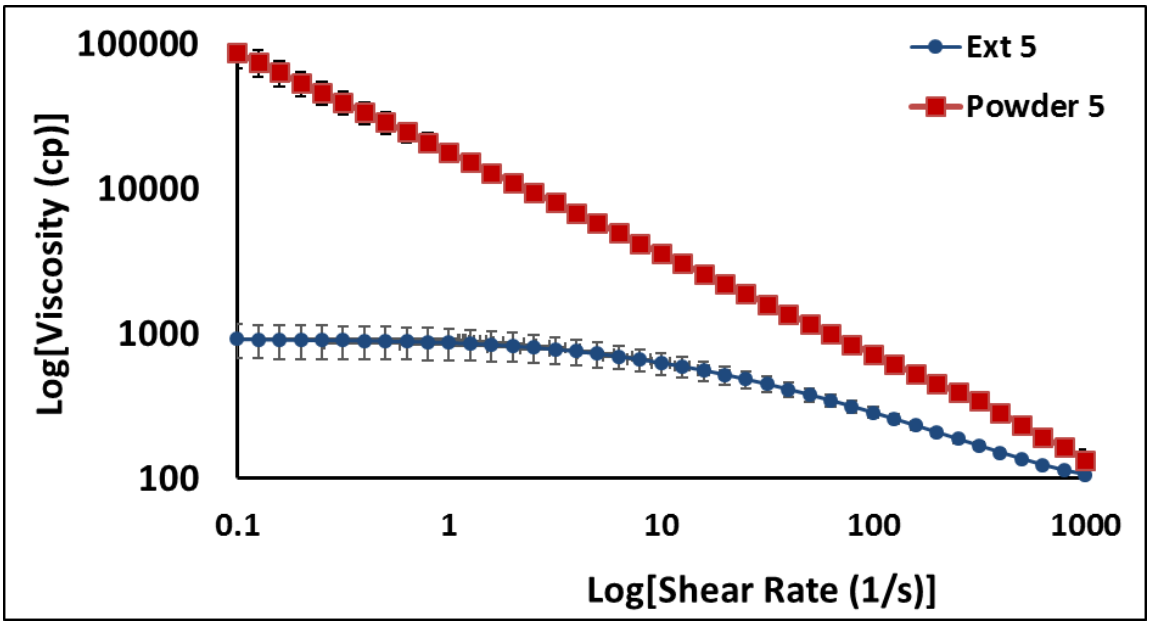

Figure 38: Shear rate vs. viscosity for F5 pre-HME and post-HME at 25 °C

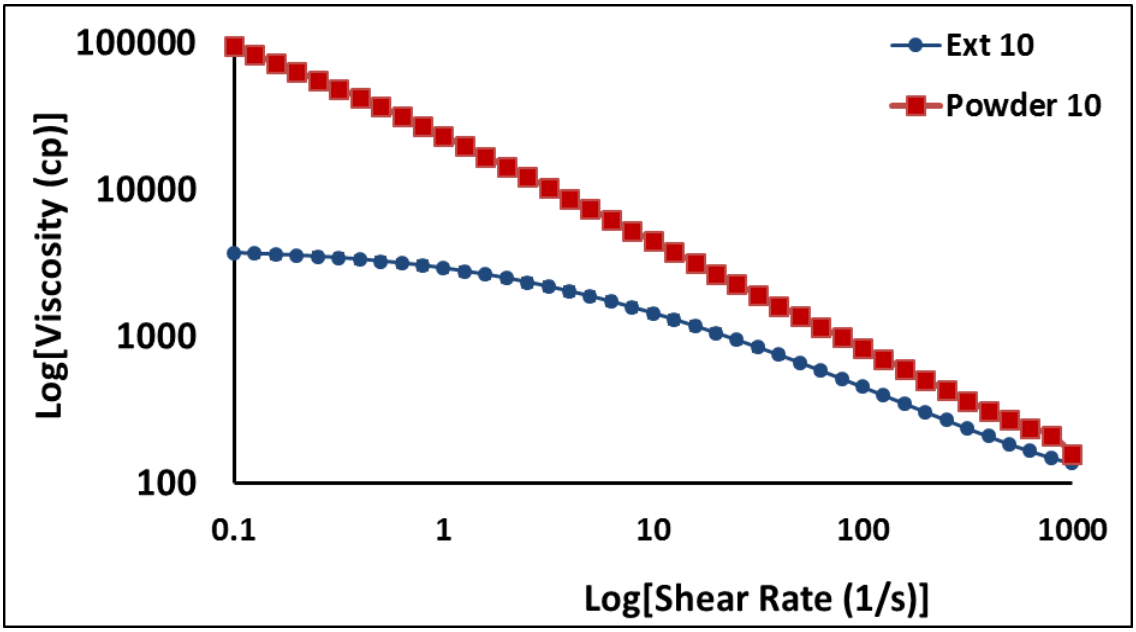

Figure 39: Shear rate vs. viscosity for F10 pre-HME and post-HME at 25 °C

Flow curves of F5 and F10 (pre-HME) are depicted in Figure 40. Similarly, flow curves of F5 and F10 (post-HME) can be seen in Figure 41. The corresponding viscosities at shear rate 1 $\mathbf{s^{-1}}$ are listed in table 23. It is apparent from the values of viscosity in Table 1 that both F5 and F10 tablets were susceptible to similar degradation resulting in lower viscosity, however, a higher viscosity loss was observed for F5 compared to F10 after the HME process. This can be related to the less crystalline structure of PEO 301 causing a more rapidly degradation. Crowley *et al*. studied the stability of PEO with molecular weight of 100,000, 600,000, and 1,000,000 Daltons [122]. They reported a similar conclusion that degradation occurred more rapidly with lower molecular weight polymers (MW of 100,000). Additional studies by Maclains and Booth concluded that PEO crystallinity was at maximum at molecular weight of 6000 and decreased with increasing molecular weight [142]. Even though their study contradicts ours it is noteworthy to mention that they reported the results for PEO molecules ranging in molecular weight from 2×10^4 to 1.6×10^6. Undoubtedly, both PEO 301 and PEO 303 are extremely sensitive to degradation during extrusion. More extensive research would be required to clearly understand the correlation between their degradation process and crystallinity.

As can be seen in Table 23, F10 tablets are more viscous than F5 tablets. One may conclude that the higher viscosity of F10 tablets is indicative of a decrease in API release content and consequently a slower dissolution rate. However, the dissolution data in the earlier section showed that F5 and F10 tablets released the drug at a similar rate. One possible explanation is that the difference between the viscosities of F5 and F10 is less than one order of magnitude, and one or higher order of magnitude viscosity difference would be required for dissolution profiles to be different. Alternatively, it is possible that the release

rate depend not only on the viscosity of the polymer but also on other factors, such as the polydispersity of the molecular weight, not considered in these experiments. Evidently, there would be more research required in this field to understand the correlation between viscosity of PEO tablets and their dissolution profiles.

Table 23: Percent viscosity loss (%) for F5 and F10 formulations pre-HME and post-HME @shear rate 1 s^{-1}

Formulation	Powder (cp)	Extrudate (cp)	Viscosity loss (%)
5	17823	866	95
10	23116	2907	87
%RSD	18	77	

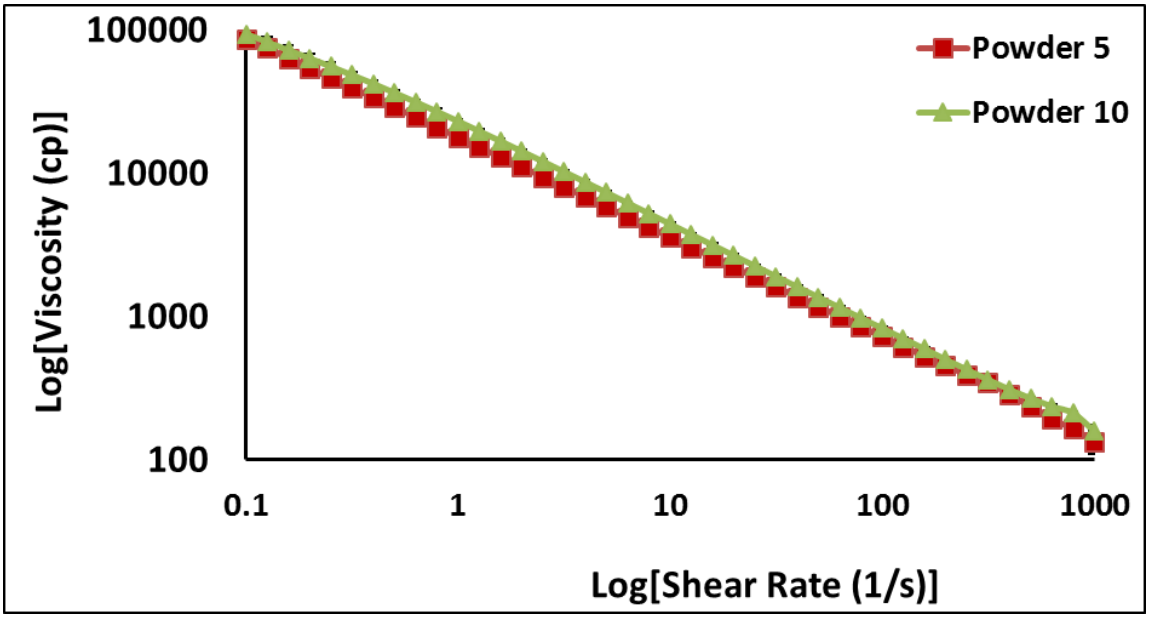

Figure 40: Shear rate vs. viscosity for the powder blends of F5 and F10 (pre-HME) at 25°C

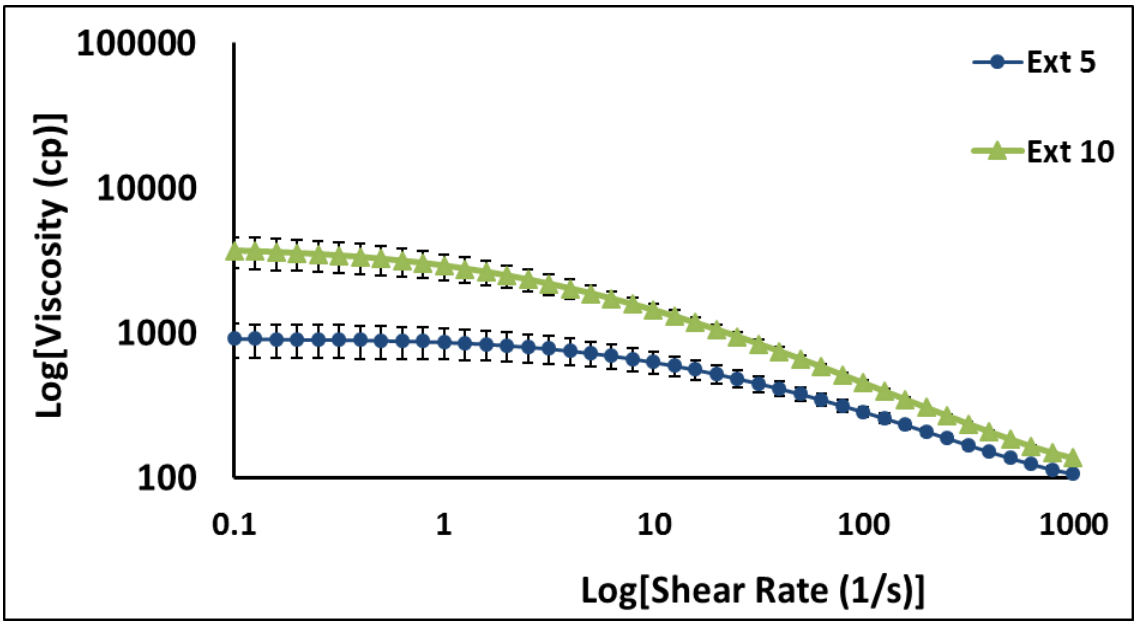

Figure 41: Shear rate vs. viscosity for the F5 and F10 tablets (post-HME) at 25 °C

As can be observed from Figure 41, the viscosity becomes independent of shear rate at very low shear rates. As the shear rate is increased, the viscosity decreases sharply due to the strong effects of shearing on entanglements that are attributed to the effect of high molecular weight. We now consider quantitative relationships for the dependence of viscosity on shear rate. The simplest relationship is the power law equation or Ostwald de Waele Model (1) where n is the power law index and K is the consistency index which is a measure of the consistency of the substance [143]. The model is the simplest approximation of shear-thinning behavior of fluids, and values of n=1 denotes the Newtonian fluid and values of n < 1 shows shear-thinning treatment. Converting the equation below into logarithmic form, the next equation can be obtained.

$$\mu = K\gamma^{n-1}$$

$$\ln(\mu) = \ln(K) + (n-1)\ln(\gamma)$$

The power index, n, was calculated from the slope of the plot of the logarithm of the apparent viscosity as a function of the shear rate (equation 2) for the melt solutions. The calculated slope was estimated at the mid-point of the linear range of the plot of equation. The data is presented in Table 24. As shown in the table, both solutions have values of less than one indicating a shear-thinning behavior. However, F10 tablet containing PEO 303 shows a slightly higher shear-thinning behavior compared to F5 tablet that contains PEO 301. Additionally, the viscosity of F10 tablet starts to decrease at a lower shear rate than that of F5 tablet. This may be explained by the effect of molecular weight distribution (MWD) on shear thinning behavior of tablets. It has been observed that polymers with broad MWD show the onset of shear thinning at lower shear rates [144]. And the viscosity of the molecule with MWD, especially with high molecular weight, is more shear sensitive than a molecule with MWD with lower molecular weight.

Table 24: Power law model constants, K and n, for F5 and F10

Extrudate	n	STDEV
5	0.65	0.03
10	0.50	0.02

5.3.3 Weight-average molecular weight and number-average molecular weight

Table 25 summarizes the number-average molecular weight (Mn) and weight-average molecular weight (Mw) based on the theoretical molecular weight values of each

component. As can be seen from the table, both the number-average and the weight-average molecular weights increase with increasing amount of high-molecular weight polymer in the sample. Mw is more sensitive to the addition of high molecular weight polymer which can be expected from the definition of the two averages. Weight-average molecular weight puts weight on the heavier molecules such as PEO 301 and PEO 303 in the formulation more strongly than number-average molecular weight.

Table 25: Formulation characteristics used in the study including %fraction of each component, the weight-average molecular weight, the number-average molecular weight, and the rate of release at t_{50}

F#	CPM (%)	PEO (303) 7M (%)	PEO (301) 4M (%)	PEO (750) 300K (%)	Mw (g/mol)	Mn (g/mol)	r_{50} (%/min)
1	6	0	0	94	282023	6386	0.39
2	6	0	7.5	86.5	559523	6396	0.31
3	6	0	17.9	76.1	944323	6409	0.31
4	6	0	43.2	50.8	1880423	6441	0.25
5	6	0	94	0	3760023	6507	0.12
6	6	4.2	0	89.77	563423	6392	0.38
7	6	9.9	0	84.13	945413	6399	0.34
8	6	23.9	0	70.1	1883323	6418	0.29
9	6	52	0	42	3766023	6455	0.19
10	6	94	0	0	6580023	6511	0.13

The time when 50% of the API in the tablet releases into the dissolution medium, t_{50}, is a standard way to quantify the release rate of the tablet. The value of t_{50} depends on the length

of the slower initial part of the release profile and the release rate during the linear period. More specifically, we evaluated the slope at 50% release, r_{50}, because this point falls in the linear part of all the release profiles. This was accomplished by fitting a straight line through the experimental data between 10% and 70% drug release. The values of r_{50} are listed in Table 25.

The values of r_{50} is plotted against the weight-average molecular weight (Mw) in Figure 42 and the number-average molecular weight (Mn) in Figure 43. The results in Figure 42 indicate that both F1 - F5 and F6 - F10 follow straight line. The value of r_{50} decreases with molecular weight in both Figures, however, it decreases at a higher rate for F1-F5 tablets. Also, r_{50} is similar in value for the formulations at approximately 5 million and 7 million molecular weight corresponding to F5 and F10 tablets. This can be explained by the similar viscosities of F5 and F10 at the swollen gel layer at the tablet surface which was elaborated in the previous sections.

Comparing the tablets with similar weight-average molecular weight such as F2 and F6 (0.5 M), F3 and F7 (1M), F4 and F8 (2M), and F5 and F9 (4M) we observe that all the tablets containing PEO 303 (red dots on Figure 42) release faster compared to the tablets containing PEO 301 (blue dots). This observation indicates that the ratio of high molecular weight PEO to low molecular weight PEO drives the diffusion mechanism in the drug release. In other words, the fraction of high molecular weight controls the overall release rate regardless of which high MW polymer is used. The faster release in these formulations can also be explained by the faster dissolution of low molecular weight polymer ratio. This observation was also made by Korner *et al*. when they studied tablets with mixed ratios of two grades of PEO; Polyox WSR N-10 (100,000 MW) and Polyox WSR N60-K (2,000,000

MW) [145]. As mentioned above, the correlation between the rate of release of CPM and the weight-average molecular weight is different for F1-F5 and F6-F10. One explanation could be that the rate of release is not only a function of weight-average molecular weight but also polydispersity. But assuming F6-F10 tablets are more polydisperse than F1-F5 tablets it appears that the increase of polydispersity does not affect the release rate of F5 and F10 tablets. This further confirms the findings in earlier sections that release rate of tablets with high fractions of high molecular weight is a function of viscosity rather than polydispersity.

As can be seen in Figure 43, the data from both F1 – F5 and F6 – F10 tablets superimpose. This means that both polymers behave similarly and follow a common trend. It is also evident that based on number-average molecular weight, the data is skewed differently. In other words, the weight on different long chains and short chains are distributed evenly, and the effect of PEO 301 and PEO 303 is not as distinct. The data in Figure 43 shows that the number-average molecular weight gives a good prediction of the drug release rate irrespective of which high molecular weight PEO is used.

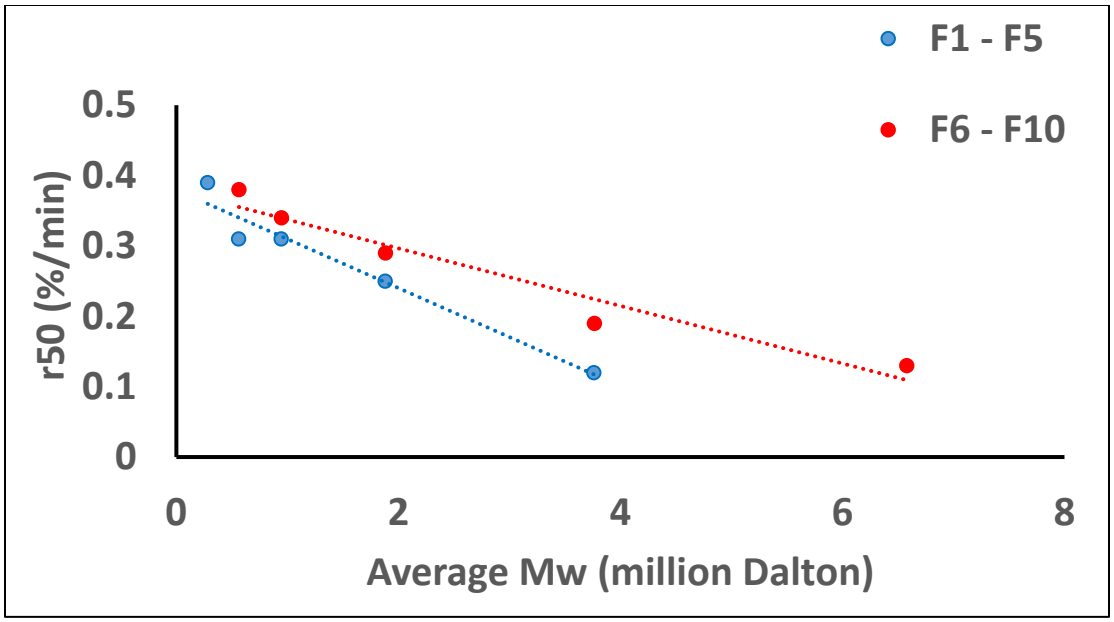

Figure 42: Rate of dissolution @ 50% release (r_{50}) vs. weight-average molecular weight (Mw)

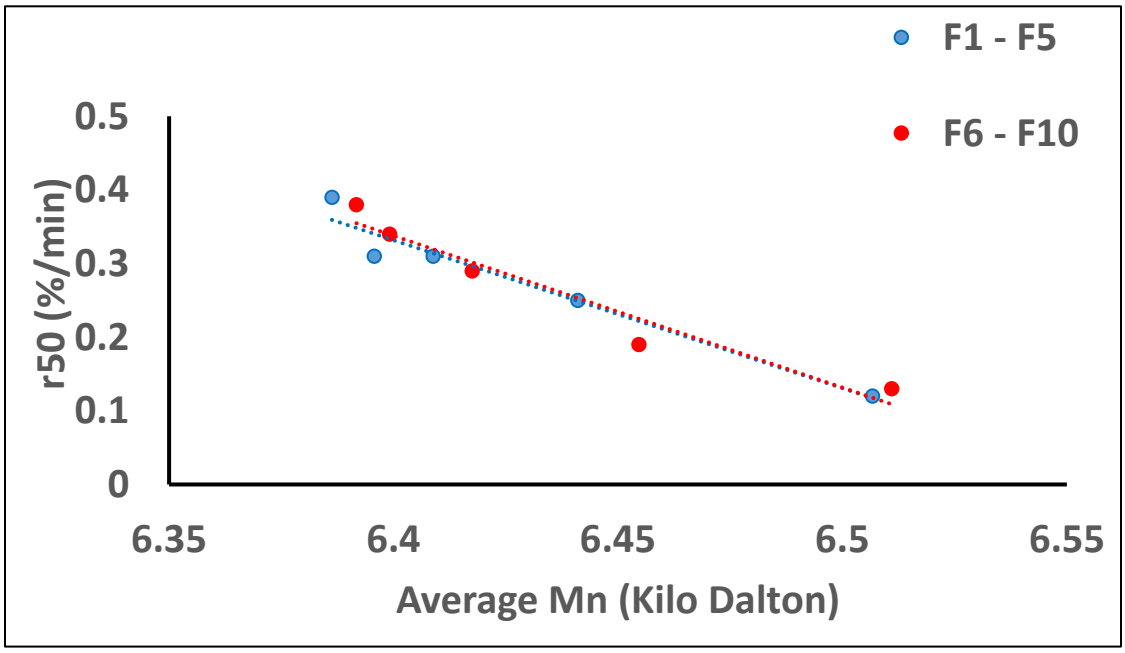

Figure 43: Rate of dissolution @ 50% release (r_{50}) vs. number-average molecular weight (Mw)

5.4 Conclusion

In this case study, we explored the properties of polyethylene oxide to manufacture tamper resistant formulations using high molecular weight PEO by hot melt extrusion. We investigated the correlation between molecular weight of PEO and extrudate attributes such as dissolution and viscosity. The dissolution results indicated that F5 and F10 tablets released similarly despite having different molecular weights. Even though F5 and F10 tablets had different viscosities the results confirmed that less than one order of magnitude of viscosity difference was not sufficient for the tablets to release drug at different rates. Additionally, it was found that number-average molecular weight had a good correlation with drug release rate compared to weight-average molecular weight. The results also indicated that as the polymer fraction of higher molecular weight increased, the dissolution of the drug decreased.

Although there has been a lot of progress by pharmaceutical industry to produce abuse deterrent products, no formulation is currently able to fully prevent drug abuse. Progress on identifying and understanding excipients and manufacturing processes to prepare abuse deterrent formulations still remains to be made. Thus, the significance of this work lies in the development of formulation composition and physical characteristics for abuse-deterrent formulations. The results from this study could be used to guide the development of such formulations which so far has indicated that it has not altered the trajectory of opioid overdose and addiction.

Chapter 6: Conclusions and future work

The work presented in this dissertation focused on building blocks of two continuous manufacturing processes; direct compression continuous manufacturing (DCCM) and continuous hot melt extrusion (CHME). The 1st case study included a direct compression continuous manufacturing line, and the study was designed to integrate RTRt tools. The 2nd case study focused on a continuous hot melt extrusion process which was set up to examine effects of formulation properties and performance of polyethylene oxide (PEO) tablets. The objective in both case studies was to develop and employ tools for real-time release testing. This chapter summarizes the work presented in this dissertation and outlines recommendations for future work.

6.1 Conclusions

As mentioned, tablets are among the most prevalent dosage forms in the US pharmaceutical market, and the interest in continuous manufacturing of tablets has grown significantly in the past few years. However, there is still a knowledge gap in building quality into the final product. The first aim focused on conducting a case study in a direct compression continuous manufacturing (DCCM) of tablets in the pilot plant at Rutgers. The DCCM line comprised of gravimetric feeders, a de-lumping mill, a continuous mixer, and a tablet press. We used designed experiments to evaluate the effect of variability in critical process parameters (CPP) on the critical quality attributes (CQA) of tablets. Chapter 2 of the dissertation includes the details pertaining to the completion of aim 1.

Towards completing the second and third aim we provided an approach to the implementation of real-time release testing to predict the tensile strength of tablets in a

continuous manufacturing line. We accomplished this task by characterizing tablets at line using ultrasound and diametrical compression test, while correlating the tensile strength of the tablets to the relative density of the tablets as well as to the speed of sound. The study confirmed that there was a strong agreement between the predicted and experimental values of tablet tensile strength. Chapter three of the dissertation includes the details for the partial completion of aim 2.

To further complete the second aim, we presented a methodology for predicting dissolution profiles non-destructively as a quality control method in a continuous direct compression manufacturing line. This work showed the feasibility of predicting dissolution profiles and demonstrated that real-time prediction of dissolution profiles could be a possible control method which can subsequently be integrated into the control strategy in continuous manufacturing to enable continued process performance and product quality. Application of such a strategy will not only add to the process knowledge but also along with other PAT tools would lower laboratory and personnel costs and increase product quality. Chapter four completes the details towards the completion of aim 2.

In aim 4, we examined the effects of formulation on tablet quality, with special focus on drug release and abuse-deterrent attributes, as they pertain to opioid products. The formulation properties and the performance of multiple grades of high molecular weight polyethylene oxide (PEO) as the main matrix forming material were investigated in a continuous hot melt extrusion process. We studied the release mechanism of chlorpheniramine maleate (CPM) from matrix tablets prepared by hot melt extrusion. The weight-average molecular weight of PEO was found to be linearly correlated with the drug release rate of the extruded tablets in F1-F5 and F6-F10 tablets. The number-average

molecular weight showed similar correlation, however, the correlation became independent of the type of PEO irrespective of whether the high molecular weight is PEO 301 or PEO 303 and can give a good prediction of the drug release rate irrespective of which high molecular weight PEO is used. We also found a good correlation between the polymer release rate and the tablet viscosity. The work in this study will allow us to optimize the formulation of opioid products and manufacture tablets with desired dissolution profile towards maximizing abuse deterrent attributes. Chapter five completes the details towards the completion of aim 4.

6.2 Recommendation

Based on the work presented in this dissertation, there are several potential areas of future study. Three specific directions are detailed here.

The analysis of ultrasound data in chapter three revealed that the speed of sound (SOS) was sensitive to the amount of acetaminophen in the tablet. Figure 15 showed that tablets with the lowest amount of acetaminophen showed lower SOS. That means that the sound waves were travelling more slowly in the tablets with low drug content. According to the Newton-Laplace equation, the fastest sound wave will be in a material that is rigid (hard) and that has a large elasticity modulus and/or low density. This suggests that tablets with very low acetaminophen content may have a less rigid structure. However, it is important to note that the main excipient in the formulation is lactose monohydrate, and the drug, acetaminophen, is a very elastic material. Speed of sound is highly influenced by the material, therefore, the type of the drug and the excipient may have a contributing factor in the speed of sound in the tablet. Future work such as using different excipients with various

elasticities will allow for in depth examinations of relations between formulation and speed of sound.

The dissolution data in chapter four was fitted to the Weibull model, the model coefficients were correlated with the process variables, and those two multilinear equations were used for the prediction of the model parameters of the target tablets which were subsequently plugged into the Weibull model to acquire the dissolution profiles. To fully validate the hypothesis that dissolution profiles can be predicted, additional dissolution models must be tested and the corresponding dissolution models be evaluated.

The data in chapter five pertained to the use of three polymers; PEO 750 (300,000 MW) as a plasticiser, PEO 301 (4,000,000 MW), and PEO 303 (7,000,000). Ten formulations were prepared based on different ratios of high molecular weight to low molecular weight PEO. It is suggested that tablets with various ratios of high molecular weight/low molecular weight ratio be made to confirm with additional data that the fraction of high molecular weight polymers controls the drug release rate.

Effect of polydispersity on drug release rate has not been studied extensively. The molecular weight distributions, the number-average molecular weights and the weight-average molecular weights, and polydispersity are determined using size exclusion chromatography. Correlating polydispersity with drug release will deepen our understanding of the role of high molecular weight polymers in drug release.

A technique used to measure the molecular weight of polymers is the intrinsic viscosity (IV) technique. The IV is determined by the measurement of the viscosity of the dilute solution of the polymer in an appropriate solvent. The measured intrinsic viscosity

can be plotted against the measured weight-average molecular weight of tablets. Ideally, the correlation should follow the Mark–Houwink equation. The Mark–Houwink equation describes the relationship between the molecular weight of a polymer and IV of the solution as in equation below:

$[\eta] = kM^a$

where $[\eta]$ is the polymer intrinsic viscosity, M is the polymer molecular weight, and k and a are constants. The correlation between the intrinsic viscosity and molecular weight of tablets and deviation from the Mark–Houwink equation will indicate polydispersity or monodispersity in tablets.

The viscosity measurements were only taken for two formulations; F5 and F10. To confirm the relationship between viscosity and rate of dissolution, it is important that the viscosity of all formulations to be measured to see whether viscosity can predict release rate of PEO tablets. Additionally, intrinsic viscosity can be correlated to intrinsic viscosity to understand whether intrinsic viscosity can be a predictor of dissolving tablet characteristics. Furthermore, one would like to apply these to other polymers and understand whether these conclusions will extend to other polymers as well.

References

1. Arnum, P.V., *Outlining Implementation Strategies for Lean Manufacturing.* Pharmaceutical Technology, 2007.
2. Markarian, J., *Optimizing Solid Dosage Manufacturing.* Pharmaceutical Technology, 2014. **38**(3).
3. Drakulich, A., *A Look Ahead in Biomanufacturing.* BioPharm International, 2013. **26**(1).
4. Plumb, K., *Continuous Processing in the Pharmaceutical Industry: Changing the Mind Set.* Chemical Engineering Research and Design, 2005. **83**(6): p. 730-738.
5. Fisher, A.C., et al., *Advancing pharmaceutical quality: An overview of science and research in the U.S. FDA's Office of Pharmaceutical Quality.* Int J Pharm, 2016. **515**(1-2): p. 390-402.
6. Lee, S.L., et al., *Modernizing Pharmaceutical Manufacturing: from Batch to Continuous Production.* Journal of Pharmaceutical Innovation, 2015. **10**(3): p. 191-199.
7. FDA. 2018; Available from: https://www.fda.gov/Drugs/DrugSafety/DrugRecalls/default.htm.
8. Woodcock, J., *What to expect in next 25 years of medicine, in AAPS Annual meeting.* 2011. **Washington, D.C.**
9. FDA. *Modernizing the Way Drugs Are Made: A Transition to Continuous Manufacturing*. 2017; Available from: https://www.fda.gov/Drugs/NewsEvents/ucm557448.htm.
10. Yu, L.X. and M. Kopcha, *The future of pharmaceutical quality and the path to get there.* International Journal of Pharmaceutics, 2017. **528**(1): p. 354-359.
11. EMA, *Guidelines on Real Time Release Testing (formerly Guidelines on Parametric Release), Final.* March 2012.
12. Leskinen, J.T.T., et al., *Real-time tablet formation monitoring with ultrasound measurements in eccentric single station tablet press.* International Journal of Pharmaceutics, 2013. **442**(1): p. 27-34.
13. Hakulinen, M.A., et al., *Ultrasound Transmission Technique as a Potential Tool for Physical Evaluation of Monolithic Matrix Tablets.* AAPS PharmSciTech, 2008. **9**(1): p. 267-273.
14. Akseli, I., B.C. Hancock, and C. Cetinkaya, *Non-destructive determination of anisotropic mechanical properties of pharmaceutical solid dosage forms.* Int J Pharm, 2009. **377**(1-2): p. 35-44.
15. Liu, J. and C. Cetinkaya, *Mechanical and geometric property characterization of dry-coated tablets with contact ultrasonic techniques.* Int J Pharm, 2010. **392**(1-2): p. 148-55.
16. Stephens, J.D., et al., *Ultrasonic real-time in-die monitoring of the tablet compaction process-a proof of concept study.* Int J Pharm, 2013. **442**(1-2): p. 20-6.
17. Stephens, J.D., et al., *Wireless transmission of ultrasonic waveforms for monitoring drug tablet properties and defects.* Int J Pharm, 2013. **442**(1-2): p. 35-41.
18. Akseli, I., et al., *Development of predictive tools to assess capping tendency of tablet formulations.* Powder Technology, 2013. **236**: p. 139-148.
19. Razavi, S.M., et al., *Toward predicting tensile strength of pharmaceutical tablets by ultrasound measurement in continuous manufacturing.* International Journal of Pharmaceutics, 2016. **507**(1): p. 83-89.
20. Razavi, S.M., M. Gonzalez, and A.M. Cuitiño, *Quantification of lubrication and particle size distribution effects on tensile strength and stiffness of tablets.* Powder Technology, 2018. **336**: p. 360-374.
21. Boccaccini, D.N.B., A.R., *Dependence of Ultrasonic Velocity on Porosity and Pore Shape in Sintered Matrials.* Journal of Nondestructive Evaluation, 1997. **16**(4): p. 187-192.

22. FDA, *Guidance for Industry: Extended-Release Solid Oral Dosage Forms - Development, Evaluation, and Application of In Vitro/In Vivo Correlations.* 1997.
23. FDA, *Guidance for Industry, Dissolution Testing of Immediate Release Solid Oral Dosage Forms.* 1997.
24. FDA, *Guidance for industry SUPAC-Immediate release solida oral dosage forms: scale up and postapproval changes, chemistry, manufacturing and controls, in vitro dissolution testing and in vivo bioequivalence documentation.* 1995.
25. Mercuri, A., et al., *Understanding and predicting the impact of critical dissolution variables for nifedipine immediate release capsules by multivariate data analysis.* International Journal of Pharmaceutics, 2017. **518**(1): p. 41-49.
26. Huang, J., et al., *Quality by design case study: An integrated multivariate approach to drug product and process development.* International Journal of Pharmaceutics, 2009. **382**(1): p. 23-32.
27. Kaul, G., et al., *Quality-by-Design Case Study: Investigation of the Role of Poloxamer in Immediate-Release Tablets by Experimental Design and Multivariate Data Analysis.* AAPS PharmSciTech, 2011. **12**(4): p. 1064-1076.
28. Andersson, M., A. Ringberg, and C. Gustafsson, *Multivariate methods in tablet formulation suitable for early drug development: Predictive models from a screening design of several linked responses.* Chemometrics and Intelligent Laboratory Systems, 2007. **87**(1): p. 125-130.
29. Ring, D.T., Oliveira J.C.O., Crean, A., *Evaulation of the influence of granulation processing parameters on the granule properties and dissolution characteristics of a modified release drug.* Advanced Powder Technology, 2011. **22**(2): p. 245-252.
30. Wang, Y., et al., *Statistical comparison of dissolution profiles.* Drug Development and Industrial Pharmacy, 2016. **42**(5): p. 796-807.
31. Douroumis, D., *Hot-melt extrusion: Pharmaceutical applications*. 2012: Wiley Online Library.
32. Markl, D., et al., *Supervisory control system for monitoring a pharmaceutical hot melt extrusion process.* AAPS PharmSciTech, 2013. **14**(3): p. 1034-44.
33. Yang, L., G. Venkatesh, and R. Fassihi, *Characterization of compressibility and compactibility of poly(ethylene oxide) polymers for modified release application by compaction simulator.* J Pharm Sci, 1996. **85**(10): p. 1085-90.
34. CDC, et al., *Drug overdose deaths in the United States, 1999-2016.* NCHS data brief, no 294. Hyattsville, MD: National Center for Health Statistics, 2017.
35. FDA, *Guidance for Industry: abuse-deterrent opioids - evaluation and labeling.* Silver Spring, MD: US Department of Health and Human Services, 2015.
36. Harris, S.C., et al., *Oral abuse potential, pharmacokinetics, and safety of once-daily, single-entity, extended-release hydrocodone (HYD) in recreational opioid users.* Pain Medicine, 2017. **18**(7): p. 1278-1291.
37. Dhillon, S., *Hydrocodone Bitartrate ER (Hysingla® ER): a review in chronic pain.* Clinical drug investigation, 2016. **36**(11): p. 969-980.
38. Zhang, F. and J.W. McGinity, *Properties of sustained-release tablets prepared by hot-melt extrusion.* Pharmaceutical Development and Technology, 1999. **4**(2): p. 241-250.
39. Osorio, J.G. and F.J. Muzzio, *Effects of processing parameters and blade patterns on continuous pharmaceutical powder mixing.* Chemical Engineering and Processing: Process Intensification, 2016. **109**: p. 59-67.
40. Vanarase, A.U., Muzzio, Fernando. *Design, modeling, and real time monitoring of continuous powder mixing processes*. [Thesis] 2011; Available from: https://doi.org/doi:10.7282/T35M64S3.
41. Coulter, B., *LS 13 320 laser diffraction particle size analyzer instrument manual.* Beckman Coulter Inc, 2003. **11800**.

42. Fell, J.T. and J.M. Newton, *Determination of tablet strength by the diametral-compression test.* Journal of Pharmaceutical Sciences, 1970. **59**(5): p. 688-691.
43. Pharmacopeia, U., *United States Pharmacopeia and National Formulary (USP 37–NF 32).* Rockville, MD: US Pharmacopeia, 2014.
44. Thiele, W. and I. Ghebre-Selassie, *Pharmaceutical extrusion technology.* Informa Health Care, New York, 2003.
45. Langley, N., J. DiNunzio, and M.A. Repka, *Melt Extrusion: Materials, Technology and Drug Product Design (AAPS Advances in the Pharmaceutical Sciences Series)*. 2013: Springer.
46. Repka, M.A., et al., *Melt extrusion: process to product.* Expert opinion on drug delivery, 2012. **9**(1): p. 105-125.
47. Gryczke, A. and L. BASF SE, *Investigating process parameter mechanism for successful scale-up of a hot-melt extrusion process.*
48. Hunt, B.J. and M.I. James, *Polymer characterisation*. 2012: Springer Science & Business Media.
49. Commereuc, S., *Basic Rheology of Polymer Melts. An Introductory Polymer Science Experiment.* Journal of chemical education, 1999. **76**(11): p. 1528.
50. Santos, S., F. Gouveia, and J. Menezes, *PAT paves the way for continuous manufacturing*. 2015.
51. Hernandez, E., et al., *Prediction of dissolution profiles by non-destructive near infrared spectroscopy in tablets subjected to different levels of strain.* Journal of pharmaceutical and biomedical analysis, 2016. **117**: p. 568-576.
52. Vanarase, A.U., et al., *Real-time monitoring of drug concentration in a continuous powder mixing process using NIR spectroscopy.* Chemical Engineering Science, 2010. **65**(21): p. 5728-5733.
53. Singh, R., et al., *Real time monitoring of powder blend bulk density for coupled feed-forward/feed-back control of a continuous direct compaction tablet manufacturing process.* International journal of pharmaceutics, 2015. **495**(1): p. 612-625.
54. Sierra-Vega, N.O., et al., *Assessment of blend uniformity in a continuous tablet manufacturing process.* International journal of pharmaceutics, 2019. **560**: p. 322-333.
55. Heigl, N., et al., *Potential of Raman spectroscopy for evaluating crushing strength of tablets.* Journal of pharmaceutical innovation, 2012. **7**(2): p. 76-86.
56. May, R.K., et al., *Hardness and density distributions of pharmaceutical tablets measured by terahertz pulsed imaging.* Journal of pharmaceutical sciences, 2013. **102**(7): p. 2179-2186.
57. Leskinen, J.T., et al., *In-line ultrasound measurement system for detecting tablet integrity.* International journal of pharmaceutics, 2010. **400**(1-2): p. 104-113.
58. Akseli, I. and C. Cetinkaya, *Drug tablet thickness estimations using air-coupled acoustics.* Int J Pharm, 2008. **351**(1-2): p. 165-73.
59. Akseli, I. and C. Cetinkaya, *Air-coupled non-contact mechanical property determination of drug tablets.* Int J Pharm, 2008. **359**(1-2): p. 25-34.
60. Akseli, I., D. Dey, and C. Cetinkaya, *Mechanical property characterization of bilayered tablets using nondestructive air-coupled acoustics.* AAPS PharmSciTech, 2010. **11**(1): p. 90-102.
61. Xu, X., et al., *Correlation of solid dosage porosity and tensile strength with acoustically extracted mechanical properties.* International Journal of Pharmaceutics, 2018. **542**(1): p. 153-163.
62. Mendez, R., F. Muzzio, and C. Velazquez, *Study of the effects of feed frames on powder blend properties during the filling of tablet press dies.* Powder Technology, 2010. **200**(3): p. 105-116.

63. Xie, X. and V.M. Puri, *Uniformity of Powder Die Filling Using a Feed Shoe: A Review.* Particulate Science and Technology, 2006. **24**(4): p. 411-426.
64. Sinka, I.C., L.C.R. Schneider, and A.C.F. Cocks, *Measurement of the flow properties of powders with special reference to die fill.* International Journal of Pharmaceutics, 2004. **280**(1): p. 27-38.
65. Vanarase, A.U. and F.J. Muzzio, *Effect of operating conditions and design parameters in a continuous powder mixer.* Powder Technology, 2011. **208**(1): p. 26-36.
66. Mendez, R., Muzzio, F., & Velazquez, C. , *Powder hydrophobicity.* AIChE Journal, 2012. **58**(3): p. 697-706.
67. Ryshkewitch, E., *Compression strength of porous sintered alumina and zirconia: 9th communication to ceramography.* Journal of the American Ceramic Society, 1953. **36**(2): p. 65-68.
68. Kuentz, M. and H. Leuenberger, *A new model for the hardness of a compacted particle system, applied to tablets of pharmaceutical polymers.* Powder Technology, 2000. **111**(1): p. 145-153.
69. AULTON, M.E., H.G. TEBBY, and P.J.P. WHITE, *Indentation hardness testing of tablets.* Journal of Pharmacy and Pharmacology, 1974. **26**(S1): p. 59P-60P.
70. Prasad, K.V.R., D.B. Sheen, and J.N. Sherwood, *Fracture Property Studies of Paracetamol Single Crystals Using Microindentation Techniques.* Pharmaceutical Research, 2001. **18**(6): p. 867-872.
71. Pawar, P., et al., *The effect of mechanical strain on properties of lubricated tablets compacted at different pressures.* Powder Technology, 2016. **301**: p. 657-664.
72. Guidance, F., *Guidance for Industry: Dissolution Testing of Immediate Release Solid Oral Dosage Forms. US Department of Health and Human Services.* Food and Drug Administration, Center for Drug Evaluation and Research (CDER), 1997.
73. FDA, U., *Guidance for Industry Extended Release Oral Dosage Forms: Development, Evaluation, and Application of.* vitro/In vivo, 1997.
74. Dosage, F.E.R.S.O., *Forms Development, Evaluation And Application Of In Vitro-In Vivo Correlation. Guidance for Industry. US Department of Health and Human Services.* Food and Drug Administration, Center for Drug Evaluation and Research, 1997.
75. O'Brien, R.G. and M.K. Kaiser, *MANOVA method for analyzing repeated measures designs: an extensive primer.* Psychol Bull, 1985. **97**(2): p. 316-33.
76. Yuksel, N., Kanik, Arzu E., Baykara, Tamer, *Comparison of in vitro dissolution profiles by ANOVA-based, model-dependent and -independent methods.* International Journal of Pharmaceutics, 2000. **209**.
77. Siepmann, J. and F. Siepmann, *Mathematical modeling of drug dissolution.* International journal of pharmaceutics, 2013. **453**(1): p. 12-24.
78. Costa, P. and J.M.S. Lobo, *Modeling and comparison of dissolution profiles.* European journal of pharmaceutical sciences, 2001. **13**(2): p. 123-133.
79. Burham, K. and D. Anderson, *Model selection and multimodel inference: A practical information-theoretic approach. Springer.* New York, 2002.
80. Langenbucher, F., *Letters to the Editor: Linearization of dissolution rate curves by the Weibull distribution.* Journal of Pharmacy and Pharmacology, 1972. **24**(12): p. 979-981.
81. Moore, J.W.a.F., H. H., *Mathematical comparison of curves with an emphasis on in vitro dissolution profiles.* Pharmaceutical Technology, 1996. **20**: p. 64-74.
82. FDA, *Guidance for industry SUPAC-MR : modified release solid oral dosage forms : scale-up and postapproval changes, chemistry, manufacturing and controls, in vitro dissolution testing and in vivo bioequivalence documentation.* 1997.
83. ICH, *Pharmaceutical Development, Q8(R2).* 2009.
84. ICH , I.C.o.H.o.T.R.f.R.o.P.f.H.U., *Quality Risk Management Q9.* 2005.

85. ICH, I.C.o.H.o.T.R.f.R.o.P.f.H.U., *Development and Manufacture of Drug Substances (Chemical Entities and Biotechnological/Biological Entities) Q11*. 2012.
86. ICH , I.C.o.H.f.T.R.f.R.o.P.f.H.U., *Tehchnical and regulatory considerations for pharmaceutical product lifecycle management, Q12.* 2017.
87. Allison, G., et al., *Regulatory and Quality Considerations for Continuous Manufacturing. May 20–21, 2014 Continuous Manufacturing Symposium.* Journal of Pharmaceutical Sciences, 2015. **104**(3): p. 803-812.
88. Breitenbach, J., *Melt extrusion: from process to drug delivery technology.* European journal of pharmaceutics and biopharmaceutics, 2002. **54**(2): p. 107-117.
89. Baronsky-Probst, J., et al., *Process design and control of a twin screw hot melt extrusion for continuous pharmaceutical tamper-resistant tablet production.* European Journal of Pharmaceutical Sciences, 2016. **87**: p. 14-21.
90. Vynckier, A.K., et al., *Hot-melt co-extrusion: requirements, challenges and opportunities for pharmaceutical applications.* Journal of pharmacy and pharmacology, 2014. **66**(2): p. 167-179.
91. Li, S., et al., *Mechanochemical synthesis of pharmaceutical cocrystal suspensions via hot melt extrusion: feasibility studies and physicochemical characterization.* Molecular Pharmaceutics, 2016. **13**(9): p. 3054-3068.
92. Melocchi, A., et al., *Hot-melt extruded filaments based on pharmaceutical grade polymers for 3D printing by fused deposition modeling.* International journal of pharmaceutics, 2016. **509**(1-2): p. 255-263.
93. Litman, R.S., O.H. Pagán, and T.J. Cicero, *Abuse-deterrent opioid formulations.* Anesthesiology: The Journal of the American Society of Anesthesiologists, 2018. **128**(5): p. 1015-1026.
94. Odian, G., *Principles of polymerization*. 2004: John Wiley & Sons.
95. Riande, E., et al., *Polymer viscoelasticity: stress and strain in practice*. 1999: CRC Press.
96. Rane, M., et al., *Application of polyethylene oxide in hydrophilic matrix tablets.* Pharma Times, 2013. **45**(3): p. 41-48.
97. POLYOX Water-Soluble Resins, N., *Patents Related to Pharmaceutical Applications.* Dow Chemical Company, 2004.
98. Harrington, R. and B. Zimm, *Degradation of polymers by controlled hydrodynamic shear1*. The Journal of Physical Chemistry, 1965. **69**(1): p. 161-175.
99. Health, N.I.o., *NIH Fact Sheets-Pain Management*. 2013.
100. Ravi Kumar, M.N. and N. Kumar §, *Polymeric controlled drug-delivery systems: perspective issues and opportunities.* Drug development and industrial pharmacy, 2001. **27**(1): p. 1-30.
101. Apicella, A., et al., *Poly (ethylene oxide)(PEO) and different molecular weight PEO blends monolithic devices for drug release.* Biomaterials, 1993. **14**(2): p. 83-90.
102. Kaur, G., et al., *Oral controlled and sustained drug delivery systems: Concepts, advances, preclinical, and clinical status*, in *Drug Targeting and Stimuli Sensitive Drug Delivery Systems*. 2018, Elsevier. p. 567-626.
103. Shojaee, S., et al., *Investigation of drug release from PEO tablet matrices in the presence of vitamin E as antioxidant.* Current drug delivery, 2015. **12**(5): p. 591-599.
104. Körner, A., et al., *Swelling and polymer erosion for poly (ethylene oxide) tablets of different molecular weights polydispersities.* Journal of Pharmaceutical Sciences, 2010. **99**(3): p. 1225-1238.
105. Körner, A., et al., *Influence of different polymer types on the overall release mechanism in hydrophilic matrix tablets.* Molecules, 2009. **14**(8): p. 2699-2716.
106. Wang, L., et al., *Design and evaluation of hydrophilic matrix system containing polyethylene oxides for the zero-order controlled delivery of water-insoluble drugs.* AAPS PharmSciTech, 2017. **18**(1): p. 82-92.

107. Choi, S.-U., J. Lee, and Y. Wook Choi, *Development of a directly compressible poly (ethylene oxide) matrix for the sustained-release of dihydrocodeine bitartrate.* Drug development and industrial pharmacy, 2003. **29**(10): p. 1045-1052.
108. Kim, C.J., *Drug release from compressed hydrophilic POLYOX-WSR tablets.* Journal of Pharmaceutical Sciences, 1995. **84**(3): p. 303-306.
109. Moroni, A. and I. Ghebre-Sellassie, *Application of poly (oxyethylene) homopolymers in sustained release solid formulations.* Drug Development and Industrial Pharmacy, 1995. **21**(12): p. 1411-1428.
110. Efentakis, M. and M. Vlachou, *Evaluation of high molecular weight poly (oxyethylene)(Polyox) polymer: studies of flow properties and release rates of furosemide and captopril from controlled-release hard gelatin capsules.* Pharmaceutical Development and Technology, 2000. **5**(3): p. 339-346.
111. Maggi, L., R. Bruni, and U. Conte, *High molecular weight polyethylene oxides (PEOs) as an alternative to HPMC in controlled release dosage forms.* International journal of pharmaceutics, 2000. **195**(1-2): p. 229-238.
112. Shrivastava, A., *Introduction to plastics engineering*. 2018: William Andrew.
113. Podzimek, S., *Light scattering, size exclusion chromatography and asymmetric flow field flow fractionation: powerful tools for the characterization of polymers, proteins and nanoparticles*. 2011: John Wiley & Sons.
114. Atkins, P.W., J. De Paula, and J. Keeler, *Atkins' physical chemistry*. 2018: Oxford university press.
115. Sheu, W.-S., *Molecular weight averages and polydispersity of polymers.* Journal of Chemical Education, 2001. **78**(4): p. 554.
116. Yin, N., Z.X. Zeng, and W.L. Xue, *Intrinsic viscosity–number average molecular weight relationship for poly (1, 4-butylene adipate) diol.* Journal of applied polymer science, 2010. **117**(4): p. 1883-1887.
117. Snejdrova, E. and M. Dittrich, *Pharmaceutically used plasticizers*, in *Recent advances in plasticizers*. 2012, IntechOpen.
118. Zhu, Y., et al., *Solid-state plasticization of an acrylic polymer with chlorpheniramine maleate and triethyl citrate.* International Journal of Pharmaceutics, 2002. **241**(2): p. 301-310.
119. Wilson, A., *Plasticizers: Principles and Practice, The Institute of Materials*. 1995, Cambridge University Press, Cambridge.
120. Repka, M.A. and J.W. McGinity, *Influence of vitamin E TPGS on the properties of hydrophilic films produced by hot-melt extrusion.* International journal of pharmaceutics, 2000. **202**(1-2): p. 63-70.
121. Gutiérrez-Rocca, J. and J.W. McGinity, *Influence of water soluble and insoluble plasticizers on the physical and mechanical properties of acrylic resin copolymers.* International Journal of Pharmaceutics, 1994. **103**(3): p. 293-301.
122. Crowley, M.M., et al., *Stability of polyethylene oxide in matrix tablets prepared by hot-melt extrusion.* Biomaterials, 2002. **23**(21): p. 4241-4248.
123. Desai, D., et al., *Selection of solid-state plasticizers as processing aids for hot-melt extrusion.* Journal of pharmaceutical sciences, 2018. **107**(1): p. 372-379.
124. Ma, L., L. Deng, and J. Chen, *Applications of poly (ethylene oxide) in controlled release tablet systems: a review.* Drug development and industrial pharmacy, 2014. **40**(7): p. 845-851.
125. Borgquist, P., et al., *A model for the drug release from a polymer matrix tablet—effects of swelling and dissolution.* Journal of controlled release, 2006. **113**(3): p. 216-225.
126. Colombo, P., et al., *Drug diffusion front movement is important in drug release control from swellable matrix tablets.* Journal of pharmaceutical sciences, 1995. **84**(8): p. 991-997.

127. Colombo, P., et al., *Analysis of the swelling and release mechanisms from drug delivery systems with emphasis on drug solubility and water transport.* Journal of Controlled Release, 1996. **39**(2-3): p. 231-237.
128. Colombo, P., R. Bettini, and N.A. Peppas, *Observation of swelling process and diffusion front position during swelling in hydroxypropyl methyl cellulose (HPMC) matrices containing a soluble drug.* Journal of Controlled Release, 1999. **61**(1-2): p. 83-91.
129. Colombo, P., et al., *Swellable matrices for controlled drug delivery: gel-layer behaviour, mechanisms and optimal performance.* Pharmaceutical science & technology today, 2000. **3**(6): p. 198-204.
130. Harland, R.S., et al., *Drug/polymer matrix swelling and dissolution.* Pharmaceutical research, 1988. **5**(8): p. 488-494.
131. Siepmann, J. and N. Peppas, *Hydrophilic matrices for controlled drug delivery: an improved mathematical model to predict the resulting drug release kinetics (the "sequential layer" model).* Pharmaceutical Research, 2000. **17**(10): p. 1290-1298.
132. Siepmann, J., A. Streubel, and N. Peppas, *Understanding and predicting drug delivery from hydrophilic matrix tablets using the "sequential layer" model.* Pharmaceutical research, 2002. **19**(3): p. 306-314.
133. Leskinen, J., *Acoustic Techniques for Pharmaceutical Process Monitoring.* Academic Dissertation, University of Eastern Finland, Kuopio, Finland, 2013.
134. Cussler, E.L., *Diffusion: Mass Transfer in Fluid System*, ed. r. ed. 2009: Cambridge University Press.
135. Sojoudi, A. and S.C. Saha, *Shear thinning and shear thickening non-Newtonian confined fluid flow over rotating cylinder.* American Journal of Fluid Dynamics, 2012. **2**(6): p. 117-121.
136. Körner, A., et al., *Molecular information on the dissolution of polydisperse polymers: mixtures of long and short poly (ethylene oxide).* The Journal of Physical Chemistry B, 2005. **109**(23): p. 11530-11537.
137. Maggi, L., et al., *Dissolution behaviour of hydrophilic matrix tablets containing two different polyethylene oxides (PEOs) for the controlled release of a water-soluble drug. Dimensionality study.* Biomaterials, 2002. **23**(4): p. 1113-1119.
138. Petrović, J., et al., *Modelling of diclofenac sodium diffusion from swellable and water-soluble polyethylene oxide matrices.* Journal of Pharmacy and Pharmacology, 2009. **61**(11): p. 1449-1456.
139. Odell, J. and A. Keller, *Flow-induced chain fracture of isolated linear macromolecules in solution.* Journal of Polymer Science Part B: Polymer Physics, 1986. **24**(9): p. 1889-1916.
140. Ebagninin, K.W., A. Benchabane, and K. Bekkour, *Rheological characterization of poly (ethylene oxide) solutions of different molecular weights.* Journal of colloid and interface science, 2009. **336**(1): p. 360-367.
141. McGary Jr, C., *Degradation of poly (ethylene oxide).* Journal of Polymer Science, 1960. **46**(147): p. 51-57.
142. Maclaine, J. and C. Booth, *Effect of molecular weight on crystallization isotherms of high molecular weight poly (ethylene oxide) fractions.* Polymer, 1975. **16**(9): p. 680-684.
143. Chhabra, R.P., *Non-Newtonian fluids: an introduction*, in *Rheology of complex fluids*. 2010, Springer. p. 3-34.
144. Dealy, J.M. and K.F. Wissbrun, *Melt rheology and its role in plastics processing: theory and applications*. 2012: Springer Science & Business Media.
145. Körner, A., et al., *Tuning the polymer release from hydrophilic matrix tablets by mixing short and long matrix polymers.* Journal of pharmaceutical sciences, 2005. **94**(4): p. 759-769.

Appendices

In Press

1. **Golshid Keyvan**, Sonia Razavi, James Scicolone, Alberto Cuitino, Fernando Muzzio. Real-time prediction of tablet tensile strength by ultrasound in continuous manufacturing
2. **Golshid Keyvan**, Yifan Wang, Fernando Muzzio. An approach to predictive dissolution modelling in continuous manufacturing of solid dosage forms
3. **Golshid Keyvan**, Justin Hendrix, Elaheh Ardalani, Alberto Cuitino, Fernando Muzzio. Effect of high molecular weight polyethylene oxide (PEO) on properties of tablets in a hot melt extrusion process

Published

1. Baranwal Y, Román-Ospino AD, **Keyvan G**, Ha JM, Hong EP, Muzzio FJ, Ramachandran R. Prediction of dissolution profiles by non-destructive NIR spectroscopy in bilayer tablets. International journal of pharmaceutics. 2019 Jun 30;565:419-36.
2. Pawar P, Wang Y, **Keyvan G**, Callegari G, Cuitino A, Muzzio F. Enabling real time release testing by NIR prediction of dissolution of tablets made by continuous direct compression (CDC). International journal of pharmaceutics. 2016 Oct 15;512(1):96-107.
3. Hernandez E, Pawar P, **Keyvan G**, Wang Y, Velez N, Callegari G, Cuitino A, Michniak-Kohn B, Muzzio FJ, Romañach RJ. Prediction of dissolution profiles by non-destructive near infrared spectroscopy in tablets subjected to different levels of strain. Journal of pharmaceutical and biomedical analysis. 2016 Jan 5;117:568-76.
4. Wang Y, Snee RD, **Keyvan G**, Muzzio FJ. Statistical comparison of dissolution profiles. Drug development and industrial pharmacy. 2016 May 3;42(5):796-807.
5. Sievens-Figueroa L, Pandya N, Bhakay A, **Keyvan G**, Michniak-Kohn B, Bilgili E, Davé RN. Using USP I and USP IV for discriminating dissolution rates of nano-and microparticle-loaded pharmaceutical strip-films. Aaps Pharmscitech. 2012 Dec 1;13(4):1473-82.
6. Dubey A, Boukouvala F, **Keyvan G**, Hsia R, Saranteas K, Brone D, Misra T, Ierapetritou MG, Muzzio FJ. Improvement of tablet coating uniformity using a Quality by design approach. Aaps Pharmscitech. 2012 Mar 1;13(1):231-46.
7. Elele E, Shen Y, Susarla R, Khusid B, **Keyvan G**, Michniak-Kohn B. Electrodeless electrohydrodynamic drop-on-demand encapsulation of drugs into porous polymer films for fabrication of personalized dosage units. Journal of pharmaceutical sciences. 2012 Jul 1;101(7):2523-33.

8. Dubey A, **Keyvan G**, Hsia R, Saranteas K, Brone D, Misra T, Muzzio FJ. Analysis of pharmaceutical tablet coating uniformity by laser-induced breakdown spectroscopy (LIBS). Journal of pharmaceutical innovation. 2011 Jun 1;6(2):77-87.
9. Meng X, Yang D, **Keyvan G**, Michniak-Kohn B, Mitra S. Synthesis and immobilization of micro-scale drug particles in cellulosic films. Colloids and Surfaces B: Biointerfaces. 2011 Aug 1;86(1):181-8.